NTNU

Norwegian University of
Science and Technology

Optimization and Process Improvements of a High Temperature Heat Pump Using Butane as Working Fluid

Martin Olafsen

Master of Science in Mechanical Engineering

Submission date: March 2018

Supervisor: Trygve Magne Eikevik, EPT

Co-supervisor: Kazuhiro Hattori, Mayekawa MFG. Co., Ltd
Kousaku Nishida, Mayekawa MFG. Co., Ltd
Kengo Kagaya, Mayekawa MFG. Co., Ltd

Norwegian University of Science and Technology
Department of Energy and Process Engineering

NTNU

Norwegian University
of Science and Technology

Department of Energy
and Process Engineering

EPT-M-2017-62

MASTER THESIS

for

Student Martin Olafsen

Fall 2017

Optimization and Process Improvements of a High Temperature Heat Pump using Butane as Working Fluid

Optimalisering og prosessforbedringer av en høytemperatur varmepumpe med butan som arbeidsmedium

Background and objective

In the industrial applications it is a need for increasing the energy efficiency and reducing the use of oil and gas burners. One of the promising technologies is to introduce high temperature heat pumps to minimize the energy consumption and reduce the green house gas emissions. In this master thesis work, in cooperation with the Mayekawa company, it will be investigated a high temperature heat pump using butane as working fluids. The heat pump will use waste heat from industry and operate between temperature levels of 80°C to 160°C. At the high temperature side the heat pump will heat oil, to be used to produce steam. The future aim with the heat pump is to produce steam at 200°C. Initially the heat pump cycle is a standard one stage system with a three stage turbo compressor and an internal heat exchanger to avoid the compressor to enter the two phase region during compression. To further improve the COP for the process, it will be investigated to use either an ejector or a turbo expander.

The following tasks are to be considered:

1. Literature review of high temperature heat pumps, especially in transcritical operations
2. Development of a simulation tool for simulations and analysis
3. Optimization of the heat pump cycle, including process improving design
4. Comparing simulation results with measurements of prototype
5. Make a draft scientific paper of the main results in the thesis
6. Make proposal for further improvements of the system

-- " --

Within 14 days of receiving the written text on the master thesis, the candidate shall submit a research plan for his project to the department.

When the thesis is evaluated, emphasis is put on processing of the results, and that they are presented in tabular and/or graphic form in a clear manner, and that they are analyzed carefully.

The thesis should be formulated as a research report with summary both in English and Norwegian, conclusion, literature references, table of contents etc. During the preparation of the text, the candidate should make an effort to produce a well-structured and easily readable report. In order to ease the evaluation of the thesis, it is important that the cross-references are correct. In the making of the report, strong emphasis should be placed on both a thorough discussion of the results and an orderly presentation.

The candidate is requested to initiate and keep close contact with his/her academic supervisor(s) throughout the working period. The candidate must follow the rules and regulations of NTNU as well as passive directions given by the Department of Energy and Process Engineering.

Risk assessment of the candidate's work shall be carried out according to the department's procedures. The risk assessment must be documented and included as part of the final report. Events related to the candidate's work adversely affecting the health, safety or security, must be documented and included as part of the final report. If the documentation on risk assessment represents a large number of pages, the full version is to be submitted electronically to the supervisor and an excerpt is included in the report.

Pursuant to "Regulations concerning the supplementary provisions to the technology study program/Master of Science" at NTNU §20, the Department reserves the permission to utilize all the results and data for teaching and research purposes as well as in future publications.

The final report is to be submitted digitally in DAIM. An executive summary of the thesis including title, student's name, supervisor's name, year, department name, and NTNU's logo and name, shall be submitted to the department as a separate pdf file. The final report in Word and PDF format, scientific paper and all other material and documents should be given to the academic supervisor in digital format on a memory stick at the time of delivery of the Master Thesis.

☐ Work to be done in lab (Water power lab, Fluids engineering lab, Thermal engineering lab)
☐ Field work

Department of Energy and Process Engineering, October 13th 2017

Prof. Trygve M. Eikevik
Academic Supervisor
e-mail: trygve.m.eikevik@ntnu.no

Research Advisors:
Dr. Kazuhiro Hattori, Mayekawa MFG. Co., Ltd, e-mail: kazuhiro-hattori@mayekawa.co.jp
Dr. Kousaku Nishida, Mayekawa MFG. Co., Ltd, e-mail: kousaku-nishida@mayekawa.co.jp
Kengo Kagaya, Mayekawa MFG. Co., Ltd, e-mail: kengo-kagaya@mayekawa.co.jp

Preface

This master thesis was carried out at the Department of Energy and Process Engineering at the Norwegian University of Science and Technology (NTNU), in cooperation with Mayekawa MFG. CO., Ltd. In conjunction with the master thesis I attended an internship at the Research and Development center of Mayekawa, during the autumn 2017. The thesis investigates a transcritical high temperature industrial heat pump system using butane as working fluid. The system investigated corresponds to one which is being designed and tested by Mayekawa. Information received from Mayekawa has been vital, and is the main source of material used in this thesis.

I would like to thank my academic supervisor Trygve M. Eikevik for his advice and counsel. I would like to thank Dr. Kazuhiro Hattori, Vice Director of the Research and Development Center, who along with Professor Eikevik arranged the opportunity of my thesis, and internship at Mayekawa. At Mayekawa I would like to give special thanks to my co-advisor Dr. Kousaku Nishida, the leader of my work team there, who gave indispensable help during and after my internship and supplied vital information for this thesis. I would also like to thank my co-advisor Kengo Kagaya for his help and instruction while at Mayekawa. I am very grateful for the stay at Mayekawa and for the teachings I received there.

The prototype of the heat pump system was not completed and no practical measurements were prepared by the time I returned to Norway. Therefore no such measurements are included in the thesis, and no comparison between practical and simulation results is made. The main body of work of this thesis lies within creating and running the heat pump simulation, which required a significant amount of time.

Martin Olafsen
March 2018

Abstract

With the ability to recover waste heat from industrial processes there is a huge potential to reduce the ever increasing requirement for energy. Globally industry consumes over half of the energy used, and large part of this energy is demanded at high temperature. Industrial waste heat is often at too low temperature to be used effectively, due to high temperature demands in industrial processes. With industrial heat pump system waste heat can be recovered efficiently to create high quality heat. Using the waste heat the required amount of primary energy is reduced, which reduces the environmental impact of the heat production.

In this thesis a transcritical high temperature industrial heat pump is examined. A simulation of the heat pump is made in MatLab. The simulation is examined in a variety of working conditions such as: reduced supply water flow rate, variation of suction superheat and variation of discharge pressure in the transcritical area. The theoretical performance of the system is evaluated. It is found that the system is able to achieve the goal of delivering above 300 kW of heat when heating oil from 80°C to 160°C, while working at a COP of 4. It is further shown that heating up to 180°C is within the capacity of the system. Butane, a natural refrigerant, is used as the working fluid.

The largest improvement in performance is found when reducing the compressor rpm to 90% due to a large reduction in the compressor friction loss. At 90% rpm a COP of 4.7 is achieved, but at the expense of reduced butane flow rate and reduced amount of produced heat. The system is further adapted with an ejector. With the ejector implemented it is found that the system may achieve a theoretical COP of 4.7 while being able to deliver a large amount of heat.

Sammendrag

Med evnen til å gjenvinne spillvarme fra industrielle prosesses skapes et enormt potensial for å redusere det stadig økende kravet for energi. Globalt bruker industri mer enn halvparten av energien brukt, og stor del av denne energien kreves ved høy temperatur. Industriell spillvarme er ofte ved for lav temperatur til å kunne brukes effektivt, på grunn av de høye temperaturkravene i industrielle prosesser. Med industrielle varmepumpesystem kan spillvarme effektivt bli gjenvunnet for å lage høy kvalitets varme. Ved bruk av spillvarme reduseres behovet for primærenergi, som reduserer den miljømessige innvirkningen av varmeproduksjon.

In denne oppgaven blir en transkritisk høytemperatur industriell varmepumpe studert. En simulering av varmepumpen blir laget i MatLab. Simuleringen blir studert ved varierte arbeidsforhold som: redusert mengde tilførselsvann, variasjon i kompressor sugetemperatur, og variasjon i utslippstrykk fra kompressor i transkritisk område. Butan, som er en naturlig kjølevæske, brukes som arbeidsmedium. Den teoretiske effektiviteten av systemet blir evaluert.

Analysene viser at systemet er i stand til å oppnå målet om å levere mer enn 300 kW med varme, ved oppvarming av olje fra 80°C til 160°C, mens det oppnås en COP på 4. Det blir videre visst at systemet er i stand til å varme opp til 180°C. Den største forbedringen i effektivitet gjøres ved reduksjon i kompressorens turtall ned til 90%, på grunn av en stor reduksjon i friksjonstap. Ved 90% rpm oppnås en COP på 4.7, men det kommer på kostnad av reduksjon i massestrømmen av butan. Systemet får integrert en ejektor. Med ejektoren implementert viser analysen av system oppnår en teoretisk COP på 4.7, mens det er i stand til å levere en stor menge varme.

Contents

List of Figures

List of Tables

Nomenclature

Symbol	Meaning	Unit
Latin letters		
A	Area	[m^2]
c_p	Specific heat capacity	[kJ/kgK]
D	Diameter	[m]
f	Friction factor	[-]
g	Gravity	[m/s^2]
G	Mass flux	[kg/m^2s]
h	Enthalpy	[kJ/kg]
H	Height	[m]
k	Thermal conductivity	[W/mK]
L	Length	[m]
$\dot{m}$	Mass flow rate	[kg/s]
P	Pressure	[kPa]
$\dot{Q}$	Heat transfer	[kW]
R	Turns characteristic value	[-]
T	Temperature	[°C]
u	Velocity	[m/s]
U	Overall heat transfer coefficient	[W/m^2K]
V_s	Compressor displacement	[m^3/h]
$\dot{W}$	Work	[kW]
x	Gas quality	[-]
X_{tt}	Lockhard Martinelli Parameter	[-]
Abbreviations		
COP	Coefficient of performance	[-]
CFC	Chlorofluorocarbon	[-]
GWP	Global warming potential	[-]
HCFC	Hydrochlorofluorocarbon	[-]
HFC	Hydrofluorcarbon	[-]
HP	High pressure	[-]
IHX	Internal heat exchanger	[-]
ln	Natural logarithmic	[-]
LMTD	Logarithmic mean temperature difference	[-]
LP	Low pressure	[-]
ODP	Ozone depletion potential	[-]
Pr	Prandtl number	[-]
Re	Reynolds number	[-]
rpm	Rounds per minute	[-]
SGH	Steam Glow Heat Pump	[-]
tol	Tolerance	[-]
VHPC	Volumetric heat pump capacity	[kJ/m^3]
Greek letters		
α	Heat transfer coefficient	[W/m^2K]

δ	Wall thickness	[m]
ζ	Mixer characteristic value	[-]
η	Efficiency	[-]
λ	Volumetric efficiency	[-]
μ	Dynamic viscosity	[kg/ms]
ν	Kinematic viscosity	[m^2/s]
π	Pressure ratio	[-]
ρ	Density	[kg/m^3]

Subscripts

alt	Alternative	[-]
aux	Auxiliary	[-]
but	Butane	[-]
comp	Compressor	[-]
cond	Condenser	[-]
crit	Critical	[-]
d	Design	[-]
diff	Diffuser	[-]
dis	Discharge	[-]
ele	Element	[-]
eq	Equivalent	[-]
evap	Evaporator	[-]
g	Gas phase	[-]
gc	Gas cooler	[-]
h	Hydraulic	[-]
hp	Heat pump	[-]
in	Inlet	[-]
l	Liquid phase	[-]
m	Mean	[-]
max	Maximum	[-]
min	Minimum	[-]
mix	Mixer	[-]
noz	Nozzle	[-]
out	Outlet	[-]
ref	Refrigerant	[-]
sh	Superheat	[-]
suc	Suction	[-]
sys	System	[-]
w	Wall	[-]

1 Introduction

1.1 Background

With the ability to recover waste heat from industrial processes there is a huge potential to reduce the ever increasing requirement for energy. Globally industry consumes over half of the energy used, a large part of this energy is demanded at high temperatures. Industrial waste heat is often is often at too low temperature to be used effectively, due to high temperature demands in industrial processes. With industrial heat pump system waste heat can be recovered efficiently to create high quality heat. Using the waste heat the required amount of primary energy is directly reduced, which reduces the environmental impact of the heat production. Continual improvement of components improves the potential of high temperature heat pumps and increases the temperature and pressure limits. Heat pump systems have several advantages over the traditional boiler systems, such as increased process control and higher efficiency.

Beside the increasing energy requirements, there is an increasing demand on the environmental aspects of energy and heat production. In heat pump systems several traditional working fluids are being phased out, in favor for natural working fluid, with low to no environmental impact.

Mayekawa Global (Mycom) is a large, Japan based, international company with departments specialized within production of heat pumps and heat pump components. The end goal of the project is to produce a industrial high temperature transcritical heat pump, able to produce a large amount of heat at temperature up to 200°C, with a COP above 3.5. In this thesis one of Mayekawa's part-goals to create such a high temperature heat pump is examined. The heat pump system is mainly examined with heating oil in the 80°C to 160°C range. A brief examination of heating oil from 100°C to 180°C is made.

1.2 Objective

The objective of this thesis is to create a heat pump simulation of a high temperature heat pump system. Using the simulation various conditions will be tested, and the performance of the heat pump will be evaluated. The system is further adapted with an ejector, and the solution is evaluate whether or not it is a viable improvement of the system.

The results made should not necessarily be viewed as strict conclusions, but rather indications of performance and feasibility of the cases examined.

1.3 Outline of thesis

Chapter 2 gives a presentation of high temperature heat production options. The main focus is on heat pump systems. Some current commercially available high temperature heat pumps are presented.

Chapter 3 presents relevant theory about heat pump systems, including transcritical systems, working fluids and ejectors.

Chapter 4 presents general characteristics of the components used in the project and the heat pump simulation.

Chapter 5 briefly presents the case and the working conditions of the heat pump system.

Chapter 6 presents theory, correlations, and relevant information to simulate the individual parts of the heat pump system.

Chapter 7 describes the system configurations and procedure of the heat pump simulation.

Chapter 8 presents the results found in the various simulations.

Chapter 9 presents how the simulation model is adapted to include an ejector. Relevant theory, equations and efficiencies are presented, along with the procedure of the simulation. Results from the adapted ejector system are presented.

Chapter 11 compares and discusses the previously presented results.

Chapter 12 gives a conclusion of the thesis and suggestions for further work.

2 High Temperature Industrial Heat Pumps

A heat pump is a device that increases the temperature of low quality heat to a higher temperature. The goal of using an industrial heat pump is to design it such that the benefits of using waste heat exceeds the cost of driving the heat pump. High temperature industrial heat pumps are a set of systems which deliver heat at high temperatures at large capacity. Industrial heat pumps work in the medium and high power range, above 50 kW. They are used for heat recovery and heat upgrading in industry, and also for heating, cooling and air-conditioning in buildings, as well as for district heating [Jakobs, 2010]. In industry the industrial heat pumps can either be used for process heating or preheating. In general they improve the energy efficiency of industrial processes, and reduce the primary energy consumption [Soroka, 2007].

2.1 Industry usage

More than 80% of the total energy use in industry consists of the need of heat in the form of steam at different pressure levels and for firing furnaces [Kleefkens and Spoelstra, 2014]. Industrial heat pumps should be able to produce heat in the range of 100°C to 250°C, the temperature lift should preferably be up to 100°C. The purpose of the heat produced of high temperature heat pumps varies greatly upon the temperature produced. The potential for heat pumps in various industries can be assessed based on the required temperature level and the amount of energy consumed at the temperature. In Germany, at temperatures above 140°C there is a large potential in food industry for reducing the cost of pasteurization, sterilization, drying and evaporation.There is also a large potential in the chemical industry, shown in figure 1 [Wolf et al., 2012].

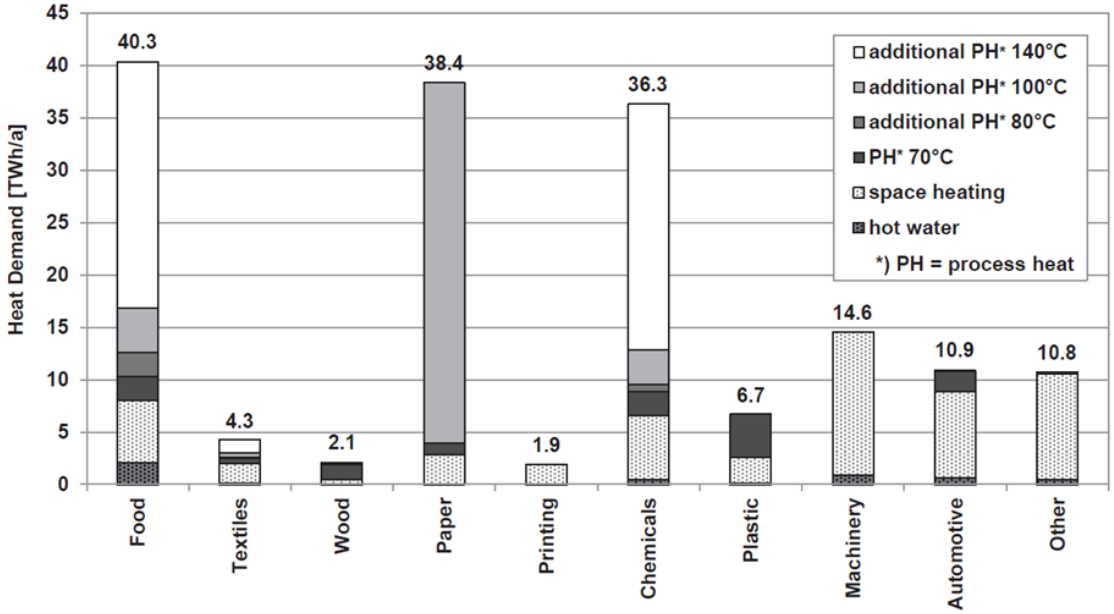

Figure 1: Potential for heat pumps in German industry

Recoverable waste heat and process heat at moderate temperatures is found in food processing, paper and pulp, refineries and chemical industry. Above 100°C it is mainly chemical,

petrochemical, metal production and some paper processes which require large amounts of heat, shown in figure 2 [Lauterbach et al., 2011].

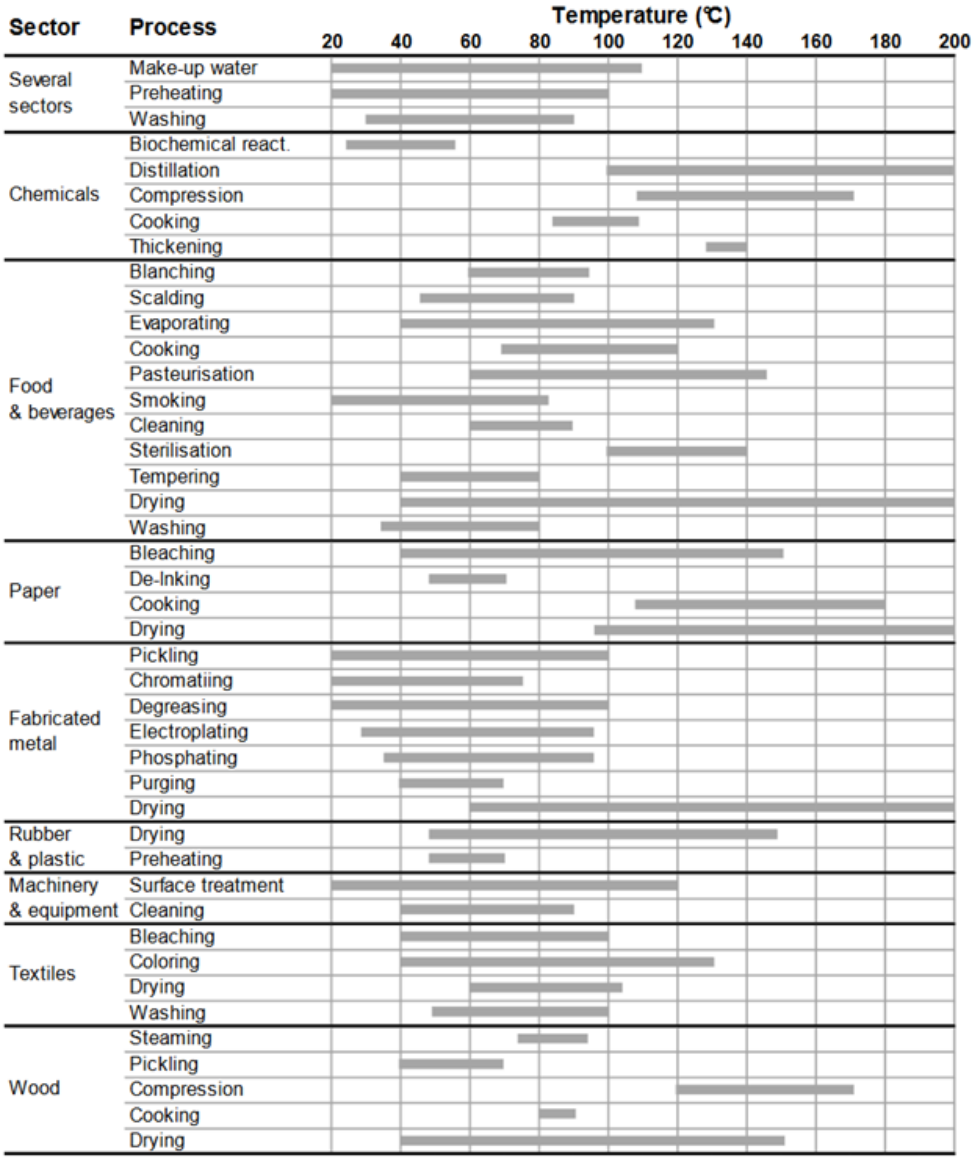

Figure 2: Typical temperature range of common industrial processes

2.2 Current technology

2.2.1 Steam boilers

The most used and most conventional method of steam generation is to heat the water by boilers. Boilers typically run on fuels such as oil, gas, coal, wood, and waste, or use heat sources such as solar, nuclear or electrical energy. There are also indirect systems which run by recovering heat from processes or equipment such as gas turbines and diesel or gas engines [Parsons, 1992].

Typically in a steam boiler fuel is burnt in a furnace and hot gas is produced. The heat

is then transferred from the gas to the water. There are two main types of steam boilers: fire tube and water tube boilers. In fire tube boilers there are a number of pipes through which hot gas from the combustion chamber passes. Surrounding these tubes is a reservoir of water. In water tube boilers there is water in tubes being heated by surrounding hot gas. With fire tube boilers the steam is limited to low pressure as the water and the steam is contained in the same reservoir. Water tube boilers are more expensive, but allows for larger heating surface and higher pressure steam can be produced [Malmcom, 2016].

The efficiency of a steam boiler is defined as how large part of the heat supplied by the fuel is delivered to the steam as it leaves the boiler. Contrary to the efficiency of heat pumps, this efficiency can never be greater than 1 for boilers. The boilers are illustrated in figure 3 [Brain, 2008] .

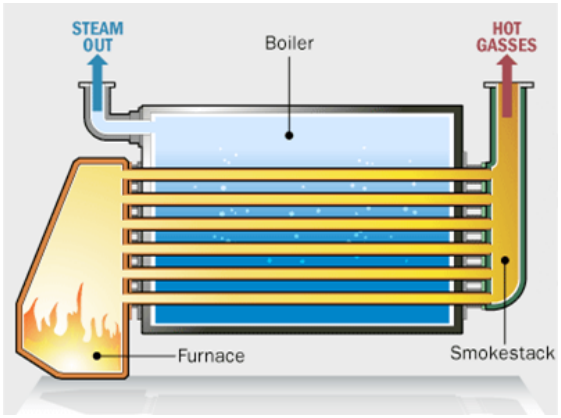

(a) Fire tube boiler

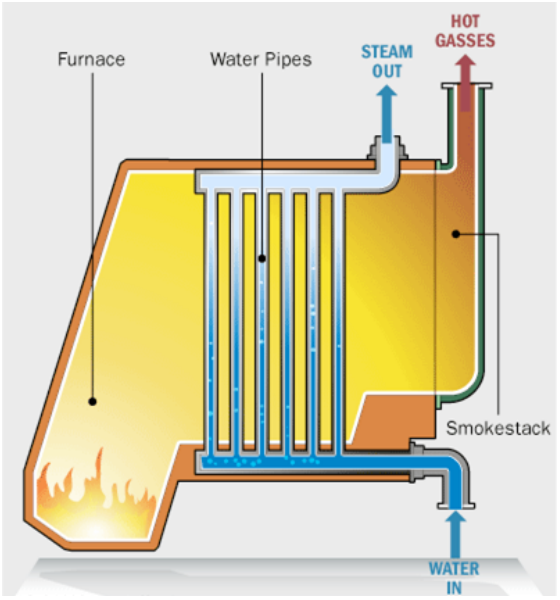

(b) Water tube boiler

Figure 3: Illustration of steam boilers

2.2.2 Heat recovery

A common byproduct of high temperature industrial process is condensate. Typically this condensate contains low quality heat, but it may still be a large reserve of energy. The heat can either be used directly in a heat exchanger to heat air, fluid or a process, or the quality of the heat can be improved. One of the ways to improve the quality is to use the enthalpy of the liquid to flash some of the liquid to steam at lower pressure. The flash steam can be used to heat air, water, or other liquids or it can be used directly in processes with lower pressure steam requirements. In a flash tank/drum partial evaporation occurs when the pressure of saturated liquid is reduced. The pressure is lowered over an expansion valve.

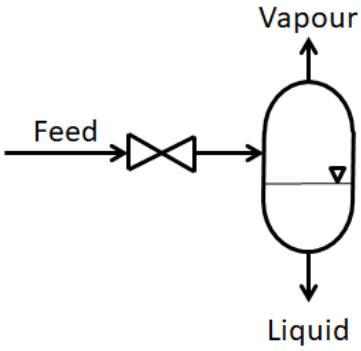

Figure 4: Illustration of a flash drum

If the temperature of the condensate is below 100°C it will require reheating to regenerate steam. The condensate can be used directly with relatively high efficiency to heat domestic hot water with a shell-and-tube or a plate-type heat exchanger. [Parsons, 1992]

2.2.3 Industrial heat pumps

There are several advantages to using heat pump systems instead of the traditional boiler systems:

- Lower environmental impact
- More cost-efficient
- May utilize otherwise wasted process heat
- Allows for higher process control
- Reduces emission of pollutants

The main disadvantages are:

- Limited temperature range
- Complex systems, which may restrict where they can be installed
- High investment cost

Industrial heat pumps examples are closed cycle vapor compression(CCC), open cycle mechanical vapor recompression(MVR), thermal vapour recompression (TVR), absorption heat pumps and lithium bromide (LiBr) heat transformers [Kleefkens and Spoelstra, 2014]. The different systems are adapted to different conditions and temperatures, these along with estimations of COP is shown in table 1.

IHP type	COP	Maximum sink temp. [°C]	Maximum temp. lift [°C]
CCC	3 - 8	120	80
MVR	5 - 30	190	90
TVR	1.2 - 3	130	40
Absorption I	1.6 - 1.7	100	50
Heat Transformer	1.6 - 1.7	150	60

Table 1: COP and temperature levels of various IHP systems

2.2.4 Closed cycle compression

The typical heat pump. Consists of a working fluid which moves in a cycle. The working fluid receives heat at low temperature in the evaporator, is compressed and pumped to the condenser, where it delivers heat at high temperature.

The CCC system is explained more closely in the theory chapter.

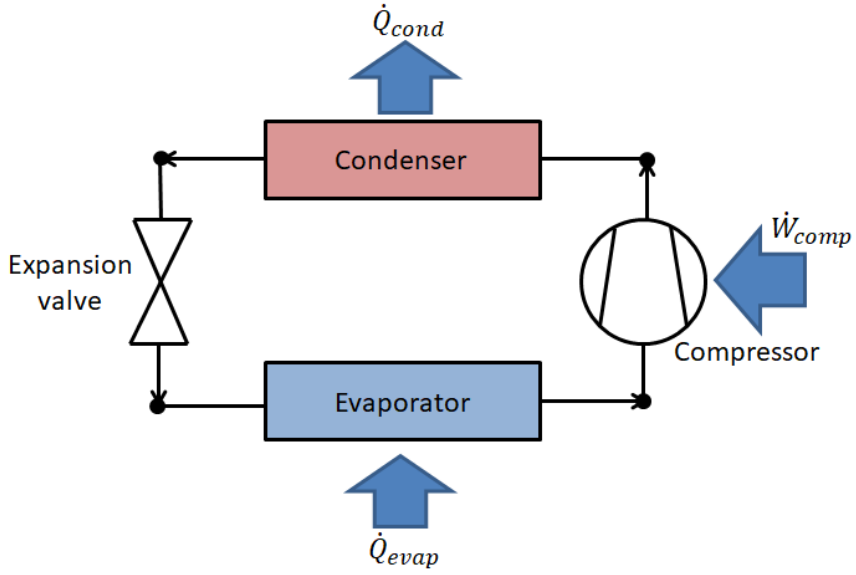

Figure 5: Principle sketch of a CCC system

2.2.5 Open cycle mechanical vapour recompression

In this process the pressure of waste gas in increased, and in the process the temperature is increased. The most common vapour compressed is steam. After being compressed the waste vapour condenses in a heat exchanger, delivering heat to at high temperature. The most important design aspect in MVR systems is the choice of compressor [Soroka, 2007].

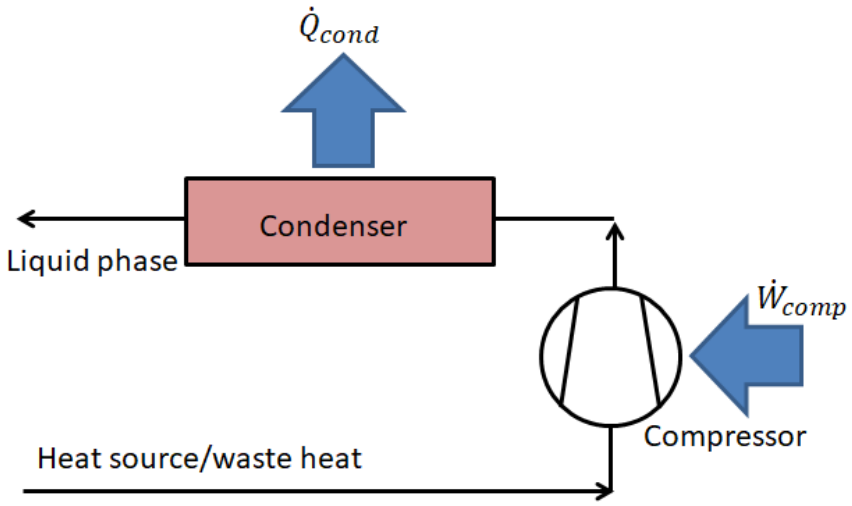

Figure 6: Principle sketch of a MVR system

2.2.6 Thermal vapour recompression

In TVR systems the work is done by an ejector and high pressure vapour. This system is often called an ejector. This system is driven by heat, not mechanical energy. This allows for new application areas, for example where there is a large difference between fuel and electricity prices.

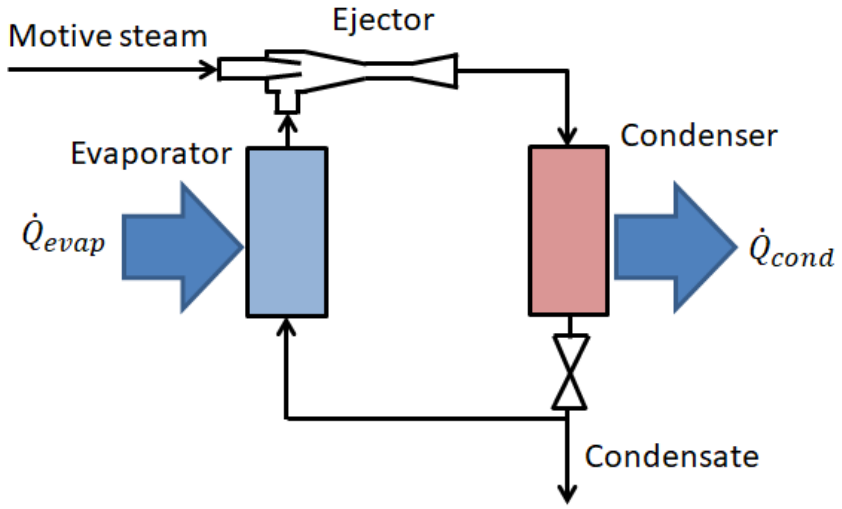

Figure 7: Principle sketch of a TVR system

The TVR system has a modest COP, but it is reliable, has relatively low investment cost and has low to no cost of usage.

2.2.7 Absorption Heat Pump

Absorption heat pumps use the principle that the boiling point for a mixture is higher than for the corresponding pure, volatile fluid. According to [U.S. Department of Energy,

2003] absorption heat pumps can deliver large temperature lifts. There are two kinds of absorption systems: absorption heat pumps and and heat transformers. The difference between the two systems is the pressure level in the four main heat exchangers (evaporator, absorber, desorber and condenser) [Soroka, 2007]. The only absorption system used in industrial application uses a combination of lithium bromide and water. This system allows for temperature up to 100°C. An example of a absorption system is shown in figure 8 [U.S. Department of Energy, 2003].

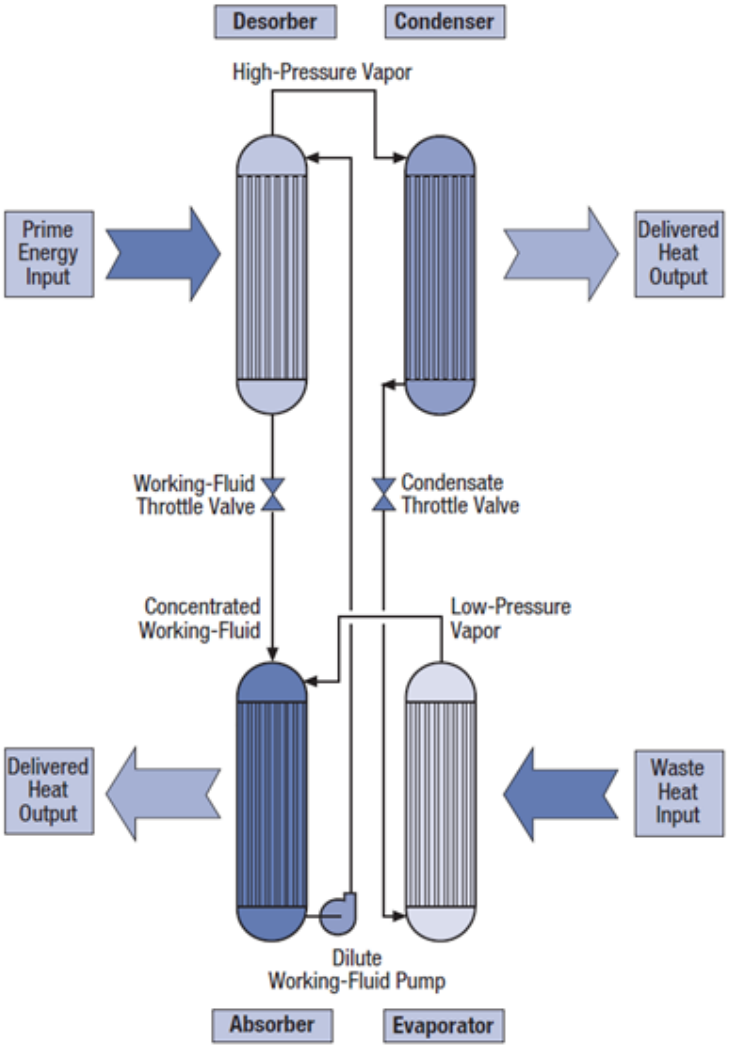

Figure 8: Principle sketch of an absorption system

2.3 Next generation systems

2.3.1 Working fluids

The main reason for the limited temperature range of several heat pumps solutions has been the working fluids. Especially when using condensers there is a demand for a high critical temperature to be able to run the system efficiently, while also enabling the delivery of heat at high temperature. In addition there is the demand of safety, low GWP and low ODP. According to [Kleefkens and Spoelstra, 2014] four ideal working fluid are identified, all of

which have the required qualities for subcritical high temperature systems.

Working fluid	T_{crit}[°C]	Flammable or toxic	ODP	GWP
R1233zd	166	No	0.0003	6
R1336mzz	171	No	0	9
LG6	>165	No	0	1
MF2	>145	No	0	<10

Table 2: Ideal working fluids

2.3.2 Thermoacoustic heat transformer

The dynamics and working principle of the thermoacoustic system is quite complex, however the implementation of the system is relatively simple. The system converts heat to acoustic power which then can pump heat up to higher temperature levels. The system is environmentally friendly and has no moving parts. The system may be implemented into the existing system at an industrial site. The acoustic power can alternatively be transformed into electrical power [Karlsson et al., 2016]. The system is illustrated in figure 9 [Kleefkens and Spoelstra, 2014].

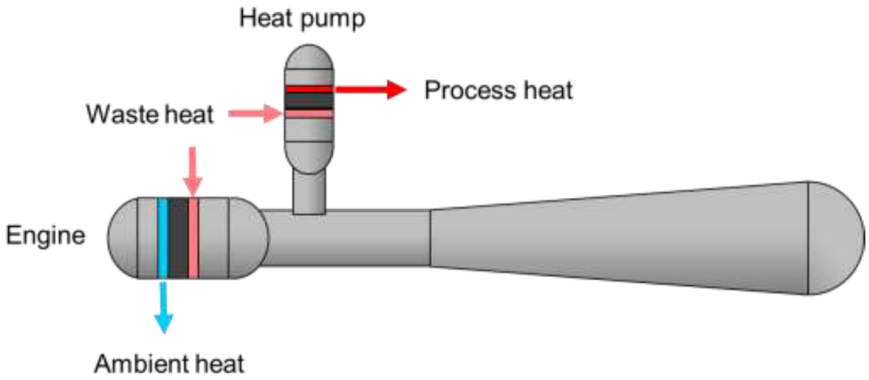

Figure 9: Principle sketch of thermoacoustic heat transformer

2.3.3 Hybrid heat pumps

Hybrid heat pumps use a combination of compression and absorption to run the heat pump cycle. A hybrid heat pump can improve several features of normal vapour recompression heat pump. The hybrid system is more flexible regarding temperature on both the heat source and sink side, has more precise capacity control and can improve the COP at high gliding temperature when using secondary fluids. Several forms of hybrid heat pumps are developed so far, an example is shown in figure 10 [Kim et al., 2013]. Hybrid systems deliver heat at up to 250°C, with a temperature lift of at least 50 K. System effectiveness is above 25%, and in total the electrical COP is on average above 5 [Kleefkens and Spoelstra, 2014].

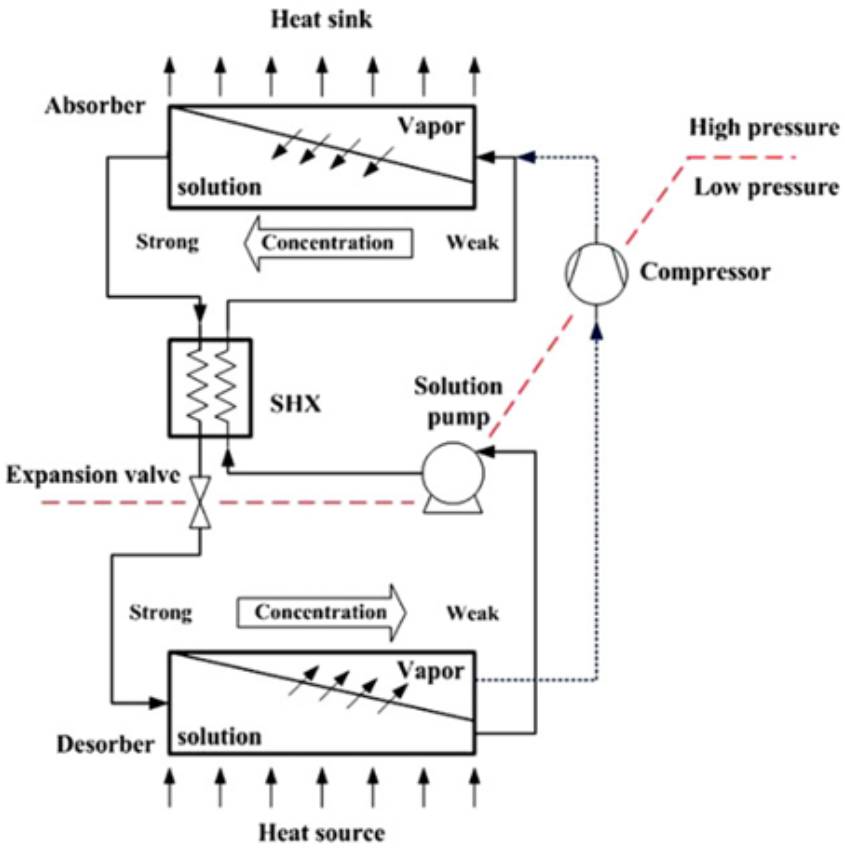

Figure 10: Principle sketch of a hybrid heat pump system

2.4 High temperature heat pump examples

2.4.1 Viking Heat Engines

A Norwegian company, Viking Heat Engines, have had promising pilot tests of their high temperature heat pump, The HeatBooster. While delivering heat above 150°C a COP close to 3 was achieved. The results were made using a heat source at 90°C, meaning a temperature lift of 60 K. The heat pump has been shown to deliver heat at up to 160°C. The HeatBooster is delivered commercially and is delivered in the 200 kW size. Viking Heat Engines have plans to release the heat pump commercially in the megawatt range in 2019 [Viking Heat Engines, 2017].

2.4.2 Kobe Steel

In 2011 the Steam Grow Heat pump (SGH) was co-developed by Kobe Steel, LTD. and electric companies in Japan. Two systems were designed one for steam supply temperature of 120°C (SGH120), and one for steam supply of 165°C (SGH165) [Kaida et al., 2015]. In design there was focus on efficient use of unused thermal energy by waste heat recovery and upgrading, and reduction of dissipation heat loss by placing the system close to processes in distribution arrangement. In addition it was deemed important to enhance the reliability of the system, while maintaining high efficiency and low initial cost.

The SGH120 is composed of a heat pump unit and a flash tank. The source water is received at 35-70°C. Heat is sent from the source water to pressurized circulating water. In the flash tank the pressurized water is decompressed and evaporated. The flash steam produced (up to 120°C, 0.1 MPaG) is supplied to various processes, while the remaining saturated water is sent back to the heat pump unit.

The SGH165 has a steam compressor in addition to the system described for the SGH120. To avoid superheat of the discharge steam, water is injected into the compressor. The SGH165 may produce discharge steam up to 175°C, 0.8MPaG. When producing the design temperature of 165°C, a COP of 2.5 is achieved [Watanabe et al., 2014].

For the SGH120 the refrigerant R245fa is used, while a mixture of R134a and R245fa is used for the SGH165. Due to the high pressure ratio and temperature compared to existing heat pumps, a newly developed screw compressor is equipped.

For the SGH165 [Kaida et al., 2015] concluded: it is more important to secure higher heat source temperature than feed water temperature. The system COP was the highest when working on full load. It was found that the COP was insufficient for a wide range of heat source water temperatures. Additionally it was reported that while working on part load that the COP_{hp} was approximately twice the COP_{sys}. The SGH165 has to use a steam compressor in addition to the heat pump compressor when finding COP_{sys} which inflates the power required by the system as a whole when compared to the heat pump itself. The system is illustrated in figure 11 [Watanabe et al., 2014].

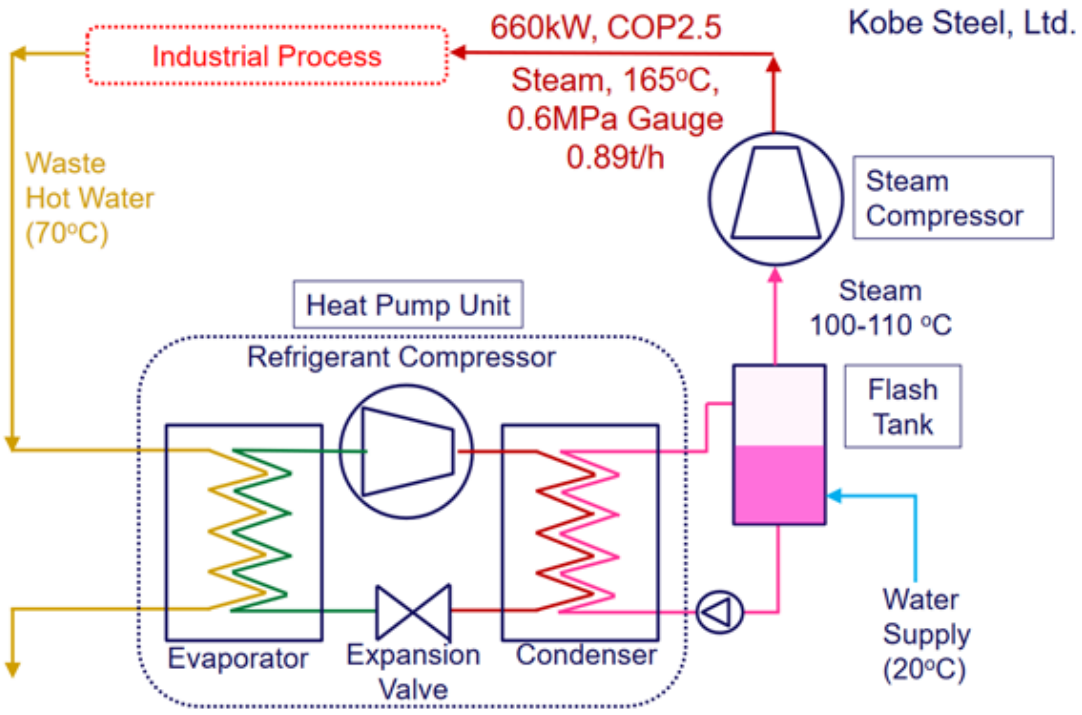

Figure 11: Kobe Steel SGH165 overview

2.4.3 Mayekawa pentane heat pump

Mayekawa has developed a heat pump able to produce steam at 150°C with a COP above 3 [Mugabi et al., 2014]. Pentane was chosen as the working fluid as it is a natural refrigerant

with a low environmental impact, while still being able to produce a high COP. Pentane has a critical temperature of 196.4°C. PAG oil was used as lubricant because of its thermal and chemical stability at high temperature levels, in addition PAG oil can supply sufficient viscosity up to high temperatures. An evaporation temperature of 80°C and a condensing temperature of 160°C was used. The system used a screw compressor which could be used at high temperature levels [Mugabi et al., 2014]. The system is illustrated in figure 12 [Mugabi et al., 2014].

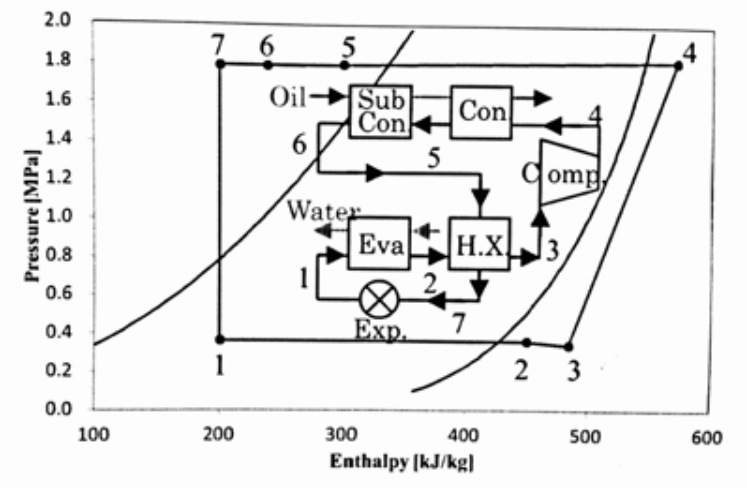

Figure 12: Mayekawa pentane industrial heat pump log P-h diagram

3 Theory

3.1 Closed cycle compression

A basic heat pump cycle consists of four components. A compressor, a condenser, an expansion valve, and an evaporator.

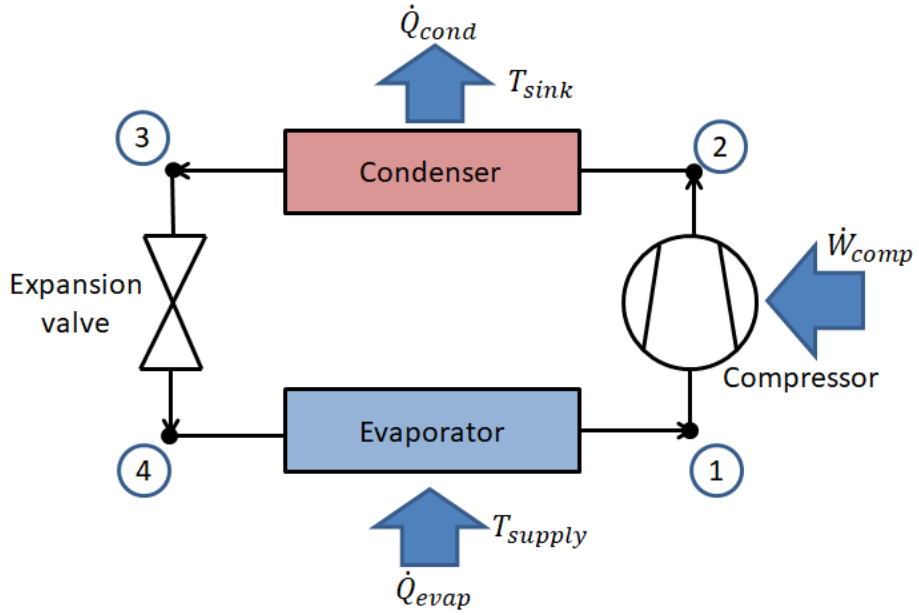

Figure 13: Principle sketch of a heat pump cycle

The compressor runs the cycle. An engine receives electrical power which it transforms into mechanical power and delivers to the compressor ($\dot{W}_{\text{comp}}$). The compressor sucks low pressure gas out of the evaporator, and releases high pressure gas into the condenser. As the compressor sucks gas out of the evaporator it maintains the evaporation pressure. In the condenser the working fluid condenses, and releases heat ($\dot{Q}_{\text{cond}}$) at high temperature to a heat sink. The temperature is decided by the condensing pressure and the working fluid. The now liquid working fluid passes into the expansion valve. Over the valve the pressure of the working fluid is reduced back to evaporation pressure. With the pressure reduced, the working fluid enters the evaporator, where it receives heat ($\dot{Q}_{\text{evap}}$) at low temperature and evaporates, before it again enters the compressor as gas.

Ideal compression is isentropic. An isentropic process assumes that the process is both adiabatic and reversible. Which means that there is no friction and no transfer of heat out of the system. The work done during such a process is the minimal work or the Carnot work. In a real system there will always be several losses, both in the compressor, and in the other components.

To measure the effectiveness of a heat pump process there is the coefficient of performance(COP). COP is a dimensionless quality which states how much useful heat is received from the process, compared to the amount of electricity applied. COP can be defined for both heating or cooling. In this thesis the interest is only in heating. Two different COPs are defined:

$$COP_{hp} = \frac{\dot{Q}_{cond}}{\dot{W}_{comp}} = \frac{\dot{Q}_{evap} + \dot{W}_{comp}}{\dot{W}_{comp}} \tag{1}$$

$$COP_{sys} = \frac{\dot{Q}_{cond}}{\dot{W}_{sys}} = \frac{\dot{Q}_{cond}}{\dot{W}_{comp} + \dot{W}_{aux}} \tag{2}$$

$\dot{W}_{aux}$ is auxiliary power used to run the cycle. COP_{hp} expresses the COP of the heat pump itself. The only power used by the heat pump is in the compressor. COP_{sys} expresses the COP of the whole system, this means that all electrical power used is included. When COP is referred to in this thesis it means COP_{hp}.

3.2 Transcritical cycles

In a transcritical cycle the working fluid is compressed up to a pressure beyond the critical pressure of the working fluid. In such a system the working fluid is not condensed at high pressure, instead it is cooled at transcritical pressure in a gas cooler. The heat from the working fluid is extracted over a range of temperature, with a variable heat capacity. Because of this temperature span, the process is well suited for heating over a gliding temperature, contrary to subcritical heat pumps, where condensation occurs at constant temperature. For example, by heating water or oil which enters at a relatively low temperature and leaves at high temperature, it is possible to extract a large amount of heat out of the working fluid in a transcritical heat pump. CO_2 is the most common working fluid in transcritical heat pumps. CO_2 is for example well suited for hot water heating up to 60-80°C. A T-s diagram of a transcritical CO_2 is shown in figure 14.

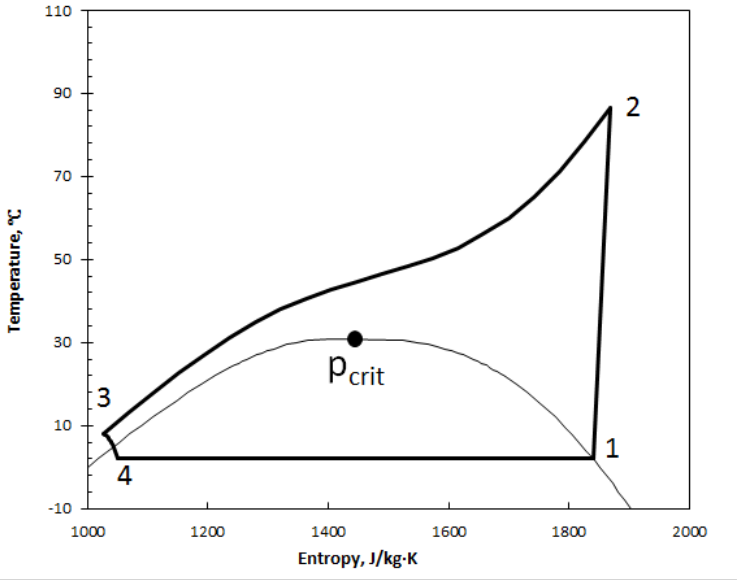

Figure 14: Transcritical CO_2 heat pump cycle shown in Ts-diagram

If the heat sink is at constant temperature, it is most advantageous to have a subcritical system, which delivers heat at a constant temperature. If the temperature of the heat sink

varies, it is beneficial to have a system which delivers heat at a variable temperature. In either case the goal is to achieve a sufficiently large temperature gap, while at the same time not producing an excess of temperature which reduces the efficiency of the system. In a transcritical cycle it is of high importance to extract as much heat as possible before sending the working fluid through the expansion valve. If it isn't possible to cool the working fluid sufficiently before expansion the performance is drastically reduced, due to the throttling loss when reducing the pressure. Around the critical point there is rapid change of properties of working fluids in that area relatively small changes in pressure and temperature may yield large changes in the amount of heat extracted.

At high temperature and relatively low pressure (while in transcritical conditions) the behaviour of working fluids can be compared to a gas, or steam. While at relatively low temperature (above critical point) working fluids behaves more like a liquid. This has a large impact on for example the heat transfer coefficient and specific heat capacity. Meaning that the temperature and choice of pressure has a large effect on the gas cooler performance. In transcritical conditions, if pressure is increased the fluid takes on properties more similar to that of liquids. This means that the viscosity increases, the Reynolds number is reduced, and therefore the heat transfer coefficient is reduced. There is also the consideration of temperature; a higher discharge pressure generally means a higher discharge temperature, which indicates that more heat can be extracted from the working fluid at high temperature.

[Sarkar et al., 2007] examined the optimization of compressor discharge pressure in transcritical cycles. It was found from performance analyses that an optimum compressor discharge pressure exists, where the cycle achieves the greatest COP. The optimum discharge pressure depends upon evaporation temperature, gas cooler exit temperature, internal heat exchanger efficiency and compressor isentropic efficiency. It was found that the gas cooler exit temperature has a greater effect than evaporation temperature on optimum pressure for ammonia, propane and isobutane (n-butane was not examined). Lower evaporation temperature yields higher optimum discharge pressure due to divergent nature of the constant entropy lines [Sarkar et al., 2007]. The results is shown in figure 15.

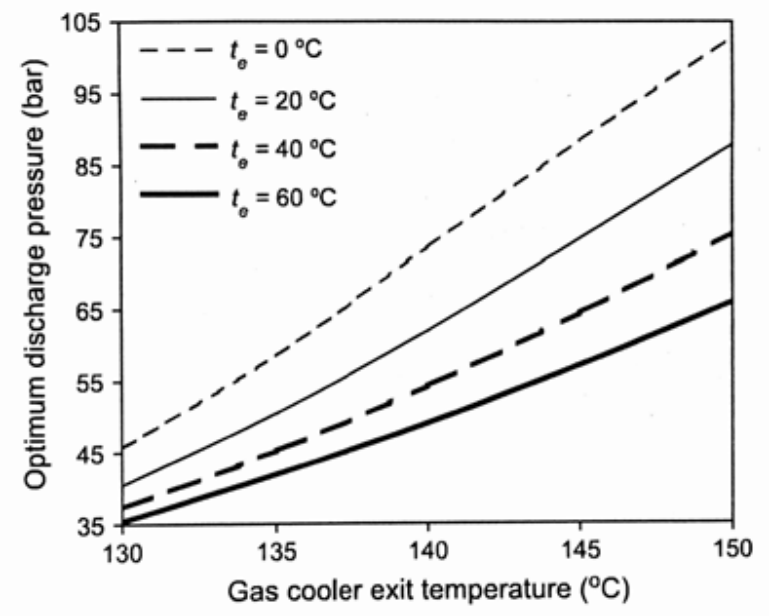

Figure 15: Variation of optimum discharge pressure for a transcritical isobutane cycle

3.3 Working fluids

The choice of working fluid in a heat pump has a large impact on the overall performance and on the overall COP. The ideal working fluid should be non-flammable, non-toxic, should have a low GWP, no ODP, and a high critical temperature [Kleefkens and Spoelstra, 2014]. As different working fluids have different thermodynamic and physical properties, it is important to select one with fitting properties for the cycle. The heat of evaporation of the working fluid effects the amount necessary to circulate in the cycle. This directly effects the necessary diameter of the pipes, the capacity of the compressor and the size of the heat exchangers, which all together has a large impact on the cost and the design of the system. Not only efficiency has to be considered, but several criteria. Among the most important criteria are [Eikevik, 2016]:

- Safety
- Reliability
- Suitable thermodynamic and physical properties
- Environmental impact
- Price and availability

The fluid needs to be stable, and to not corrode the material of the heat pump. In cases where oil is used in the system, the working fluid needs to be compatible. Since the 1980s the choice of working fluids has been influenced by environmental impact [Eikevik, 2016]. Both the effect on the ozone depletion and the greenhouse effect is being considered. Chlorofluorocarbons (CFCs) were banned from the market in 1987. Hydrofluorocarbon (HFCs), with an ozone depletion potential (ODP) of zero, became popular and have been widely used. However, HFCs have been shown to have large global warming potential (GWP), therefore legal regulations have been created to decrease the usage of fluorinated greenhouse gases. The EU regulation on F-gases states that the amount of HFCs on the European market will be gradually reduced, by 2030 the amount of HFCs on the market is to be reduced by 79% [Eikevik and Hafner, 2016].

With the regulation in the place the usage of the "natural five" has been increasing. Air, water, CO_2, ammonia and hydrocarbons are all fluids with low to no environmental impact [Mayekawa, 2009]. With proper usage and newer technology these working fluids have been found to be able to compete with the previously used environmentally harmful working fluids.

3.3.1 Butane

The chemical formula for butane is C_4H_{10}. This may refer to n-butane(normal butane) and isobutane. n-butane has the carbon atoms linked in a straight line, while isobutane is branched and is created from n-butane. In context of this thesis butane refers to n-butane. Butane is commonly used as a fuel, propellant and refrigerant. Butane is a gas at room temperature and atmospheric pressure. It is highly flammable, colourless, and easily liquified.

	t_{crit}	P_{crit}	ODP	GWP	Safety group	Autoignition temperature
Butane	152.0°C	3 796 kPa	0	15	A3	365°C

Table 3: Characteritics of butane

Butane is as all hydrocarbons highly flammable. This creates several demands to the facilities when using large amounts of butane in heat pump cycles. Specifically there needs to be proper ventilation, along with sufficient gas detection systems in place. The temperature of the working fluid should be kept at minimum 100°C below autoignition temperature.

Butane has relatively low viscosity compared to other working fluids. This is an advantage in the heat pump cycle, as it reduces the pressure loss produced in the components. This is noticeable in the pipelines, and in the various heat exchangers. At higher pressure cycles the pressure loss typically increases, meaning that low viscosity is more advantageous in transcritical cycles. In figure 16 the viscosity of several common working fluids at varying temperature are compared, with butane having the lowest viscosity.

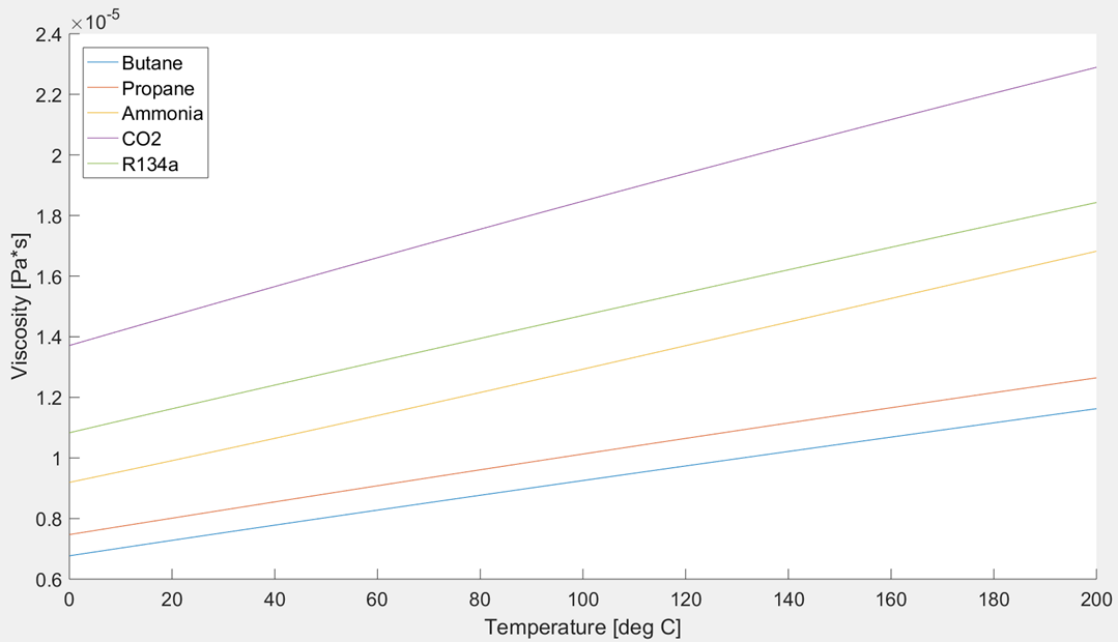

Figure 16: Viscosity of several working fluids, depending on temperature

When choosing the temperature and pressure level of the transcritical heat pump cycle it is important to keep in mind the variation of heat capacity. It is not necessary that a higher discharge pressure(which leads to higher discharge temperature) leads to a higher efficiency or larger amount of delivered heat. Depending on the temperature of the heat sink, some pressure is going to be more efficient, this should be considered when designing the system and choosing the compressor discharge pressure.

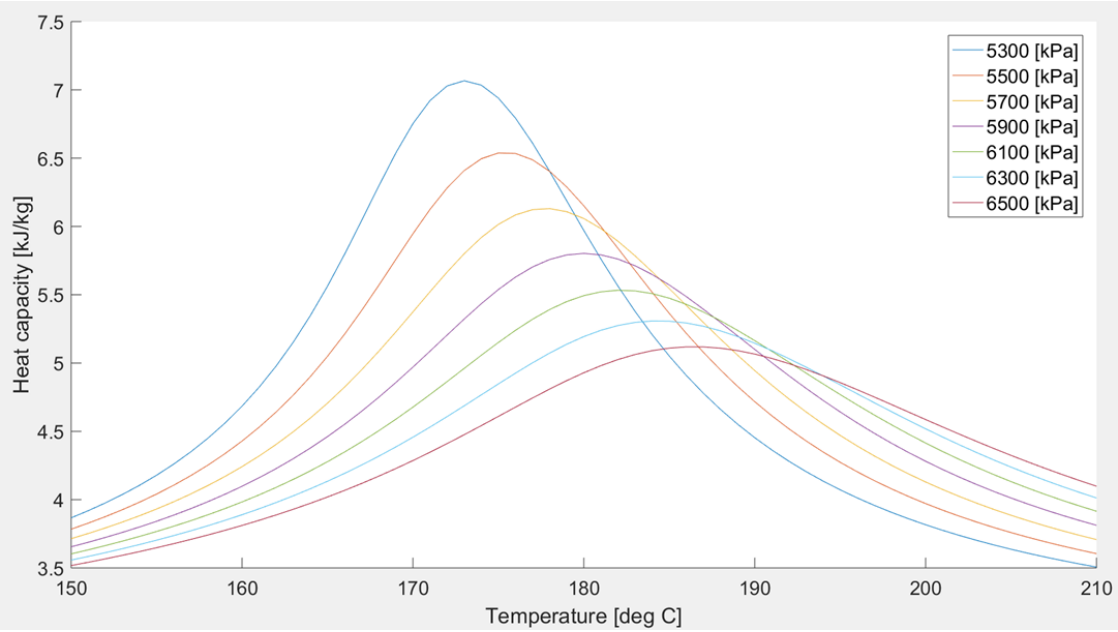

Figure 17: Heat capacity of butane at varying transcritical pressure

Figure 17 shows the heat capacity of butane at varying transcritical pressure, and temperature. The sum of the heat capacity is higher at lower pressure, but when increasing the pressure, the heat capacity peak is moved towards higher temperatures. Heat capacity at high temperature is more valuable. Depending on the requirements of the system the ideal gas cooler pressure will vary. The point at which highest heat capacity is achieved at a transcritical pressure is the pseudo-critical point. It's at the point defined by pseudo-critical temperature which corresponds to a pseudo-critical pressure, shown by the peaks in figure 17. Figure 18 shows the ts diagram of butane with constant pressure lines.

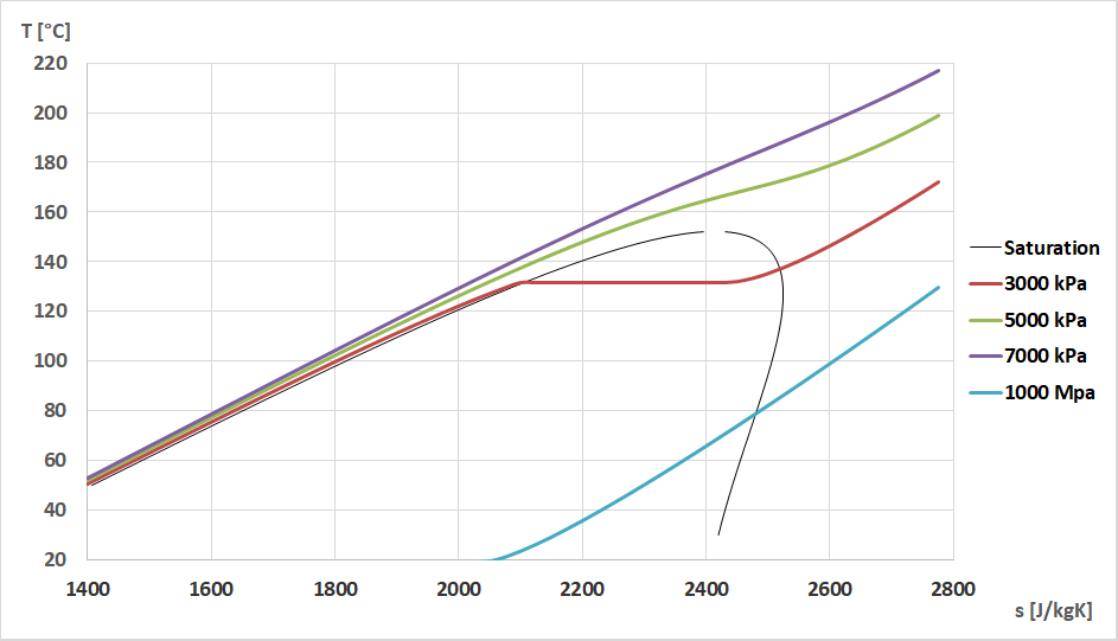

Figure 18: Shows the ts diagram of butane at varying pressure

3.4 Ejector System

In an ejector system the expansion valve is replaced by an ejector. The ejector allows the system to utilize the expansion loss to lift the suction pressure of the compressor. An ejector works by using conversion of pressure to kinetic energy. An ejector consists of four main sections: nozzle, suction, mixer and diffuser, as shown in figure 19.

Motive supercritical gas enters the motive nozzle. In the nozzle there is a large increase in velocity, as well as a large pressure reduction. The gas from the evaporator enters through the suction nozzle. The much higher velocity of the motive flow causes a suction of the suction flow. The two flows join together in the mixing chamber, in the mixer a series of shock waves occur. After the mixer the stream enters the diffuser where pressure is increased and velocity is reduced. In the diffuser the reverse of the motive nozzle happens. Kinetic energy in form of velocity is converged to higher internal energy. The internal energy of the suction flow is increased, and importantly the pressure at the outlet of the ejector is higher than the suction pressure.

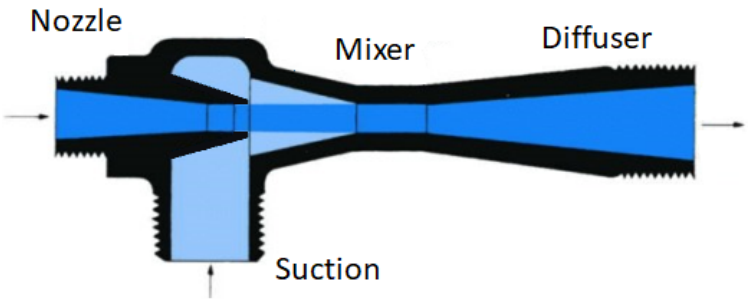

Figure 19: Illustration of an ejector

Since the pressure of the flow from the suction is increased the required pressure ratio of the compressor is reduced. This reduces the necessary amount of work, and will usually increase system performance along with COP. The potential mass flow of the compressor is also usually increased, as pressure ratio and mass flow of compressors normally are inversely correlated. Higher mass flow increases the potential heat delivered by the heat pump.

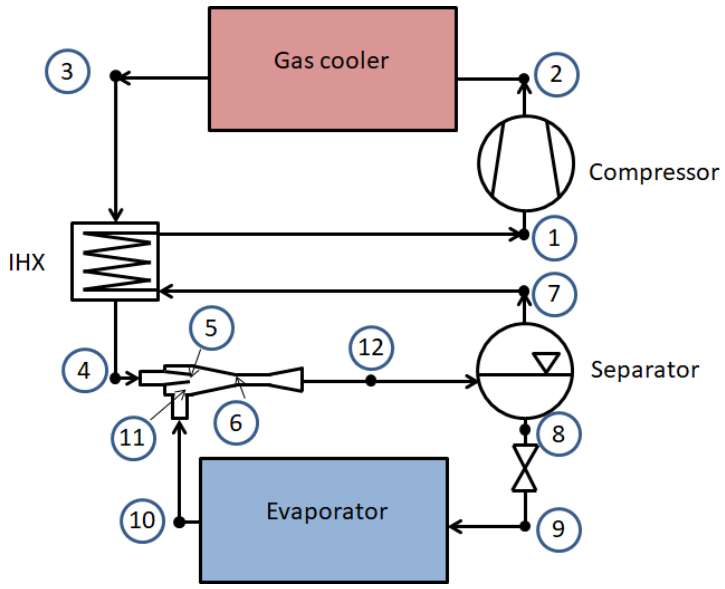

Figure 20: Principle model of the heat pump cycle with ejector

3.4.1 Equations

The equations used to solve the ejector are mainly variations of conservation of energy, mass and momentum. These are used over the different sections of the ejector which act as control volumes. Energy and mass conservation are used freely over the control volumes, while the momentum equation requires the efficiency of the control volume to be 100%.

Energy conservation

$$\sum \left(h + \frac{u^2}{2}\right)_{in} = \sum \left(h + \frac{u^2}{2}\right)_{out} \tag{3}$$

Mass conservation

$$\sum \left(\rho \cdot A \cdot u\right)_{in} = \sum \left(\rho \cdot A \cdot u\right)_{out} \tag{4}$$

Momentum conservation

$$\sum \left(u \cdot \dot{m} + P \cdot A\right)_{in} = \sum \left(u \cdot \dot{m} + P \cdot A\right)_{out} \tag{5}$$

3.4.2 Efficiency

As stated previously, each of the four sections of an ejector has a separate efficiency. Most of the research regarding ejectors are done on CO_2 system. [Liu and Groll, 2013] reported on the ejector efficiency in several systems with various working fluids and found that ejector efficiency vary on the ejector geometry and operation conditions. The efficiencies of the controllable motive nozzle, suction nozzle and mixing section were found to range from 0.50

to 0.93, from 0.37 to 0.90, and 0.50 to 1.00, respectively. Figure 21 shows relevant efficiencies found [Liu and Groll, 2013].

Authors	Fluid	η_m	η_s	η_{mix}	η_d
Keenan et al. (1950)	Air	1.0	1.0		
Alexis and Rogdakis (2003)	Water	0.7			0.8
Sun (1996)	LiBr–H_2O/ H_2O–NH_3	0.85	0.85		0.85
Vereda et al. (2012)	Ammonia/ lithium nitrate	0.85	0.85	0.9	0.8
Domanski (2005)	R134a	0.85–0.9	0.85–0.9		0.7
Yapici and Ersoy (2005)	R123	0.85	0.85		0.85
Yu and Li (2006)	R141b	0.9		0.85	0.85
Yu et al. (2007)	R142b	0.85		0.95	0.85
Elbel and Hrnjak (2004)	CO_2	0.9	0.9		0.9
Li and Groll (2005)	CO_2	0.9	0.9		0.8
Ksayer and Clodic (2006)	CO_2	0.85	0.85		0.75
Ksayer (2007)	R141b	0.95	1.0	0.9–0.98	1
Deng et al. (2007)	CO_2	0.7	0.7		0.8
Sarkar (2008)	CO_2	0.8	0.8		0.75
Elbel and Hrnjak (2008)	CO_2	0.8	0.8		0.8
Sun and Ma (2011)	CO_2	0.9	0.9		0.8
Eskandari Manjili and Yavari (2012)	CO_2	0.7	0.7	0.95	0.8

Figure 21: Efficiency of ejector sections

3.4.3 Variable nozzle outlet area

One of the biggest challenges with ejector heat pump systems is that the cycle performance is sensitive to change in working conditions [Zhu and Elbel, 2016]. Different working conditions require different ejector geometries to attain maximum performance. Slight differences in geometry may have large impact on the COP. The ejectors motive nozzle throat diameter is a key parameter and may determine whether an ejector is a viable solution or not [Zhu and Elbel, 2016]. Alternatively several ejectors can be installed in the heat pump system, with the different ejectors having different geometries. Then one or more can be used at a time depending on the requirements.

4 Components

4.1 Plate heat exchanger (PHE)

PHEs are part of a group of components called compact heat exchangers, typical characteristics of this group is [Wadekar, 2000]:

- High heat transfer coefficients
- Large surface area
- Low space requirement
- Relatively low cost

PHEs consists of a series of thin, corrugated metal plates. The plates are pressed and held together in a frame. Between the plates there are gaskets which function as a seal between each plate, while also giving flow channels to the fluid, ensuring that hot and cold fluid flow in alternating channels. The plates are produced with different patterns. The pattern is design to induce turbulence. An increase in turbulence increases the heat transfer efficiency and reduces fouling [ETSU and WS Atkins Consultants Ltd., 2000].

PHEs have a wide spectrum of industries where they are used including refrigeration, air conditioning, cryogenics and food processing. They are adaptable to many uses, depending upon design choices, such as welding and choice of gasket material. PHEs allow for close approach temperatures as they have counter-current operation. The performance of the PHEs is also adaptable, as it is possible to vary the amount of heat exchanger plates used. With sufficient size, it is possible to get a thermal effectiveness above 90%. PHEs are used as evaporators, condensers and for single phase flows [Wadekar, 2000].

Common kinds of plate heat exchangers are: gasket heat exchangers, brazed heat exchangers, partially welded heat exchangers and fully welded heat exchangers [ETSU and WS Atkins Consultants Ltd., 2000].

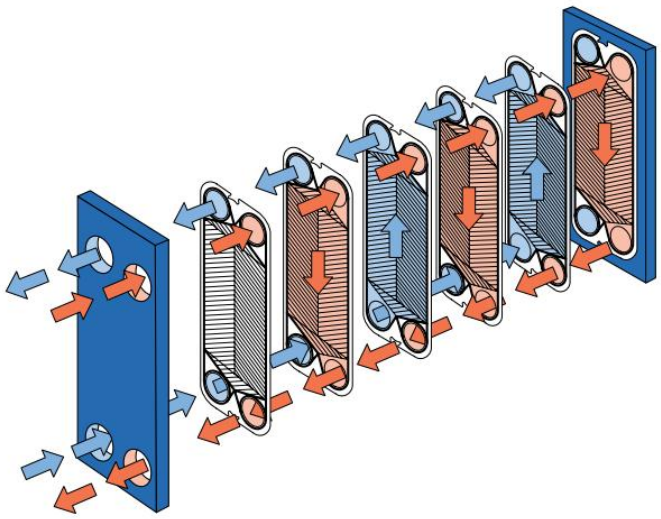

Figure 22: Illustration of a plate heat exchanger

4.1.1 Gas Cooler

Maximum efficiency of the cycle is achieved by delivering as much heat as possible in the gas cooler, while at the same time keeping the necessary work low. By reducing the temperature of the working fluid more before throttling through the expansion valve, the throttle loss is reduced. This implies that the design of the gas cooler is vital. In a transcritical heat pump cycle there is a rapid change in the specific heat capacity of the gas. The ideal discharge pressure should be found, and the gas cooler should be designed accordingly. The ideal pressure depends upon the temperature of the heat sink.

The lowest temperature difference between the working fluid and the heat sink is the pinch point. The pinch point should be located at one of the ends of the gas cooler in order to obtain maximum efficiency. If not the pinch point will reduce the heat transfer.

4.1.2 Internal Heat Exchanger(IHX)

The IHX further reduces the throttling loss by increasing the temperature of the working fluid before it is throttled through the expansion valve, increasing the efficiency of the cycle. The heat is delivered to the suction. An increase in the suction gas temperature increases the specific volume of the gas, effectively reducing the amount of mass flow through the compressor which may reduce the potential heat production of the cycle. The volumetric heat pump capacity(VHPC) is normally defined as the heat delivered in the condenser related to the specific volume of the gas at the inlet of the compressor. Here the heat delivered in the gas cooler is used instead. v_1 being the specific volume of the working fluid at the compressor inlet.

$$VHPC = \frac{\Delta h_{gc}}{v_1} \qquad [kJ/m^3] \tag{6}$$

Depending on the type of compressor used in the heat pump system there are demands on the suction gas. For a turbo compressor there can not be any condensation in the compressor stages. An internal heat exchanger help achieve this by using some of the excess heat after the gas cooler to heat the fluid before compression effectively increasing the suction superheat.

Ideally the flow on the low pressure side is single phase gas. There are situations where two phase flow will enter the IHX, and instead of producing superheat the IHX continues evaporation. The temperature on the high pressure side is of higher quality than the heat delivered in the evaporator. Assuming this, an IHX can increase the production and the quality heat. Increased suction temperature may also increase the compressor discharge temperature, allowing for heat production at higher temperature.

Figure 23 illustrates a transcritical butane heat pump cycle with an internal heat exchanger. The importance of the internal heat exchanger is clear, as Without it there would not be sufficient suction superheat into the compressor to evade condensation. This can be seen from the heat being transferred from the line between point 3 and 4 to the line between point 6 and 1. The energy used to produce the superheat is otherwise not useful.

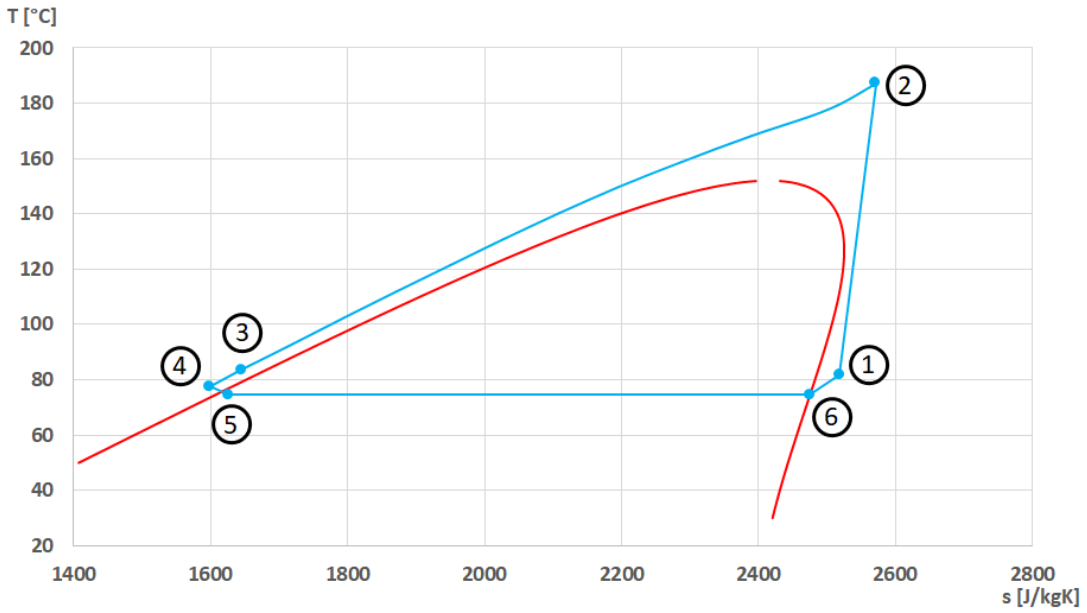

Figure 23: Ts diagram of a transcritical butane heat pump with IHX

4.2 Turbo compressor

There are three main compressor types used in industrial size applications: reciprocating compressors, screw compressors and turbo compressors. The compressors work with different displacement volumes as can be seen in figure 24 [Eikevik, 2016], with turbo compressors having the largest volume displacement. The required compressor volume displacement can be found by equation 7. $\dot{m}$ being the mass flow rate, ρ_g the density of the gas and λ being the volumetric efficiency of the compressor.

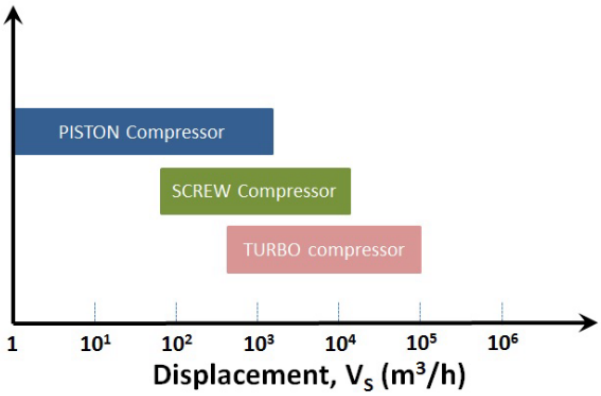

Figure 24: Typical displacement of compressors

$$V_s = \frac{\dot{m}}{\rho_g \lambda} \cdot 3600 \qquad [m^3/h] \tag{7}$$

A turbo compressor is a centrifugal compressor. Turbo compressors can be divided into axial or radial categories. As with centrifugal compressors the pressure of the working fluid

is increased by giving it high speed through an impeller. Then the increase in speed is transferred to increased pressure through a diffusor.

Instead of traditional bearings, turbo compressors use magnetic bearings. These bearings ensure that there is no direct contact between the shaft and the bearing. Because of this there is no requirement for oil in turbo compressors, and less required maintenance of the system. A turbo compressor is shown in figure 25 [Crowther and Smithart, 2004].

There are two conditions which need to be avoided in turbo compressors (illustrated in figure 26):

- Surge: Momentary reduced or reversed flow, required discharge pressure exceeds compressor output pressure capability
- Choke: Gas velocity inside the compressor approaches sonic velocity. Limits compressor capacity at a given speed.

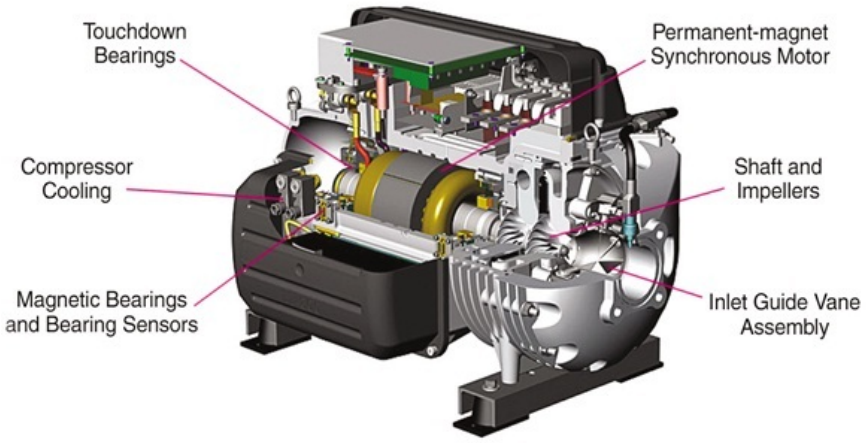

Figure 25: Illustration of a frictionless turbo compressor

In general turbo compressors are more demanding than the common piston and screw compressors. They demand a certain mass flow, and have a limited variation in the compression ratio, typically between 1.5 and 2. When reducing the pressure ratio the efficiency of piston and screw compressors typically increase, this is not always the case for turbo compressors.

The main advantage of using a turbo compressor is that it demands a very low amount or no oil at all. This is often the most important factor when using turbo compressors in high temperature systems, where oil degradation is a large concern. In addition there is no oil spilling into the other components in the heat pump, and there is no need for an elaborate oil-recovery system. [Crowther and Smithart, 2004]

Compressors have performance curves, meaning that in some area of operation the highest performance can be found. Depending on the suction state and the required pressure ratio the mass flow and the efficiency of the compressor can be found. Varying on the rpm of the compressor the pressure ratio of highest compressor efficiency and mass flow changes. An illustration of a compressor performance map is shown in figure 26 [How It Works, 2015].

In turbo compressors with the given rpm, and a given suction state either pressure ratio or mass flow rate can be decided. Not all combinations of pressure ratio and mass flow rate is

possible to achieve.

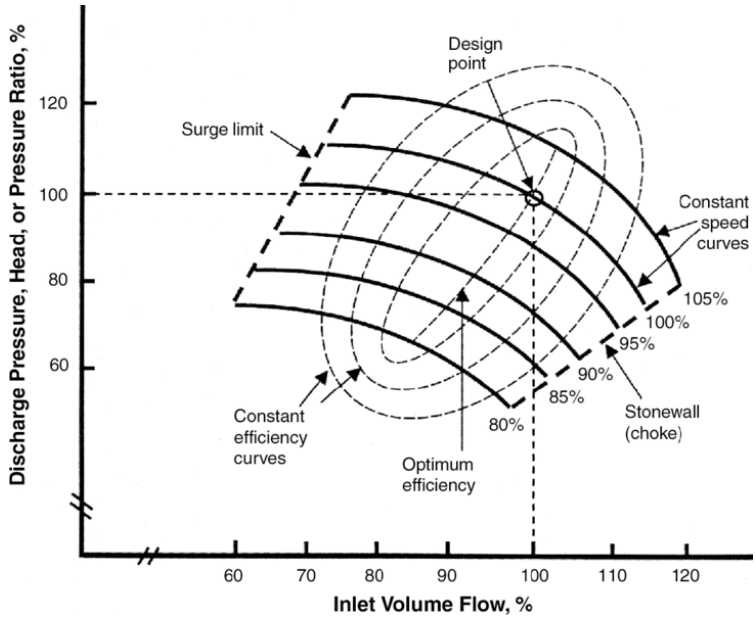

Figure 26: Illustration of compressor performance map

5 Case

5.1 Current Project

In the current state the focus is at producing oil up to 160°C. While the future goal is to heat efficiently up to 180°C and to be able to deliver heat close to 200°C. This means that the components used in the system are designed for a higher temperature than the current conditions. It also means that the size of the heat exchangers used is relatively large compared to the current requirement. The future goal of the cycle may be of heating water/steam, but in the current simulation the fluid used in the gas cooler is high temperature oil. The oil used is a heat medium oil with high thermal and oxidation stability. The properties of the oil is supplied in table 64.

5.2 Operation conditions

The operation time of the heat pump is assumed to be 4400 hours annually, which translates to 12 hours daily. A single heat pump is assumed to deliver approximately 300 kW. Over a year this equals 1 320 000 kWh. Assuming a temperature difference of oil during heating of 80°C, the mass flow of oil is approximated to 1.64 kg/s. Assuming a COP of 4, the heat delivered in the evaporator is 225 kW. Water inlet temperature at 80°C, and outlet temperature of 77°C gives an estimated water flow rate of 17.9 kg/s. The system may be closed cycle, meaning that the waste water from the industrial process is the supply water to the heat pump evaporator, or that the waste water is reheated and reused in the industrial process. The specific industrial usage of the system is not defined.

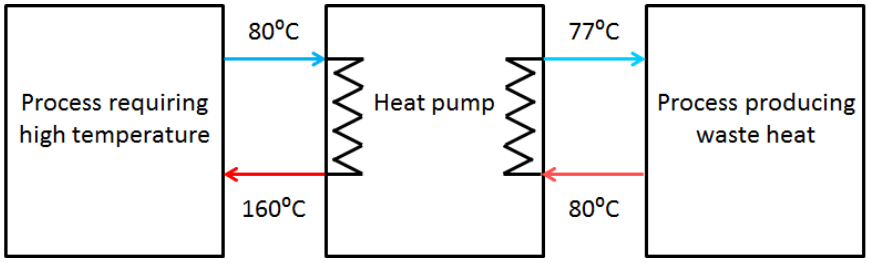

Figure 27: Overview of possible system solution

5.3 Choice of components

The simulation model is based on a heat pump cycle which is being made and tested by Mayekawa. The model is a three-stage transcritical compression heat pump. The compressors used are turbo compressors. The main reason for choosing turbo compressors is that they do not require oil. As temperature approaches 200°C there is commonly a degradation of the oil. Another advantage is the low maintenance required of turbo compressors. The downside of these compressors is the low pressure ratio, which means that for this system 3 are required in series. The compressors are made by Mayekawa, and are constructed for usage with butane.

During initial simulations done by Mayekawa butane was found to have the highest COP for heating oil from 80 to 160°C, while also being among the best for heating oil from 100 to 180°C. It was compared to R245fa, R1234ze(Z), R600a, R1234ze(E), R134a, R32, R290 and R1270. Butane has a suitable heat transfer coefficient and critical pressure, it has a low GWP value, and requires relatively low discharge pressure.

The evaporator and internal heat exchanger were chosen by Mayekawa using Alfa Laval's calculation software. A suitable number of plates was also found. The gas cooler was designed by SWEP using data from Mayekawa. The gas cooler is a prototype and is not yet in widespread production.

Compressor	Mayekawa BU 80/35
Evaporator	Alfa Laval AC-500eq
Gas cooler	SWEP CAS25T
Internal heat exchanger	Alfa Laval CBXP52
Expansion valve	Fujikin AR2000

Table 4: Components used in the heat pump design, all but the expansion valve are used in the simulation.

6 Simulation models

The simulation model is based on a butane heat pump cycle which is being tested by Mayekawa. Each of the components in the simulation are based on actual components used. The properties of the components are received from Mayekawa, and are either based on information from the producer, or simulations and testing done by Mayekawa.

The model of the transcritical heat pump cycle is developed in MATLAB(Matrix Laboratory)[Mat, 2016]. MATLAB as a platform is optimized for solving engineering and scientific problems. MATLAB is a program which supplies a numerical computing environment, several toolboxes may be added to the program. In addition to the standard MATLAB program, a REFPROP extension is used. This allows for accessing thermodynamic data directly, the data is produced by NIST[Lemmon et al., 2013]. The combination of MATLAB and REFPROP forms a good base for simulation of thermodynamic processes, such as heat pumps.

The simulation started as a simple model of a transcritical butane heat pump cycle. At first all calculations were done by simple REFPROP calculations, the assumption of ideal processes, and no pressure loss. Step by step the components were made to produce more detailed and precise results. Finally all the components were joined together to create a complete heat pump cycle.

Simplifications made in the simulation:

- The flow rate of supply water and oil is freely variable
- The temperature of water and oil is perfectly stable
- When calculating pressure drop in pipes, enthalpy is assumed to be constant
- Expansion is considered isenthalpic
- No heat is leaked to the surroundings
- No pressure drop in the compressor suction valve
- The compressor is calculated by one dimensional correlations
- Uniform flow rate over the flow area in heat exchangers

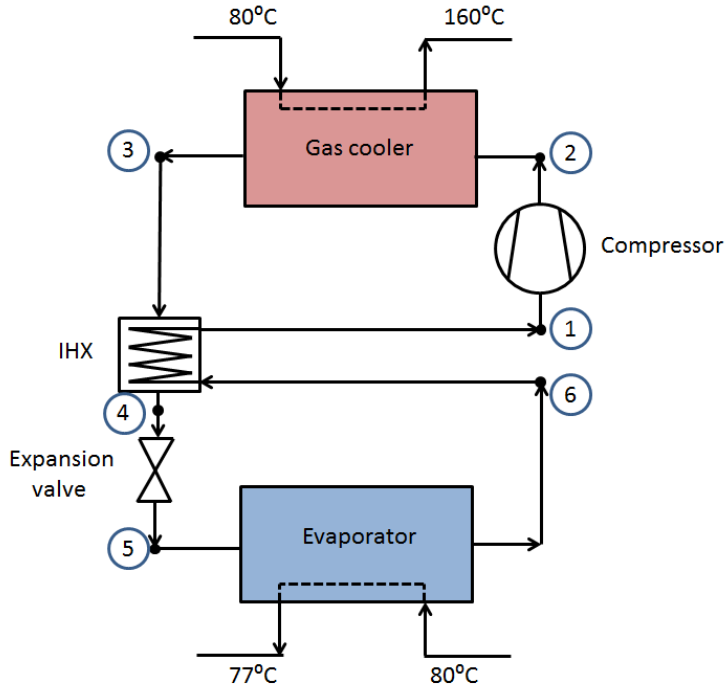

Figure 28: Principle model of the heat pump cycle simulated

6.1 Compressor

The correlations used to estimate the compressor performance were created by Mayekawa using COMPAL[Concepts NREC]. There are separate correlations for pressure ratio and required power for each compressor stage.

The subscript d means design properties. N is rpm, ρ is density, P is pressure and $\dot{m}$ is the butane flow rate. The pressure and density is calculated at the inlet to each compressor stage.

Compression ratio:

First stage

$$\begin{aligned}\pi_1 = &\Big[-1.651\Big\{\dot{m}\Big(\frac{N_d}{N}\Big)\Big(\frac{\rho_d}{\rho}\Big)\Big\}^2 + 1.750\Big\{\dot{m}\Big(\frac{N_d}{N}\Big)\Big(\frac{\rho_d}{\rho}\Big) + 1.452\Big] \\ &\times 0.5\Big\{\Big(\frac{N}{N_d}\Big) + \Big(\frac{N}{N_d}\Big)^2\Big\}\Big(\frac{\rho}{\rho_d}\Big)^{0.631}\Big(\frac{P_d}{P}\Big)^{0.556}\end{aligned} \tag{8}$$

Second stage

$$\begin{aligned}\pi_2 = &\Big[-1.651\Big\{\dot{m}\Big(\frac{N_d}{N}\Big)\Big(\frac{\rho_d}{\rho}\Big)\Big\}^2 + 1.750\Big\{\dot{m}\Big(\frac{N_d}{N}\Big)\Big(\frac{\rho_d}{\rho}\Big) + 1.452\Big] \\ &\times 0.5\Big\{\Big(\frac{N}{N_d}\Big) + \Big(\frac{N}{N_d}\Big)^2\Big\}\Big(\frac{\rho}{\rho_d}\Big)\Big(\frac{P_d}{P}\Big)\end{aligned} \tag{9}$$

Third stage

$$\begin{aligned}\pi_3 =& \Big[-1.651\Big\{\dot{m}\Big(\frac{N_d}{N}\Big)\Big(\frac{\rho_d}{\rho}\Big)\Big\}^2 + 1.750\Big\{\dot{m}\Big(\frac{N_d}{N}\Big)\Big(\frac{\rho_d}{\rho}\Big) + 1.48\Big] \\ & \times 0.5\Big\{\Big(\frac{N}{N_d}\Big) + \Big(\frac{N}{N_d}\Big)^2\Big\}\Big(\frac{\rho}{\rho_d}\Big)\Big(\frac{P_d}{P}\Big)^{1.15}\end{aligned} \tag{10}$$

Power required:

First stage

$$W_1 = \Big[30.031\Big\{\dot{m}\Big(\frac{N_d}{N}\Big)\Big(\frac{\rho_d}{\rho}\Big)\Big\} + 2.987\Big]\Big(\frac{N}{N_d}\Big)^3\Big(\frac{\rho}{\rho_d}\Big)^{0.942} \tag{11}$$

Second stage

$$W_2 = \Big[30.182\Big\{\dot{m}\Big(\frac{N_d}{N}\Big)\Big(\frac{\rho_d}{\rho}\Big)\Big\} + 2.422\Big]\Big(\frac{N}{N_d}\Big)^3\Big(\frac{\rho}{\rho_d}\Big)^{0.942} \tag{12}$$

Third stage

$$W_3 = \Big[26.053\Big\{\dot{m}\Big(\frac{N_d}{N}\Big)\Big(\frac{\rho_d}{\rho}\Big)\Big\} + 3.028\Big]\Big(\frac{N}{N_d}\Big)^3\Big(\frac{\rho}{\rho_d}\Big)^{0.946} \tag{13}$$

The efficiency of the compressor is found by comparing the work from the correlations above to isentropic compression. The maximum mass flow is set to where the pressure ratio of the third compressor stage is below 1, found by testing in the simulation. The minimum mass flow is set to equation 14, found by the simulation done by Mayekawa. Below this mass flow the risk of surge is prevalent.

$$\dot{m}_{min} = \Big\{0.5361\Big(\frac{N}{N_d}\Big)^2 + 0.0828\Big(\frac{N}{N_d}\Big)\Big\}\Big(\frac{\rho}{\rho_d}\Big)^{1.69}\Big(\frac{P_d}{P}\Big)^{0.63} \tag{14}$$

6.2 Heat exchangers

The heat exchangers are modeled using a numerical method to find the heat transfer. Each heat exchanger is divided into small control volumes. The number of sections is chosen to give valid calculation and to converge, while still being kept low to reduce computation time. The amount of control volumes in the heat exchangers varies from 30 to 50. The number of plates in the heat exchangers is kept constant.

An energy balance is used over each of the control volumes. The enthalpy/temperature at the inlet of each control volume is known or assumed, then the found heat transfer of that element is added or subtracted to find the enthalpy/temperature at the outlet. The next control volume then continues on the results. The inlet and outlet temperature of each element is found by using the heat transfer rate of each heat exchanger element.

$$h_{out} = h_{in} + \frac{\dot{Q}_{ele}}{\dot{m}} \qquad \text{[kJ/kg]} \tag{15}$$

The equation used to estimate each element is the heat transfer, as in equation 16.

$$\dot{Q} = U \cdot A \cdot LMTD \qquad \text{[W]} \tag{16}$$

U is the overall heat transfer coefficient(as in eq 17), A is the heat transfer area, and LMTD is the logarithmic mean temperature difference(as in eq 18).

$$U = \frac{1}{R_{warm} + R_{cold} + R_w} = \frac{1}{\frac{1}{\alpha_{warm}} + \frac{1}{\alpha_{cold}} + \frac{\delta}{k_w}} \quad [\mathrm{W/m^2K}] \tag{17}$$

α is the heat transfer coefficient, δ_w is the thickness of the plate wall and k_w is the thermal conductivity of the wall between the two fluids.

$$LMTD = \frac{\Delta(1) - \Delta(2)}{\ln(\frac{\Delta(1)}{\Delta(2)})} \tag{18}$$

$\Delta(1)$ and $\Delta(2)$ are respectively the temperature difference on the inlet and outlet of each control volume. Pressure drop is found from the friction factor of each control volume. The approach is found in Lee et al. [2014]. The friction factors used are produced experimentally, they therefore include all factors for pressure loss in the heat exchangers.

$$\Delta P = f \frac{L}{D_h} \frac{2 \cdot G^2}{\rho_m} \qquad [\mathrm{Pa}] \tag{19}$$

L being the length of each element, D_h being the hydraulic diameter, G being the mass flux and ρ_m being the mean density. To estimate the heat transfer in the heat exchangers the dimensionless Reynolds and Prandtl number are defined.

$$Re = \frac{G D_h}{\mu} \tag{20}$$

$$Pr = \frac{\nu}{\alpha} \tag{21}$$

μ being dynamic viscosity and ν being kinematic viscosity. A few different definitions of temperature are used to find the necessary properties of fluids, shown in equation 22.

$$\begin{aligned} T_{bulk} &= \frac{T_{in} + T_{out}}{2} \\ T_w &= T_{bulk} - \frac{\dot{Q}_{ele}}{\alpha \cdot A_{ele}} \\ T_{film} &= \frac{T_{bulk} + T_w}{2} \end{aligned} \tag{22}$$

$\mathrm{T_{in}}$ and $\mathrm{T_{out}}$ being the temperature at inlet and outlet of the heat exchanger element and $\mathrm{A_{ele}}$ being the wall area of each element.

6.3 Evaporator

In the evaporator the film properties are very close to the properties found in the bulk of the fluid, therefore the bulk temperature is used to find properties. There are separate correlations used for single phase flow, and two phase flow. In the range of vapor quality 0 to 0.1 and 0.9 to 1 the heat transfer coefficient and the friction factor is found by linear interpolation between single and two phase flow. The equivalent Reynolds number and mass flux is from [Lee et al., 2014].

$$Re_{eq,ref} = \frac{G_{eq} D_h}{\mu_l} \tag{23}$$

$$G_{eq} = G[(1 - x_m) + x_m \cdot (\rho_l/\rho_g)^{0.5}] \tag{24}$$

Where G_{eq} is the equivalent mass flux, μ_f and μ_{ref} is the dynamic viscosity of respectively fluid state and the refrigerant, x_m is the mean vapor quality, and ρ_f and ρ_g is the density of the saturated liquid and gas state of the refrigerant at the give pressure.

Friction factor is defined, using the defined $\mathrm{Re_{ref}}$ and $\mathrm{Re_{eq,\ ref}}$:

$$\begin{aligned} f_{ref} &= 1.235 Re_{ref}^{-0.0686} && \mathrm{x} \leq 0 \\ f_{ref} &= 9706.429 Re_{eq,ref}^{-1.44893} \cdot Re_{ref}^{0.401293} && 0.1{<}\mathrm{x}{<}0.9 \\ f_{ref} &= 1.235 Re_{ref}^{-0.0686} && 1 \leq \mathrm{x} \end{aligned} \tag{25}$$

The heat transfer coefficient of the evaporator is defined by equation 26.

$$\begin{aligned} \alpha_{ref} &= 0.1671 \cdot Re_{ref}^{0.866} Pr^{\frac{1}{3}} \cdot \frac{\lambda_{ref}}{D_h} && \mathrm{x} \leq 0 \\ \alpha_{ref} &= 3.3596 \left\{ 1 + \frac{1}{X_{tt}} \right\}^{0.5142} \frac{\lambda_l}{D_h} \left\{ \frac{G(1-x) D_h}{\mu_l} \right\}^{0.4909} Pr_l^{-0.00024} && 0.1{<}\mathrm{x}{<}0.9 \\ \alpha_{ref} &= 0.2093 Re_{ref}^{0.6991} Pr_{ref}^{\frac{1}{3}} \cdot \frac{\lambda_{ref}}{D_h} && 1 \geq \mathrm{x} \end{aligned} \tag{26}$$

Subscript ref denotes refrigerant, l denotes liquid, g denotes gas λ is the thermal conductivity. X_{tt} is the Lockhart-Martinele parameter as defined in [Lee et al., 2014]. x being the vapor quality.

$$X_{tt} = \left(\frac{1-x}{x} \right)^{0.875} \cdot \left(\frac{\rho_g}{\rho_l} \right)^{0.5} \cdot \left(\frac{\mu_g}{\mu_l} \right)^{0.125} \tag{27}$$

Inputs	Value
Length	0.687 [m]
Width	0.322 [m]
Plate thickness	0.0004 [m]
Plate gap	0.00178 [m]
Number of channels	199 [-]
Thermal conductivity	15.9 [W/m K]
Hydraulic diameter	0.00356 [m]

Table 5: Evaporator data

6.4 Gas Cooler

The heat transfer correlation in the gas cooler is found in [Nishida et al., 2016], it is developed by Mayekawa. There will only be transcritical butane in the gas cooler, and therefore one correlation is sufficient. In the gas cooler the film temperature of the butane and oil is used to calculate the properties to find the heat transfer.

$$\alpha = 0.3522 \cdot Re_{ref}^{0.6705} Pr_{ref}^{\frac{1}{3}} \times \frac{\lambda_{ref}}{d_h} \tag{28}$$

The pressure drop has two different equations, depending on the Reynolds number. The correlations are found from testing by Mayekawa.

$$\frac{\Delta P}{L} = 1.736 \cdot 10^4 \cdot Re^{-0.3491} \frac{G^2}{\rho} \left(\frac{\mu_w}{\mu}\right)^{0.14} \quad \text{[Pa/m]; Re<227} \tag{29}$$

$$\frac{\Delta P}{L} = 1.501 \cdot 10^4 \cdot Re^{-0.1672} \frac{G^2}{\rho} \left(\frac{\mu_w}{\mu}\right)^{0.14} \quad \text{[Pa/m]; Re} \geq 227 \tag{30}$$

Inputs	Value
Length	0.5575 [m]
Width	0.113 [m]
Plate thickness	0.00025 [m]
Plate gap	0.0008 [m]
Number of channels	139 [-]
Thermal conductivity	15.9 [W/m K]
Hydraulic diameter	0.0016 [m]

Table 6: Gas cooler data

6.5 Internal Heat Exchanger

The internal heat exchanger correlations are found by simulations done by Mayekawa using Alfa Laval simulation program. The heat transfer coefficient of the IHX is as in equation

31. In the case that the gas quality is below 1 correlations from the evaporator are used for the mixed state, it is assumed that the gas quality is never below 0.1 in the IHX. With gas quality between 0.9 and 1, linear interpolation is used.

$$\begin{aligned} \alpha_{ref} &= 3.3596\left\{1+\frac{1}{X_{tt}}\right\}^{0.5142}\frac{\lambda_l}{D_h}\left\{\frac{G(1-x)D_h}{\mu_l}\right\}^{0.4909}Pr_l^{-0.00024} && 0.1<x<0.9 \\ \alpha_{ref} &= 0.2786\cdot Re_{ref}^{0.7071}Pr_{ref}^{1/3}\cdot\frac{\lambda_{ref}}{d_h} && 1 \geq x \end{aligned} \tag{31}$$

The friction factor is as shown in equation 32.

$$\begin{aligned} f_{ref} &= 9706.429Re_{eq,ref}^{-1.44893}\cdot Re_{ref}^{0.401293} && 0.1<x<0.9 \\ f_{ref} &= 2.230Re_{ref}^{-0.03351} && 1 \geq x \end{aligned} \tag{32}$$

Inputs	**Value**
Length [m]	0.459
Width [m]	0.111
Plate thickness [m]	0.0004
Plate gap [m]	0.00179
Number of channels [-]	119
Thermal conductivity [W/m K]	15.9
Hydraulic diameter [m]	0.00358

Table 7: IHX data

6.6 Expansion valve

Over the expansion valve constant enthalpy is assumed. The only change is in the pressure and the resulting temperature.

6.7 Pressure drop in pipelines

Pressure drop in some of the pipes is included. The flow is varied between laminar and turbulent. To calculate the pressure drop the laminar flow uses the Darcy friction factor, while turbulent flow uses the Prandtl and von Karman equation [Cengel and Cimbala [2013], Kast [2010]].

$$\begin{aligned} f &= \frac{64}{Re} && \text{Re} \leq 2300 \\ \frac{1}{\sqrt{f}} &= 2\cdot\ln(Re\sqrt{f})-0.8 && \text{Re} > 2300 \end{aligned} \tag{33}$$

Depending on the available information about the components two different manners of calculating the pressure drop is used, shown in equation 34, both being a variation of the Darcy-Weisbach equation, [Cengel and Cimbala, 2013].

$$\begin{aligned} \Delta P &= \rho g \Delta H \qquad [\text{Pa}] \\ \Delta P &= f \frac{L}{D_h} \frac{\rho u^2}{2} \qquad [\text{Pa}] \end{aligned} \tag{34}$$

Only the parts of the pipe network which are expected to have an impact of the performance are considered. The pressure loss from the IHX to the compressor is important as it changes the pressure ratio of the compressor. When the pressure ratio changes, so does the efficiency and the mass flow of butane, which influences the entire cycle. The pressure loss from the compressor to the gas cooler is also included as it is relatively large. Both of these pressure drops are in the 20 - 30 kPa range. The pressure loss from the evaporator to the IHX was also considered, but the pressure loss was found to be small (estimately 5 kPa) and is therefore not included in the calculation (a table of the pipe components from the evaporator to the IHX is included in the appendix A.1).

The pressure drop from the gas cooler to the internal heat exchanger and from the internal heat exchanger to the expansion valve is not considered. This is because the impact of this pressure is low. The pressure drop itself is low, with also the ratio $\frac{\Delta T}{\Delta P}$ being low.

Beside the straight pipes there are turns, separators, mixer, and valves. The length and diameter of the components are found from the system schematics used during the design. In the tables 8 and 9 information about the components in the pipelines is given. Each type of component has a given characteristic. For pipes inner diameter (Di), for turns the radius (R) of the turn, for splitters/mixers a variable depending on the radius (ζ) of the pipe, and for valves (C_v) the flow coefficient.

Component	Type	Characteristics	Length/Amount	Comment
Pipes	40A	Di 41.2	1858 mm	-
	65A	Di 65.9	3783 mm	-
Turns	65A	R 95.3	5	-
Splitter/mixer	65A	ζ 0.3	1	Mixer
Valves	-	Cv 74	2	-

Table 8: IHX to compressor pipes

Component	Type	Characteristics	Length/Amount	Comment
Pipes	20A	Di 21.4	600 mm	Half flow rate
	32A	Di 35.5	2613.5 mm	-
	40A	Di 41.2	785.5 mm	-
Turns	20A	R 13.5	1	Half flow rate
	32A	R 47.6	3	-
	40A	R 57.2	1	-
Splitter/mixer	32A	ζ 0.8	1	Splitter
Valves	-	-	None	-

Table 9: Compressor to gas cooler pipes

7 Simulation setup

When running the simulation there are two main parameters which are defined: the superheat into the compressor, and the compressor discharge pressure. Once these two parameters are decided, and a range for the suction pressure is set, the simulation may start. The cycle is solved by converging the enthalpy after the evaporator (point 6 in figure 29), the enthalpy difference is changed by varying the suction pressure. The program needs no more input once the superheat, the discharge pressure and the suction pressure range are set.

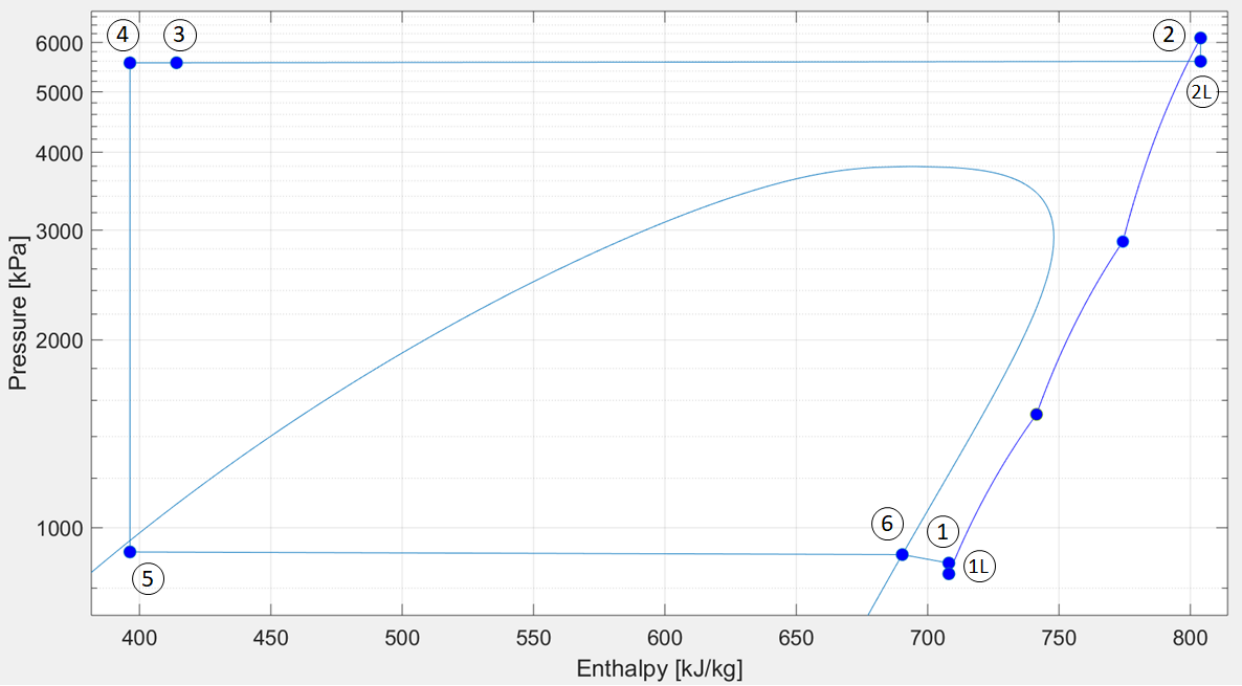

Figure 29: Log p-h diagram. Illustrates the cycle.

In figure 29 the pressure loss between the compressor and the gas cooler is exaggerated to show the various points more clearly.

7.1 Superheat into compressor

It is required that there is no condensation in any of the compression stages. To ensure this, some superheat is required into the compressor. The suction temperature is varied by the heat delivered in the evaporator and the internal heat exchanger, to ensure sufficient superheat the system varies the suction pressure.

Apart from ensuring gas phase during compression, superheat is advantageous to exploit more of the high quality heat on the high pressure side in the IHX. Depending on the temperature of the oil in the gas cooler, the superheat is changed. For oil temperature of 80-160°C, 10 K superheat is used, while for 100-180°C, 30 K superheat is used.

7.2 Compressor discharge pressure

In the gas cooler, it is assumed that the butane entering should at minimum have a 10 K temperature gap to the desired oil temperature. To heat the oil to 160°C the minimum discharge temperature is 170°C, and to heat the oil to 180°C the minimum discharge temperature is 190°C. In the simulation this is used to decide the minimum discharge pressure. If the discharge temperature is too low this is due to the corresponding discharge pressure being too low. The maximum discharge pressure is found either by assuming that the maximum pressure ratio is any compressor stage is below 2, effectively limiting the maximum pressure ratio to 8. With some input the maximum effective pressure ratio will be lower. The maximum and minimum discharge pressure decides in what range to test the system.

In practice a receiver is used to vary the discharge pressure. The receiver controls the amount of fluid in the evaporator and in the gas cooler. The receiver allows part of the mass flow to go directly from the gas cooler to the evaporator. Additionally the receiver may store butane if the amount of working fluid in one section needs to be reduced, while the other is kept constant.

In the actual system the receiver controls the amount of superheat into the compressor. If the suction superheat is too high the receiver may increase the amount of fluid in the evaporator. When the amount of fluid is increased the pressure is increased, which increases the saturation temperature. In the simulation the system is always operated a steady state, and the receiver does not effect the results.

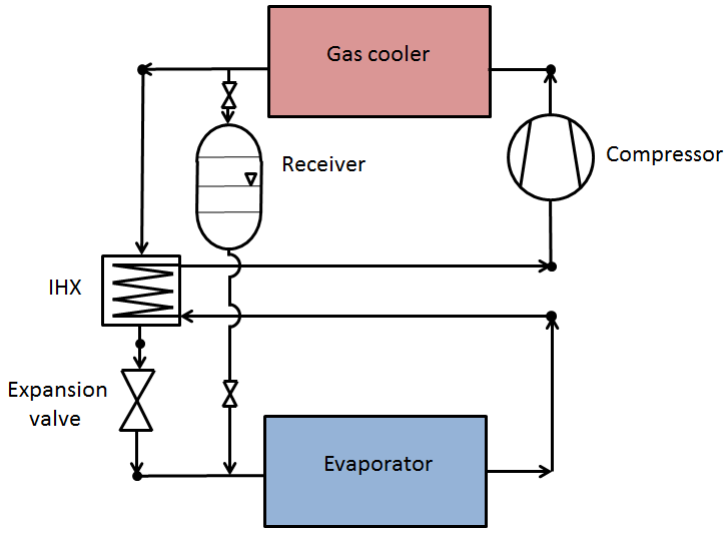

Figure 30: Principle model of the heat pump cycle with receiver

7.3 Solving procedure

The simulation program can be divided into one inner part and one outer part. The inner part is the heat pump cycle. It uses the given suction superheat, suction pressure and discharge pressure to run the heat pump itself. It does not consider the results in any way. The results are returned to the outer part of the program. The outer part examines the results and uses the secant method (eq. 36) to vary the suction pressure as needed before the next iteration of the heat pump cycles starts.

Figure 31 shows how the heat pump itself runs. The starting point of the cycle is from point 1L. From here the cycle runs two ways. First the compressor and gas coolers run, and then there is the IHX. The IHX receives data from point 1 and from point 3, and solves for point 4 and point 6_{IHX}. From point 4 the cycles moves through the throttling valve and the evaporator which produces an additional result after the evaporator, point 6_{evap}. All the results are then returned to the outer function, which evaluates the enthalpy difference of point 6_{IHX} and 6_{evap}, and finds the suction pressure of the next iteration. The outer function and the solving procedure is explained in figure 32.

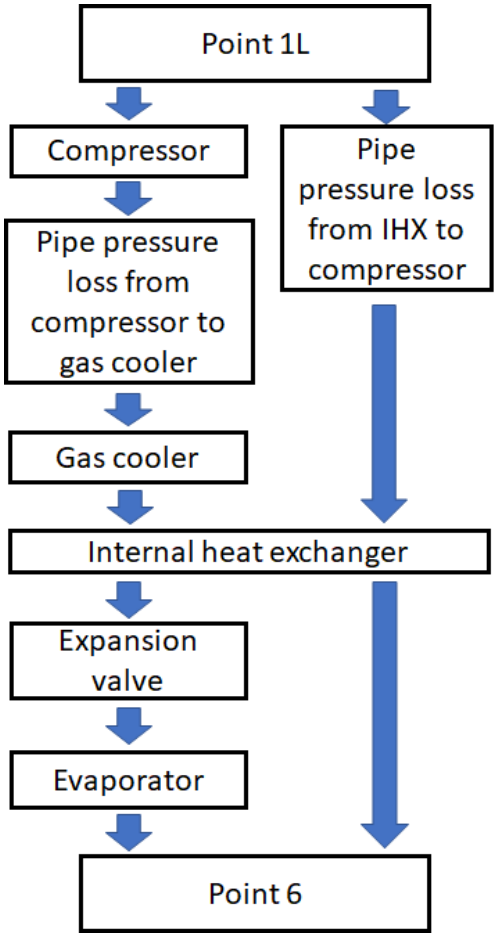

Figure 31: Flow chart of the heat pump cycle

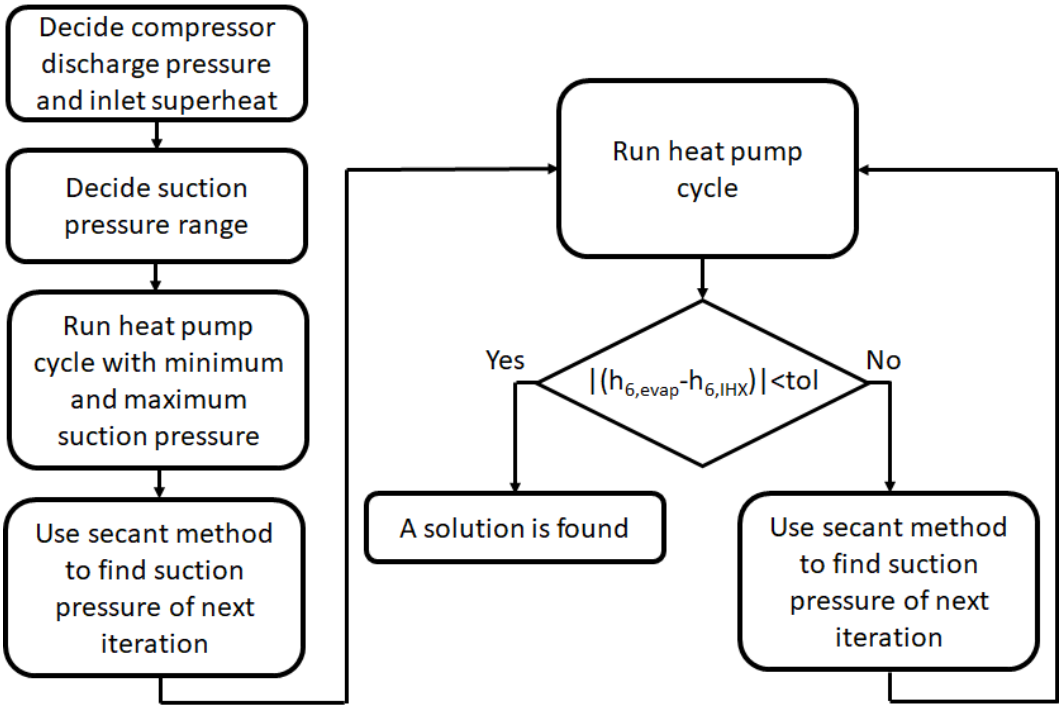

Figure 32: Flow chart of the simulation program

Given a constant compressor discharge pressure and suction superheat of the compressor the secant method is used as the root-finding algorithm to find the correct suction pressure. The secant method is given below in equation 35.

$$x_i = x_{i-1} - f(x_{i-1}) \cdot \frac{x_{i-1} - x_{i-2}}{f(x_{i-1}) - f(x_{i-2})} \tag{35}$$

In the simulation the enthalpy difference is used to converge the suction pressure which changes the secant equation to equation 36. The demand of convergence is an enthalpy difference below 100 J/kg.

$$p_{suc,i} = p_{suc,i-1} - \Delta h_{6,i-1} \cdot \frac{p_{suc,i-1} - p_{suc,i-2}}{\Delta h_{6,i-1} - \Delta h_{6,i-2}} \tag{36}$$

Δh being the absolute enthalpy difference between $h_{6,evap}$ and $h_{6,IHX}$.

Table 10 shows what each of the components in the heat pump simulation require as input, and what they produce as output. The points correspond to figure 29.

Component	Input	Output
Compressor	rpm, T_{1L}, P_{1L}, P_2	$\dot{m}_{but}$, η_{comp}, T_2, P_2
Gas cooler	$\dot{m}_{but}$, T_{2L}, P_{2L}	$\dot{m}_{oil}$, Q_{GC}, T_3, P_3
IHX	$\dot{m}_{but}$, T_3, P_3, h_1, P_1	Q_{IHX}, h_6, h_4, ΔP_{HP}, ΔP_{LP}
Evaporator	$\dot{m}_{but}$, h_5, P_5	$\dot{m}_{water}$, Q_{evap}, T_6, h_6, ΔP_{evap}

Table 10: Overview of components in the HP simulation

8 Results

The discharge pressure range for each simulation was found by testing. To find the minimum discharge pressure it was demanded that the discharge temperature had to be above 170°C. This temperature demand was chosen to ensure that there was a sufficiently large temperature gap between the butane and the oil in the gas cooler to ensure sufficient heat transfer. It is also kept in mind that the compression ratio of any stage cannot be below 1 as this would imply a significant risk of choke, which may be harmful to the compressor and stop the cycle.

The theoretical maximum compression ratio of each compressor stage was assumed to be 2, which implies a total pressure ratio of 8. If the pressure ratio is larger, there is an increased risk of surging in one of the compression stages. To find the discharge pressure range of the cycle testing was done by increasing the discharge pressure, choosing a fitting suction pressure range, and check for convergence. If the result had a discharge temperature below 170°C or a pressure ratio above 8, that result was deemed outside of the working range.

8.1 Effect of changing discharge pressure

The variation of discharge pressure allows for testing the heat pump cycle over a large range. Both the COP and the amount of heat delivered in the gas cooler is examined. This simulation is of the basic cycle which the other results are be compared to. The interest of examining the cycle over a large discharge pressure range, is to find how the performance of the heat pump cycle varies. This may indicate where the heat pump should be operated, and for which conditions the heat pump is viable to use. The point of highest COP is of high interest.

The minimum discharge pressure was found to be 4300 kPa, while the maximum was 6700 kPa. This range is found using the already mentioned minimum discharge temperature of 170°C, and the maximum pressure ratio of 8.

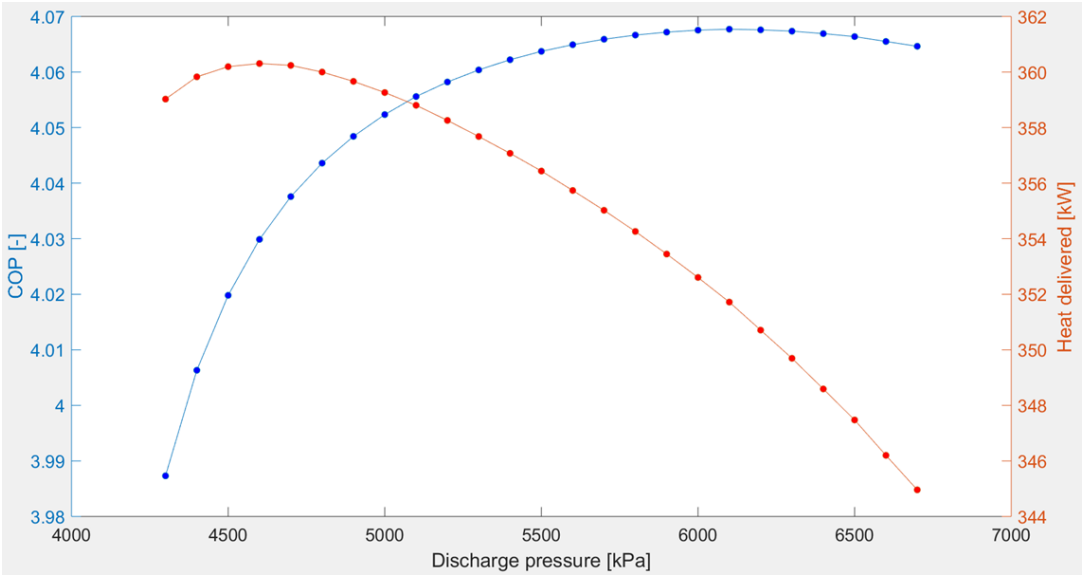

Figure 33: COP and heat delivered at varying discharge pressure

As seen in figure 33, the COP of the system is consistently above 4 except at the lowest discharge pressure, while the delivered heat is above 344 kW. This indicates that the system should be able to deliver the specifications of a COP above 3.5 and delivered heat above 300 kW. The point of highest COP is at 6100 kPa discharge pressure. This point is used as a reference point when examining other results, precise results of this point is found in table 11.

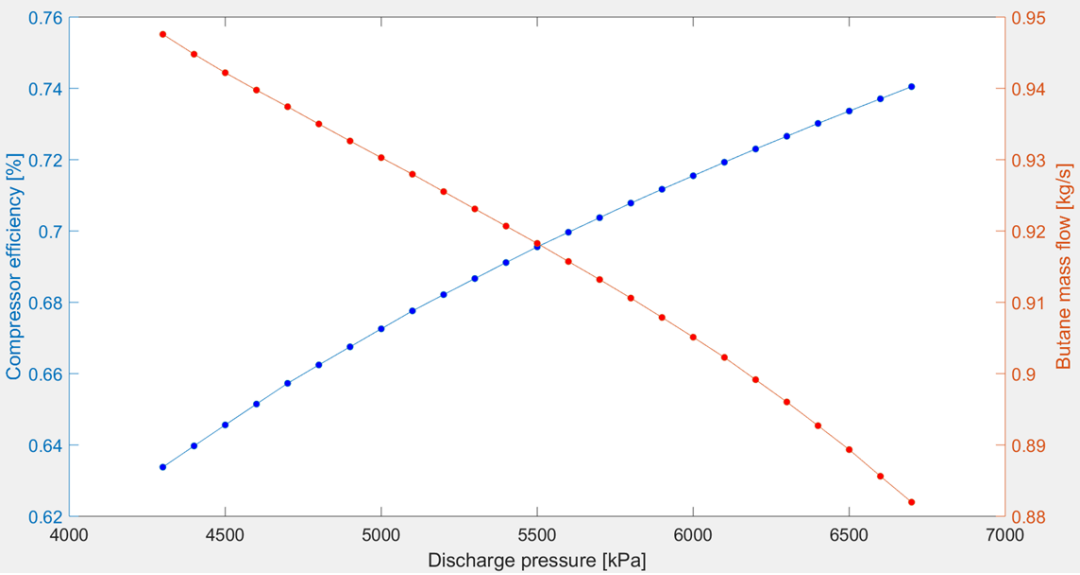

Figure 34: Compressor efficiency and butane mass flow at varying discharge pressure

At the lowest discharge pressure (4300 kPa) the pressure ratio is low (see table 11) which leads to a low compressor efficiency. At low pressure ratio there is a large butane flow rate, which ensures the delivery of a large amount of heat. The amount of heat delivered at 4300 kPa is slightly lower than the amount at 4600 kPa, this is due to the low discharge temperature from the compressor, which reduces the heat transfer rate in the gas cooler, in addition to the peak of the heat capacity being at low temperature at lower gas cooler pressure.

As the discharge pressure increases so does the compressor efficiency. This may be attributed back to the typical turbo compressor characteristics of higher efficiency at higher pressure ratio. As the pressure ratio increases so does the energy required for isenthalpic compression of butane(see figure 35). Even with the increase in compressor efficiency the increase in the pressure ratio makes the specific work of the compressor increase. Due to the reduction in flow rate, the required amount of work is reduced at higher discharge pressure.

The discharge temperature keeps increasing at higher discharge pressure. The necessary temperature difference in the gas cooler is deemed to be 10 K, at a certain point the increase in temperature of the butane becomes redundant, as the temperature already is sufficiently high. At high discharge pressure the increase in discharge temperature is diminishing. As discussed in the theory chapter; the specific heat capacity is reduced with increasing pressure, but is shifted towards higher temperature which is beneficial.

Comparing the graph of delivered heat in figure 33 and the butane mass flow rate in figure 34, it is clear that the amount of heat delivered changes very closely to the butane flow rate.

$T_{sh,\ comp}$ [K]	10	10	10
P_{dis} [kPa]	4300	6100	6700
P_{suc} [kPa]	839.7	843.3	844.5
T_{suc} [°C]	81.62	81.81	81.87
COP [-]	3.987	4.068	4.065
Heat delivered [kW]	359.03	351.72	344.96
Work [kW]	90.04	86.47	84.87
η_{comp} [%]	63.38	71.93	74.05
π [-]	5.12	7.23	7.93
T_{dis}[°C]	170.51	189.88	194.11
$\dot{m}_{butane}$ [kg/s]	0.948	0.902	0.882
$\dot{m}_{oil}$ [kg/s]	1.959	1.918	1.881
$\dot{m}_{water}$ [kg/s]	21.373	21.070	20.659
$\rho_{butane,\ suc}$ [kg/m^3]	19.66	19.74	19.77

Table 11: Results from variation in discharge pressure

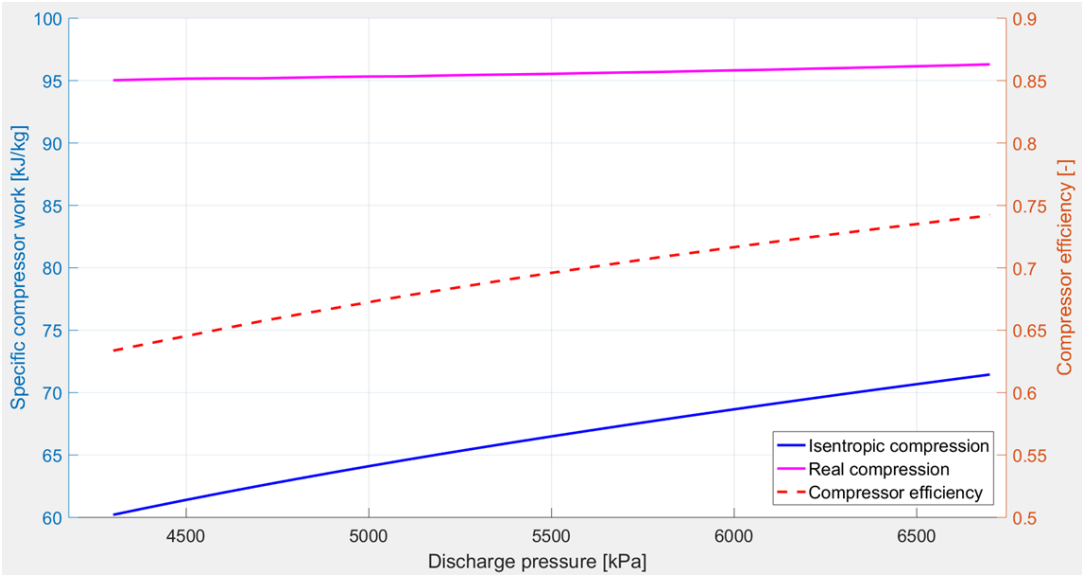

Figure 35: Comparison of isentropic vs real compressor work, with compressor efficiency.

8.2 Effect of changing suction superheat

In practice the suction superheat will not be constant, it is therefore of interest to see how the variation in superheat may effect the system. Additionally there may be a temperature which is more efficient than 10 K. 10 K was chosen to ensure that there is sufficient superheat through all the compressor stages, this may however be found to be a too high temperature or too low depending on the requirements of the discharge temperature.

In this simulation the discharge pressure is kept constant at 5700 kPa while the suction superheat is varied from 5 to 15 K. The minimum suction superheat was set to ensure no condensation during compression. While the maximum suction superheat is limited by the suction pressure, as this is reduced to create the superheat.

$T_{sh,\ comp}$ [K]	5	10	15
P_{dis} [kPa]	5700	5700	5700
P_{suc} [kPa]	839.2	841.9	753.7
T_{suc} [°C]	76.60	81.74	81.95
COP [-]	3.942	4.066	4.076
Heat delivered [kW]	363.05	355.02	285.0
Work [kW]	92.09	87.32	69.93
IHX [kW]	26.10	19.65	4.20
η_{comp} [%]	67.54	70.37	76.35
π [-]	6.79	6.77	7.56
T_{dis} [°C]	184.40	186.51	187.61
$\dot{m}_{butane}$ [kg/s]	0.968	0.913	0.716
$\dot{m}_{oil}$ [kg/s]	1.980	1.936	1.554
$\dot{m}_{water}$ [kg/s]	21.521	21.268	17.084
$\rho_{butane,\ suc}$ [kg/m^3]	20.16	19.71	17.23

Table 12: Results when changing compressor suction superheat

It was found that the system was able to run within the range of the superheat, there was no condensation even 5 K suction superheat.

To vary the suction superheat the simulation converges the suction pressure. As can be seen in table 12 the suction pressure is reduced significantly to produce 15 K superheat. This leads to a relatively large pressure ratio which leads to a reduced butane flow rate. The low saturation temperature and butane flow rate leads to a large amount of superheat being produced in the evaporator, and the amount of heat delivered in the IHX is reduced. There is a reduction in the butane flow rate which leads to a drastic reduction in the amount of heat delivered at 15 K superheat, seen in figure 36b. This is partially due to the reduced butane density at the compressor inlet. As the pressure ratio increases so does the compressor efficiency. However, with increasing pressure ratio the isentropic compressor work increases, and the actual specific work increases.

There is only a minor variation in the COP when changing the suction superheat. Notably at 5 K there is a drop in the COP. As can be seen in table 12 the compressor efficiency is the lowest at 5 K superheat, even though the pressure ratio is higher at 5 K superheat than at 10 K. This shows that not only the pressure ratio effects the compressor efficiency, but also the amount of suction superheat is an important factor.

It is interesting to note that there is only a minor increase of the discharge temperature when changing the suction superheat. Even with increased suction superheat the actual temperature into the compressor is relatively stable. This indicates that suction superheat along doesn't decide the discharge temperature, but a combination of several parameters.

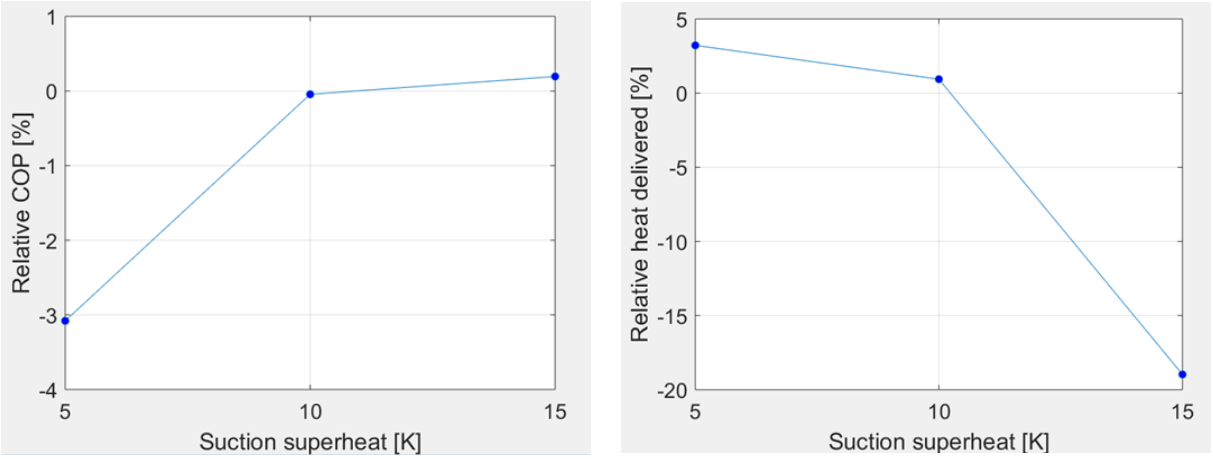

(a) Relative change in COP

(b) Relative change in delivered heat

Figure 36: Relative change in performance at 5700 kPa, at varying suction superheat

8.3 Variation of supply water outlet temperature

When running the system the amount of delivered supply water is expected to vary. In this simulation the effect of the varying the temperature at the outlet of the evaporator is examined. As the temperature of the outlet water varies the evaporator solves for the water flow rate, and the two parameters may be correlated. Lower water outlet temperature means a more efficient usage of the process waste heat, as long as the COP of the heat pump is maintained.

While keeping the supply water inlet temperature constant at 80°C the outlet temperature is varied from 72 to 78°C. The suction temperature into the compressor is set to 10 K superheat. The discharge pressure is constant at to 6100 kPa, the point of highest COP of the standard cycle. The range 72 to 78°C is where the simulation converged given the settings. At higher outlet temperature the amount of water needed would be far too large, and at lower outlet temperature the required pressure ratio would be too large for the compressor, due to the low evaporation temperature.

As can be seen in table 13, the change in the water temperature has an effect on the butane suction temperature. As the evaporator temperature is decreased, the heat delivered in the evaporator is reduced, which leads to a reduced suction temperature. To compensate, and keep the superheat constant, the suction pressure is reduced. A lower suction pressure increases the pressure ratio which reduces the mass flow. This leads to a reduction in the amount of heat delivered compared to the normal cycle. There is about a 2% drop in heat delivered by each degree of reduction in water outlet temperature. As the temperature is increased, the reverse happens. The suction pressure is increased and the pressure ratio is reduced, leading to a larger mass flow of butane, and there is a slight increase in the amount of heat delivered. This can be seen in figure 38.

Water outlet pressure	72	78
$T_{sh,\ comp}$ [K]	10	10
P_{dis} [kPa]	6100	6100
P_{suc} [kPa]	774.92	852.09
T_{suc} [kPa]	78.14	82.27
COP [-]	3.991	4.077
Heat delivered [kW]	306.47	357.49
Work [kW]	76.78	87.69
η_{comp} [%]	74.38	71.61
π [-]	7.87	7.16
T_{dis} [°C]	189.07	189.99
$\dot{m}_{butane}$ [kg/s]	0.793	0.916
$\dot{m}_{oil}$ [kg/s]	1.671	1.950
$\dot{m}_{water}$ [kg/s]	6.846	32.144

Table 13: Shows results from variation of evaporator water outlet temperature

There is only a small variation in the COP, which is the result of a variation of the pressure ratio. At lower water temperature the suction pressure is reduced, leading to a larger pressure ratio and higher efficiency. The specific compressor work increases and the COP is slight reduced at lower water outlet temperature.

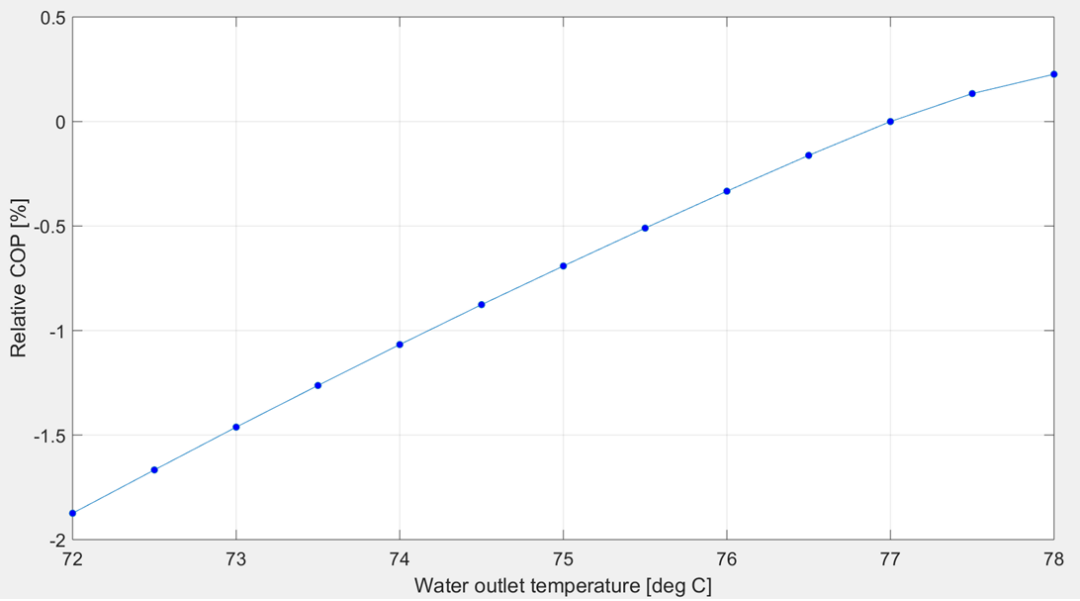

Figure 37: Relative COP at varying water outlet temperature

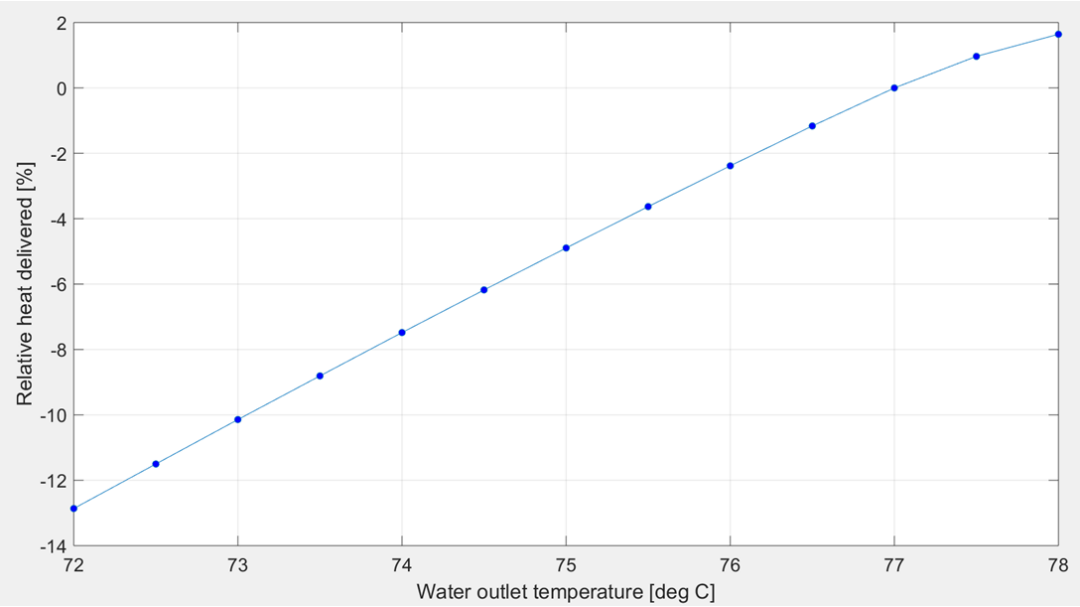

Figure 38: Relative heat at varying water outlet temperature

As seen in figure 39, with increasing water outlet temperature there is a steep increase in the required amount of water. As the water temperature increases, the temperature of the butane after the evaporator also increases. To keep the superheat at 10 K the saturation pressure is increased. This reduces the pressure ratio of the compressor, which increases the butane mass flow rate. As the butane mass flow is increased even more heat is required in the evaporator, and the amount of water has to further increase. This leads to the water flow rate to increase disproportionately to the change in water temperature.

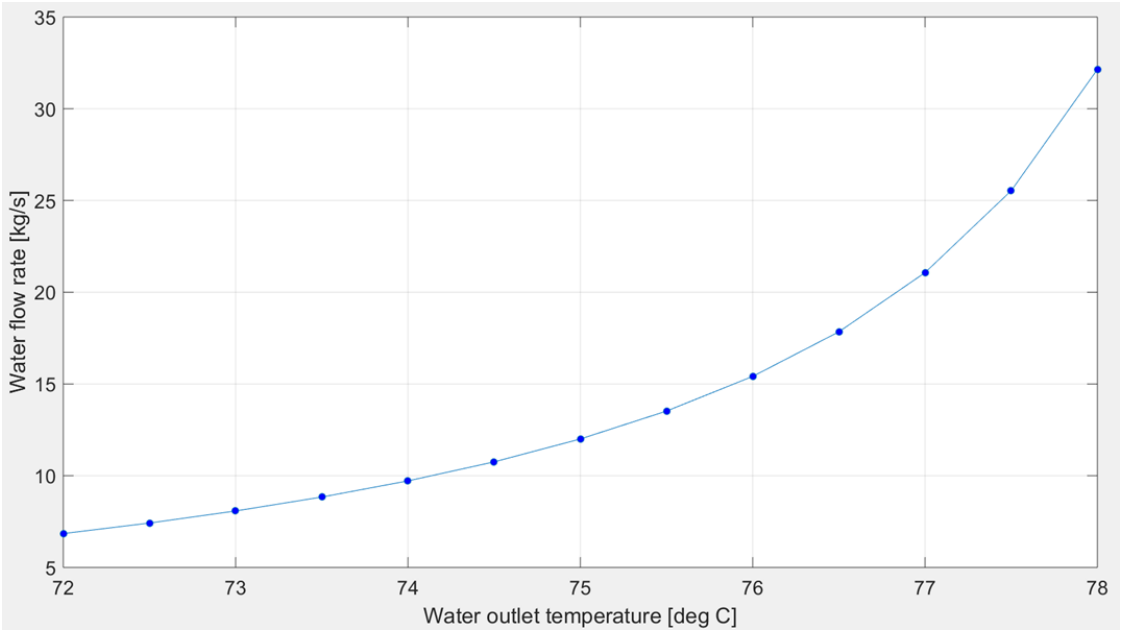

Figure 39: Variation of water flow rate when varying water outlet temperature

As with the variation in the suction superheat, there is a minimal change in the discharge temperature when varying the water temperature. Again suggesting that the discharge

pressure and the pressure ratio more important for determining the discharge temperature.

8.4 Effect of reducing compressor rpm

The design point of the compressor is at 30 K superheat and a suction pressure of 906.2 kPa. In the current project a suction superheat of 10 K is used, therefore the point of best compressor performance is going to change. In this simulation 90% rpm of the turbo compressor is examined to see how the changes in the compressor may effect the cycle, and if the COP might be improved.

In the simulation the discharge pressure is in the range 4500 to 5200 kPa, the range where the simulation converges. The demanded discharge temperature is 170°C which limits the minimum discharge pressure. The maximum pressure ratio of the compressor at 90% rpm is significantly smaller than while working at 100% rpm, which gives the limit for the maximum discharge pressure, it varies depending on the input. The point of highest COP is found at discharge pressure of 4600 kPa, this point along with the highest and lowest discharge pressure is shown in table 14.

P_{dis} [kPa]	4500	4600	5200
P_{suc} [kPa]	876.7	875.3	852.1
COP	4.726	4.731	4.674
Heat delivered [kW]	258.40	255.54	212.76
Work [kW]	54.68	54.01	45.52
η_{comp} [%]	76.00	76.66	79.85
π [-]	5.13	5.26	6.10
T_{dis} [°C]	170.62	171.96	179.15
$\dot{m}_{butane}$ [kg/s]	0.695	0.685	0.5630
$\dot{m}_{oil}$ [kg/s]	1.410	1.394	1.1603
$\dot{m}_{water}$ [kg/s]	16.186	16.006	13.290

Table 14: Selected results from variation of discharge pressure at 90% rpm.

Figure 40 and 41 show the trend of the results. It is clear that the COP is much larger when the compressor is working at 90% rpm than in the standard cycle. The COP is increased with as much as 16%. The increase in COP mainly comes from the increase in the compressor efficiency which is at best increased with 11%. The rest of the improvement comes from the reduction in isentropic compressor work. Since the reference point has a discharge pressure at 6100 kPa and a pressure ratio of 7.23 the required specific work is much larger than with a pressure ratio of 5.26 which is required for the discharge pressure of 4600 kPa at 90% rpm. Since the performance of the compressor is improved at significantly lower pressure ratio, the low isentropic work at lower pressure ratio can be exploited. When reducing the rpm of the compressor to 90% the amount of friction loss in the compressor can be reduced by up to 19% [Nishida, 2017], which may account for most of the improvement in compressor efficiency.

The performance at 90% rpm is improved from 4500 kPa to 4600 kPa discharge pressure. There is a slight increase in the compressor efficiency, along with an increase in the compressor discharge temperature. A higher discharge temperature, especially when close to

170°C, is beneficial to the gas cooler performance, along with the higher heat capacity at high temperatures. When further increasing the discharge pressure, the compressor efficiency keeps increasing, but not sufficiently to compensate for the increase in the required isentropic work, giving a reduction in COP at higher discharge pressure.

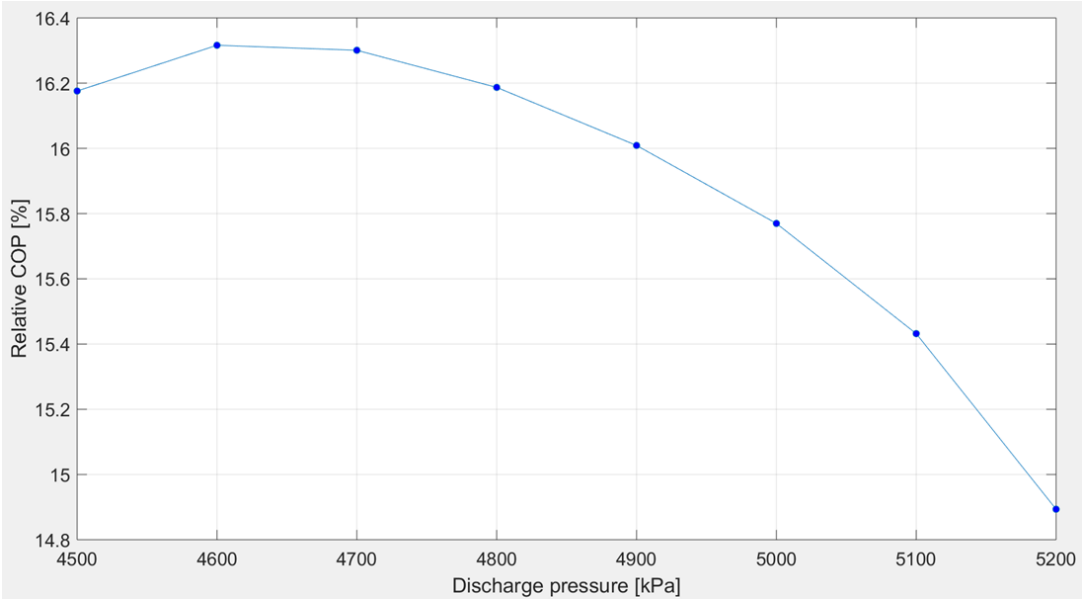

Figure 40: Relative COP with compressor at 90% rpm

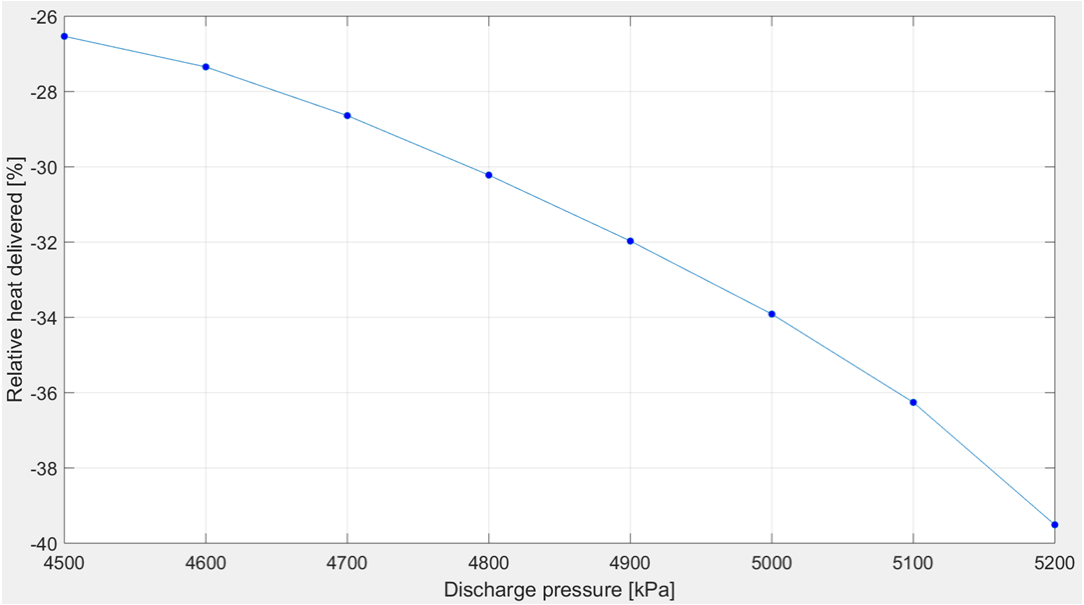

Figure 41: Relative delivered heat with compressor at 90% rpm

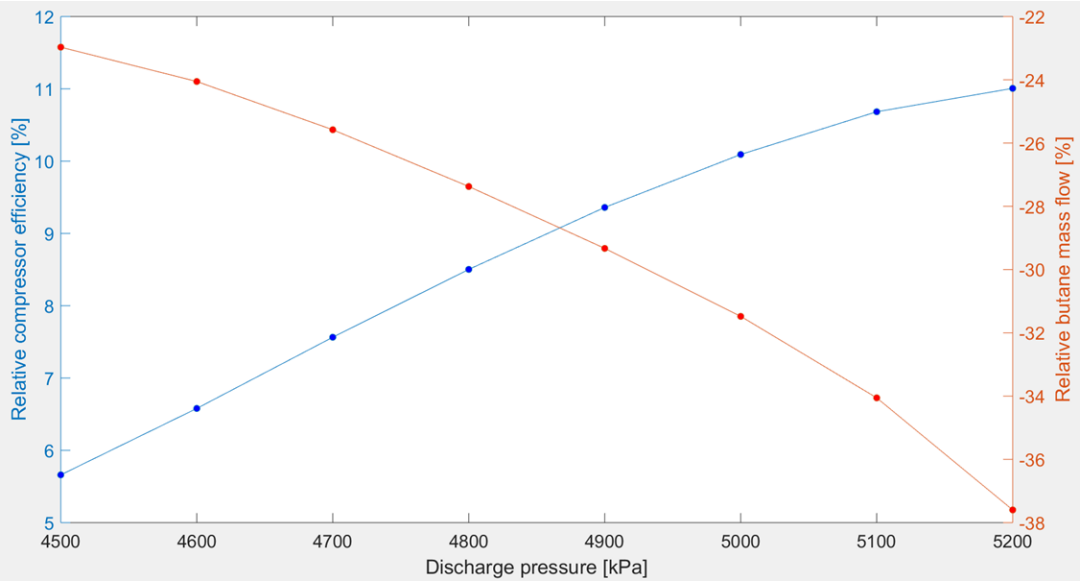

Figure 42: Relative compressor efficiency and butane mass flow with compressor at 90% rpm

The COP of the system is much higher with the compressor running at 90% rpm. Since the only change is the compressor rpm this clearly has a large effect. At reduced rpm the characteristics of the compressor changes. The mass flow through the compressor is reduced, while the efficiency is increased. The maximum pressure ratio is also significantly reduced. While the efficiency of the compressor is significantly increased, the amount of delivered heat is significantly reduced, as can be seen in figure 41. Comparing the reduction in heat to the relative mass flow rate in figure 42 it is clear that most of the reduction comes from a reduction in the butane mass flow rate. The reduced discharge pressure reduces the heat capacity at high temperature, and reduces the discharge temperature. Together they further reduce the amount of heat delivered compared to the reference point.

8.5 Effect of running cycle without internal heat exchanger

The cycle is examined without the IHX to examine its performance. The superheat into the compressor is kept at 10 K. The discharge pressure is in the range 4300 to 6400, using the minimum discharge temperature of 170°C and a maximum pressure ratio of 8. In this simulation the pressure loss in the pipelines from the evaporator to the compressor is ignored.

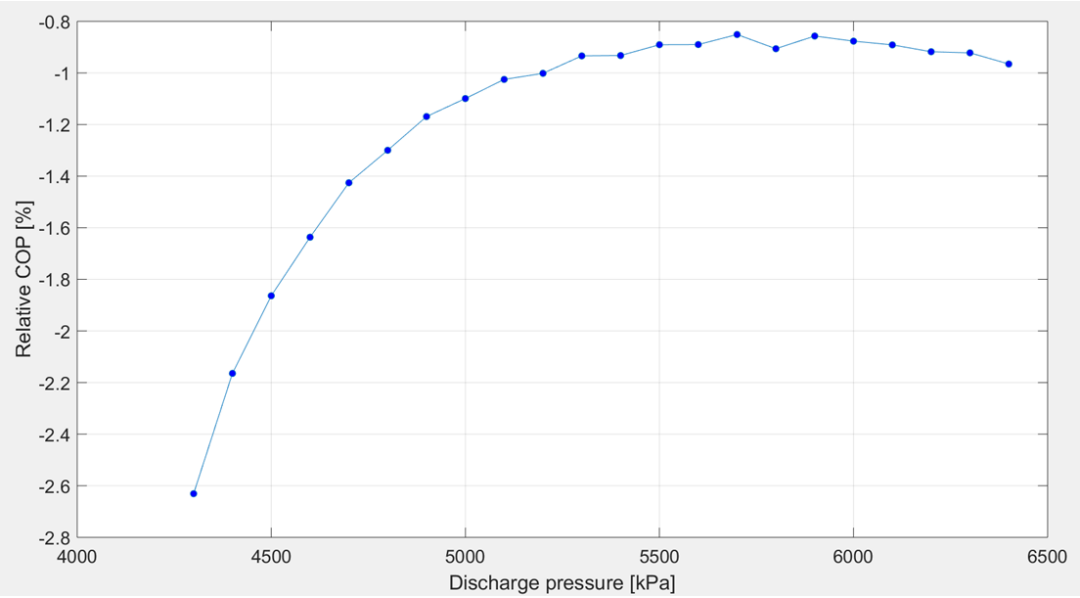

Figure 43: Relative COP without IHX

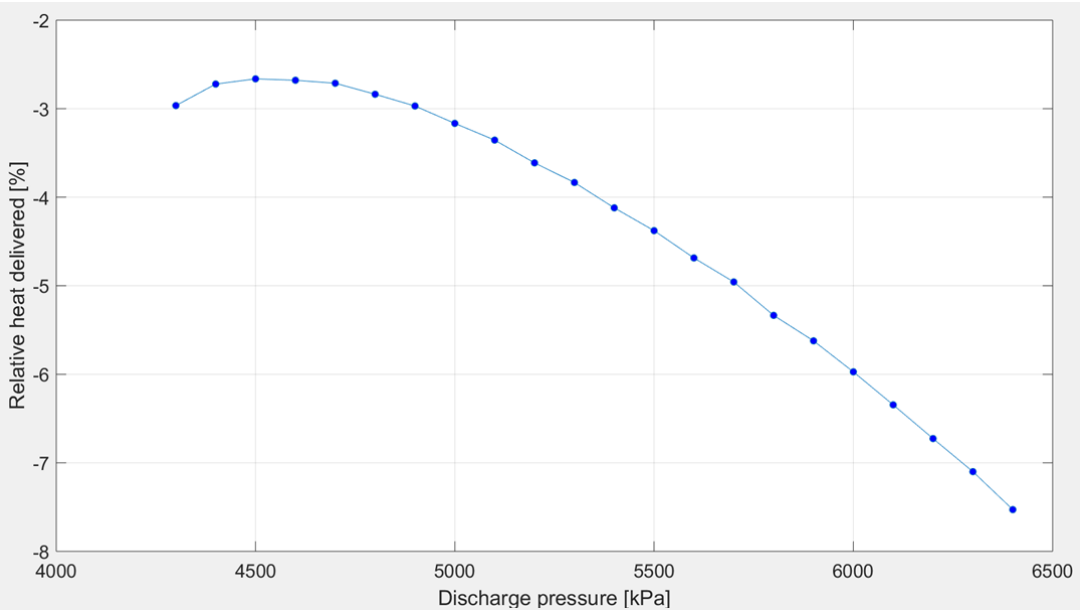

Figure 44: Relative heat delivered without IHX

The superheat into the compressor is fixed to be 10 K. Without the IHX there is no further heating after the evaporator. Since there is no variation in the temperature of the heating water in the evaporator there is only a small change in the temperature of the butane into the compressor. This means that the suction pressure is close to constant even with a large change in the discharge pressure. The suction pressure has only a variation of $\pm$ 0.04 kPa from 809.3 kPa.

Examining the results in table 15. To ensure the superheat of 10 K, the suction/saturation pressure is reduced. The low and almost constant suction pressure makes the pressure ratio increase, close to linearly. At increasing pressure ratio the flow rate of butane is reduced, this is clearly noticeable in the reduced heat delivered at higher discharge pressure. The

COP is increasing at higher discharge pressure. At low discharge pressure this is from the increase in discharge temperature which is required for good performance in the gas cooler, and the increased heat capacity at higher temperature. At increased pressure ratio the compressor performance is improved, but the isentropic work increases.

Without the IHX less of the high quality heat on the high pressure side is utilized, and the throttling loss from the expansion valve is increased. The gas quality into the evaporator is increased, as can be seen in table 15. While in fluid entering the evaporator in the reference simulation is liquid. Due to this less heat can be absorbed in the evaporator which has an effect on the system. Figure 45 shows the change in heat transfer in the heat exchanger in the standard heat pump cycle with IHX. As can be seen the amount of heat transferred in the IHX is reducing with increasing discharge pressure, indicating that the effect of the IHX is decreasing.

There is some reduction in the amount of heat delivered in the system without IHX compared to the reference simulation. As the discharge pressure increases, the difference becomes more noticeable. This is from the reduction in butane mass flow with increasing pressure ratio, due to the low suction pressure.

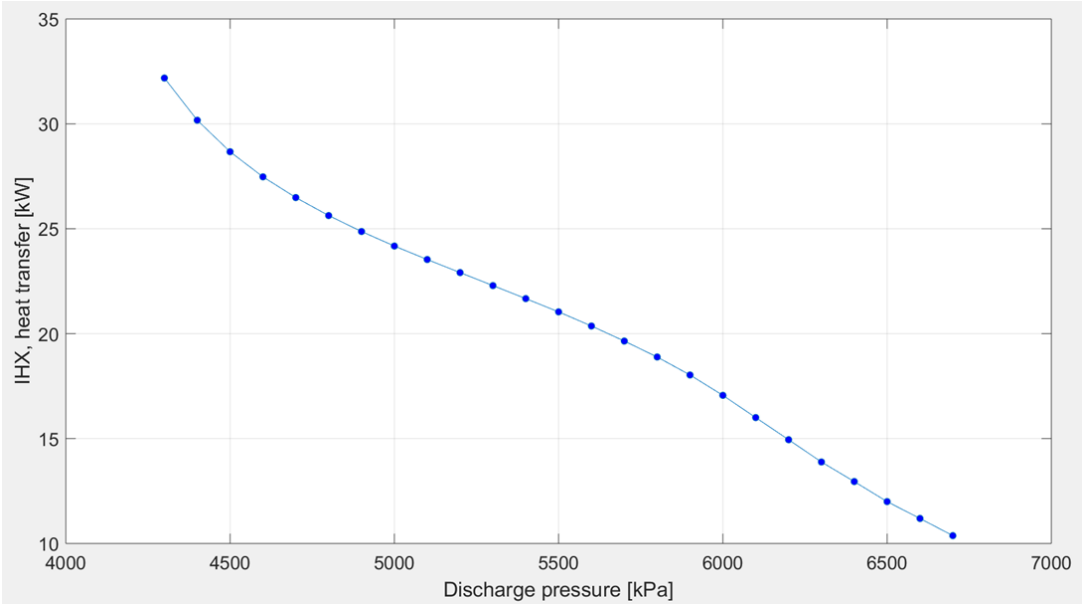

Figure 45: Heat transferred by IHX at varying discharge pressure

P_{dis} [kPa]	4300	5700	6400
P_{suc} [kPa]	809.3	809.3	809.3
COP	3.961	4.033	4.028
Heat delivered [kW]	341.29	334.28	325.24
Work [kW]	86.179	82.89	80.74
η_{comp} [%]	64.61	71.60	74.21
π [-]	5.31	7.04	7.91
T_{dis} [°C]	170.09	186.12	191.69
Evaporator gas quality [-]	0.1506	0.1213	0.1178
$\dot{m}_{butane}$ [kg/s]	0.904	0.863	0.836
$\dot{m}_{oil}$ [kg/s]	1.862	1.822	1.773
$\dot{m}_{water}$ [kg/s]	20.263	19.974	19.429

Table 15: Highest COP result along with highest and lowest discharge pressure, without IHX.

8.6 Design point

The design point of the heat pump system is to produce oil at 180°C with a discharge pressure of 5700 kPa. In this simulation the oil temperature goes from 100 to 180°C. The superheat is at 30 K. The results are shown in table 16.

Oil temperature [°C]	100 - 180
$T_{sh,\ comp}$ [K]	30
P_{dis} [kPa]	5700
P_{suc} [kPa]	842.2
COP [-]	3.833
Heat delivered [kW]	249.50
Work [kW]	65.09
η_{comp} [%]	79.73
π [-]	6.77
T_{dis}[°C]	196.26
$\dot{m}_{butane}$ [kg/s]	0.660
$\dot{m}_{oil}$ [kg/s]	1.319
$\dot{m}_{water}$ [kg/s]	14.643
$\rho_{butane,\ suc}$ [kg/m^3]	18.00

Table 16: Results from simulation at the design point

At the design point the cycle is able to produce heat at a COP above 3.8 which satisfies the goal of the system. Considering the high temperature and the large temperature lift in the system this is very promising. The delivered amount of heat however is at 249.5 kW which is significantly below the goal of 300 kW. The discharge temperature is sufficiently high. As seen in earlier results it's beneficial to have a discharge temperature more than 10 K above the required temperature in the gas cooler. This shows that the system is able to produce heat at such high temperatures.

Again the performance of the compressor changes when changing the suction superheat. The compressor efficiency is very good at 79.73%, but the butane mass flow is lacking. Due to the low mass flow the amount of heat delivered in the gas cooler is reduced. The butane mass flow is reduced by 26.9%, part of this reduction is due to reduced butane density at the compressor inlet, which is reduced by 8.6%. The rest of the difference is due to changes in the compressor performance. The reduction in COP at the design point is due to the relatively large isentropic work at high suction temperature, even with a very high compressor efficiency.

Compared to the simulation where 15 K superheat was tested here the compressor suction pressure is higher. At 15 K superheat the suction pressure had to be reduced to increase the superheat. While at design point and 30 K superheat the gas cooler outlet temperature is higher, and therefore more heat is delivered in the gas cooler, increasing the suction temperature, which allows the suction pressure to remain relatively high. In this simulation the amount of heat transferred in the IHX is 32.4 kW, which is high compared to most of the other simulations.

Figure 46 shows the ts diagram of the heat pump working at design point, using results found by the simulation. It can be seen that the IHX performs well, and increases the suction temperature significantly.

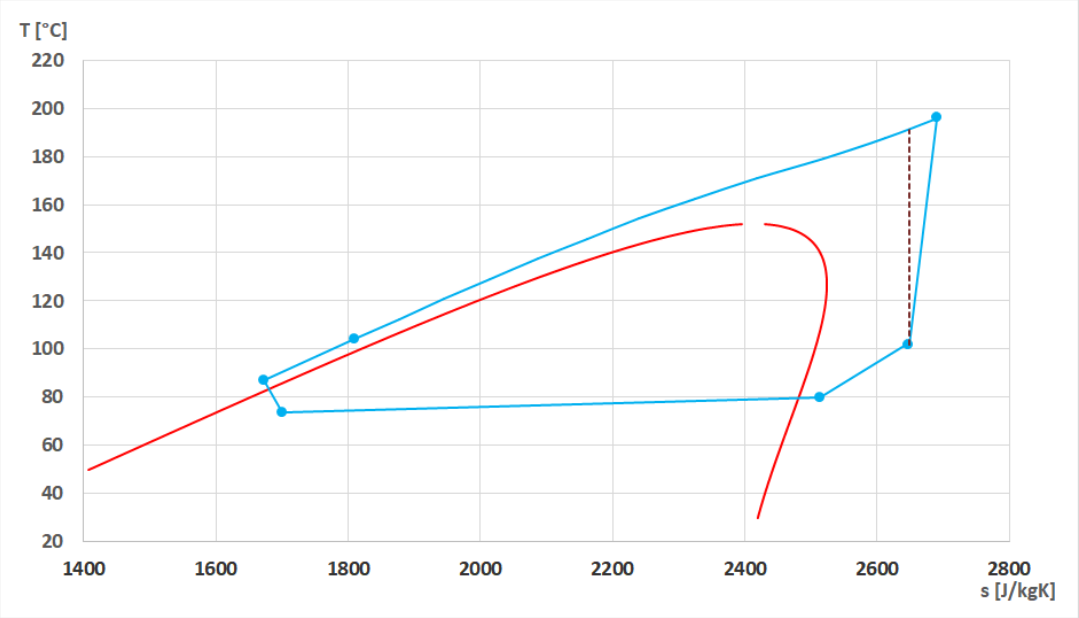

Figure 46: Ts diagram of the cycle at design point

8.7 Component Results

8.7.1 Compressor results

The compressor is tested at both 90% and 100% rpm. Table 17 shows the input used and some of the results.

Suction pressure [kPa]	852.1
Suction temperature [°C]	82.26
Suction superheat [K]	10
Discharge pressure [kPa]	4800
π [-]	5.63
Discharge temperature 100% rpm [°C]	179.37
Discharge temperature 90% rpm [°C]	174.34
η_{comp} 100% rpm [%]	68.29
η_{comp} 90% rpm [%]	78.59

Table 17: Input and result running compressor at 90% and 100% rpm

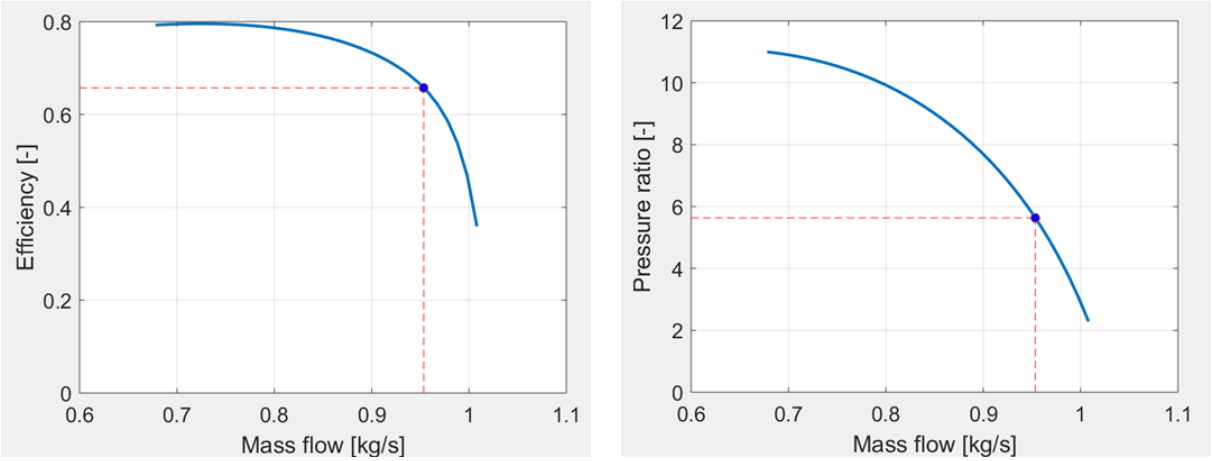

(a) Compressor efficiency vs mass flow (b) Compressor pressure ratio vs mass flow

Figure 47: Compressor results at 100% rpm

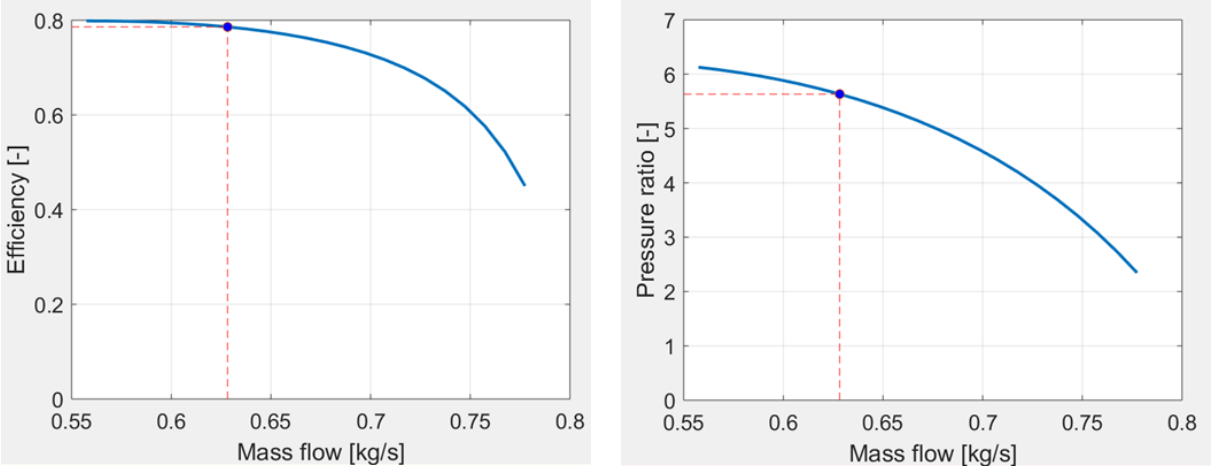

(a) Compressor efficiency vs mass flow (b) Compressor pressure ratio vs mass flow

Figure 48: Compressor results at 90% rpm

The performance of the compressor is influenced by the suction temperature, suction pressure, discharge pressure and rpm. The suction temperature, suction pressure and the rpm

decides the shape of the curves as seen in figure 47 and 48. The discharge pressure/pressure ratio decides which point along the curve serves as a solution.

In figure 47 and 48 efficiency, pressure ratio and mass flow can be correlated together. As the required pressure ratio increases the mass flow is reduced, at the same time the efficiency is increased.

Comparing the results in figure 47 and 48 there are some clear differences between the performance at 90% and 100% rpm. The maximum pressure ratio when working at 90% rpm is much lower than when working at 100%. This limits the maximum discharge pressure and the potential discharge temperature, which limits the potential temperature of the heat pump cycle. The butane mass flow rate is also much lower at 90% rpm. The efficiency however is increased. The performance at both 100% rpm has a small range of mass flow variation, as the viable pressure ratio range covers a relatively small area.

8.7.2 Evaporator

Table 18 shows the input used to test the evaporator.

Water temperature [°C]	80-77
Butane inlet temperature [°C]	75.39
Butane inlet pressure [kPa]	914
$\dot{m}_{\text{butane}}$ [kg/s]	0.902
$\dot{m}_{\text{water}}$ [kg/s]	21.079

Table 18: Shows input used to run evaporator

Figure 49 shows the temperature distribution in the evaporator of both the butane and water side. The water temperature is set to be 80°C at the inlet, and 77°C at the outlet, the water flow rate is then varied to ensure the water temperature at the outlet. For the evaporator to be able to converge there has to be some minimum temperature difference between the butane and the water, due to this the butane inlet pressure rarely exceeds 920 kPa.

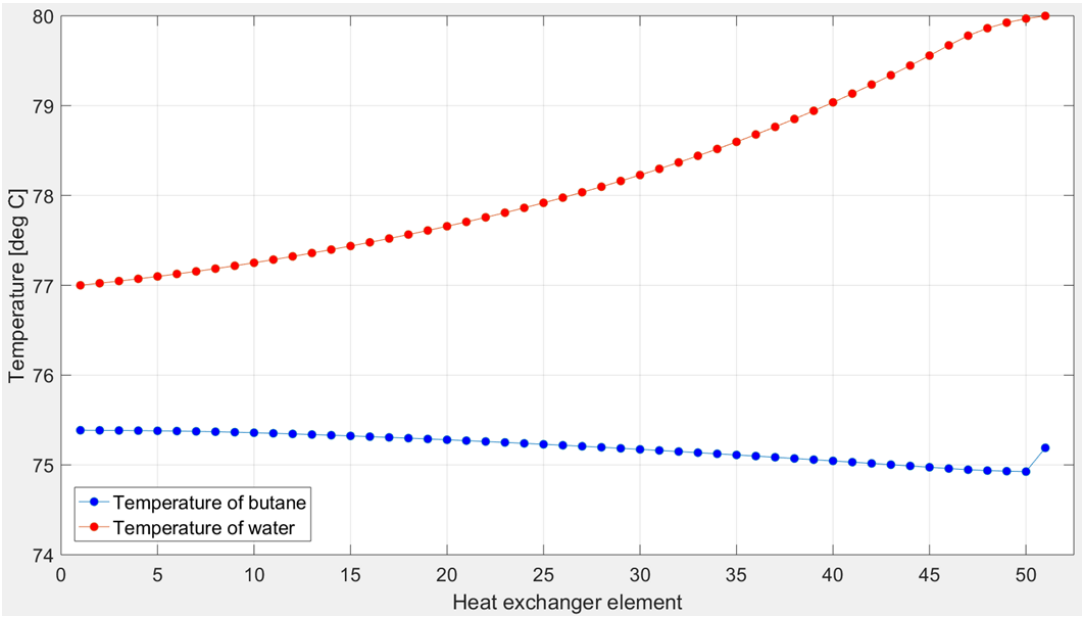

Figure 49: Temperature distribution in evaporator

There is a small pressure loss in the evaporator on both the water and the butane side(shown in figure 51). As the pressure is reduced on the butane side, the saturation temperature of the butane is also reduced. Because of this there is a slight reduction in the temperature of the butane, even with increasing enthalpy. In figure 49 the heat given from the water is used mainly as latent heat for the butane, increasing the gas quality. Finally in the last heat exchanger element the butane becomes single phase gas, and the heat is used to increase temperature. The temperature pinchpoint is at the water outlet and butane inlet side.

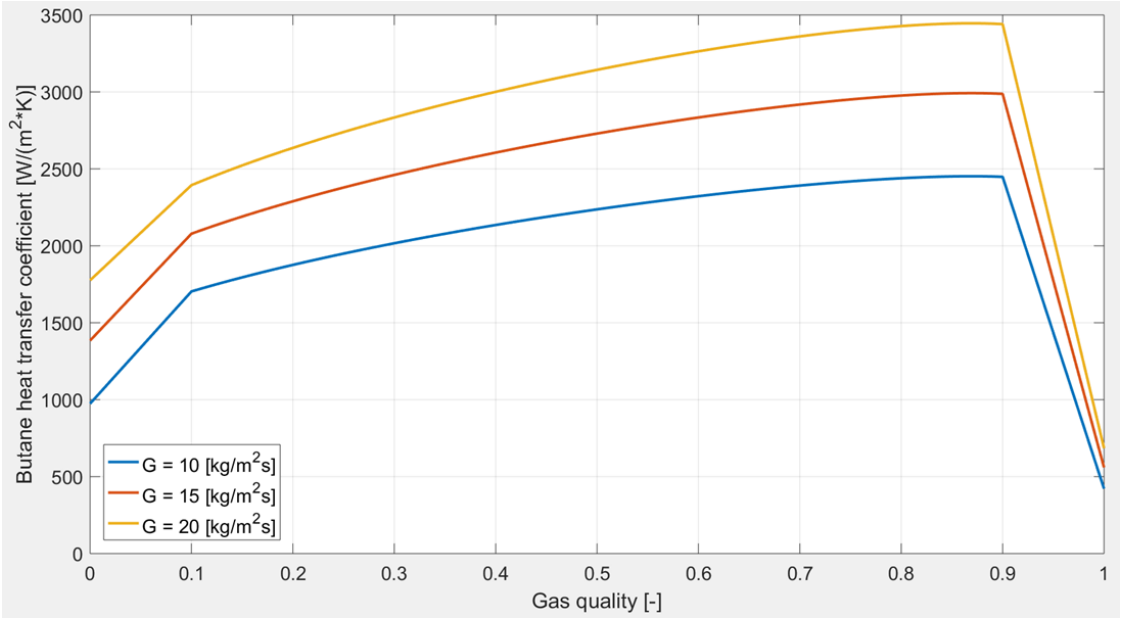

Figure 50: Heat transfer coefficient of butane at varying gas quality and mass flux

Figure 50 shows the butane heat transfer coefficient depending on gas quality, with different mass flux. In the evaporator the forced convection term is the dominant part of the heat

transfer. When the mass flux is increased the Reynolds number increases meaning more turbulent flow, and increased forced convection. When the gas quality is increased the viscosity of the butane is reduced, also increasing the Reynolds number and the heat transfer coefficient. Finally when nearing single phase gas, the dryout of the evaporator reduces the heat transfer coefficient. Figure 52 shows the heat transfer coefficient as found by Mayekawa using the Alfa Laval simulation tool. The results correspond well to the results found with the simulation tool. The same trend can be seen in the pressure drop of the evaporator in figure 51. Here the pressure drop in each element of the evaporator is increasing, until there is dryout.

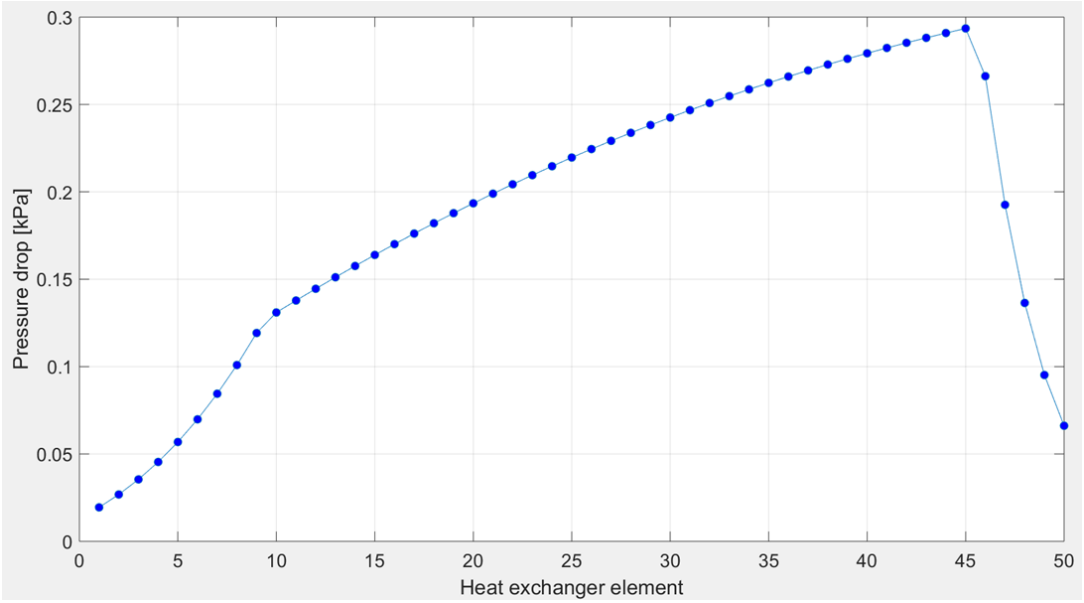

Figure 51: Butane pressure drop in evaporator

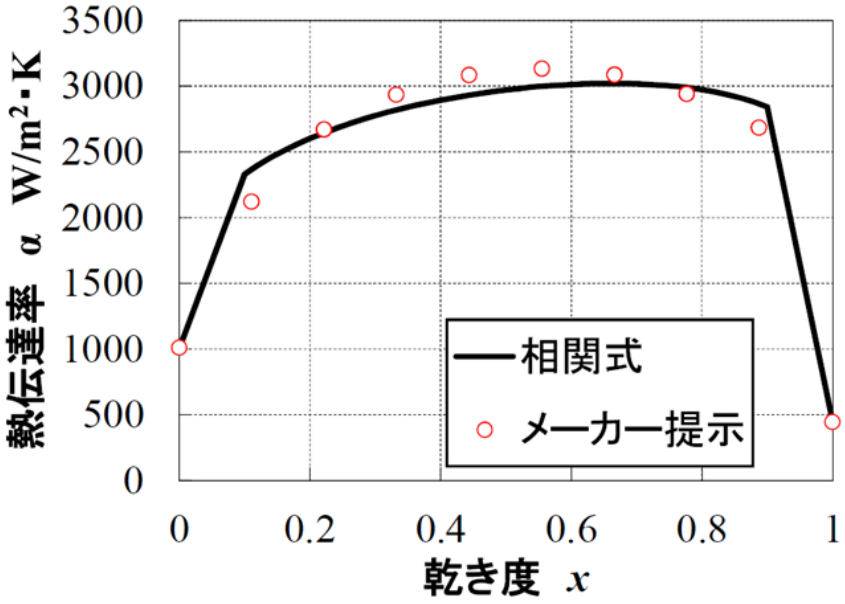

Figure 52: Heat transfer coefficient as found by Mayekawa

8.7.3 Gas cooler

The gas cooler is tested at oil temperature at 80-160°C and 100-180°C. Table 19 and 20 shows the input used and some of the results when testing the gas cooler in the simulation.

Oil temperature [°C]	80-160
Butane inlet temperature [°C]	189.86
Butane inlet pressure [kPa]	6097
$\dot{m}_{\text{butane}}$ [kg/s]	0.902
$\dot{m}_{\text{oil}}$ [kg/s]	1.917
Heat transfer [kW]	351.52

Table 19: Shows input and results from gas cooler while heating oil at 80-160°C

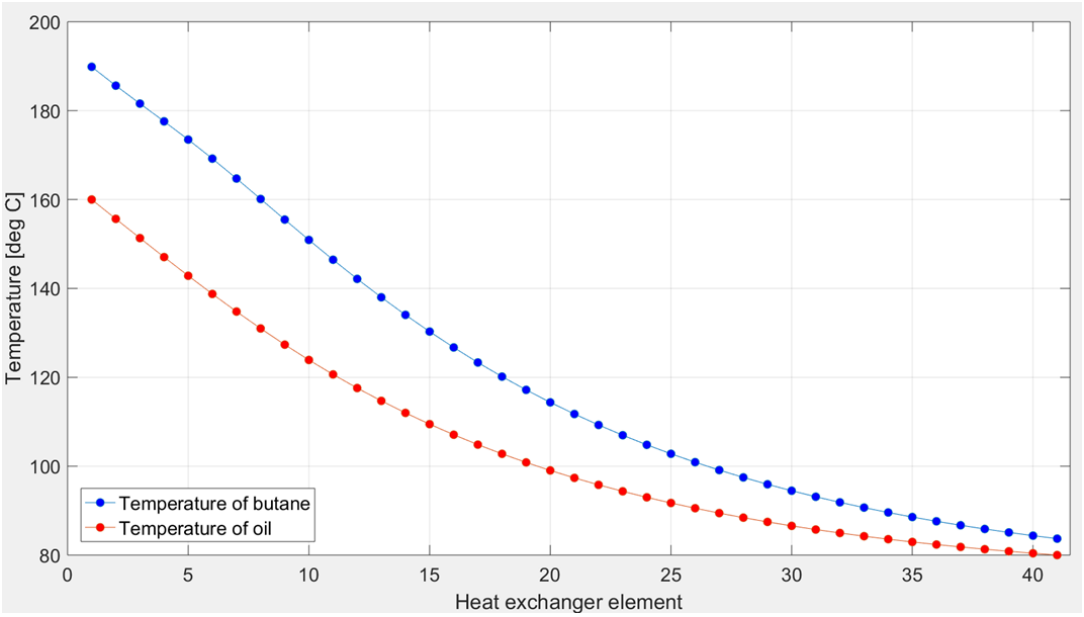

Figure 53: Temperature distribution in gas cooler. Heating oil at 80 to 160°C.

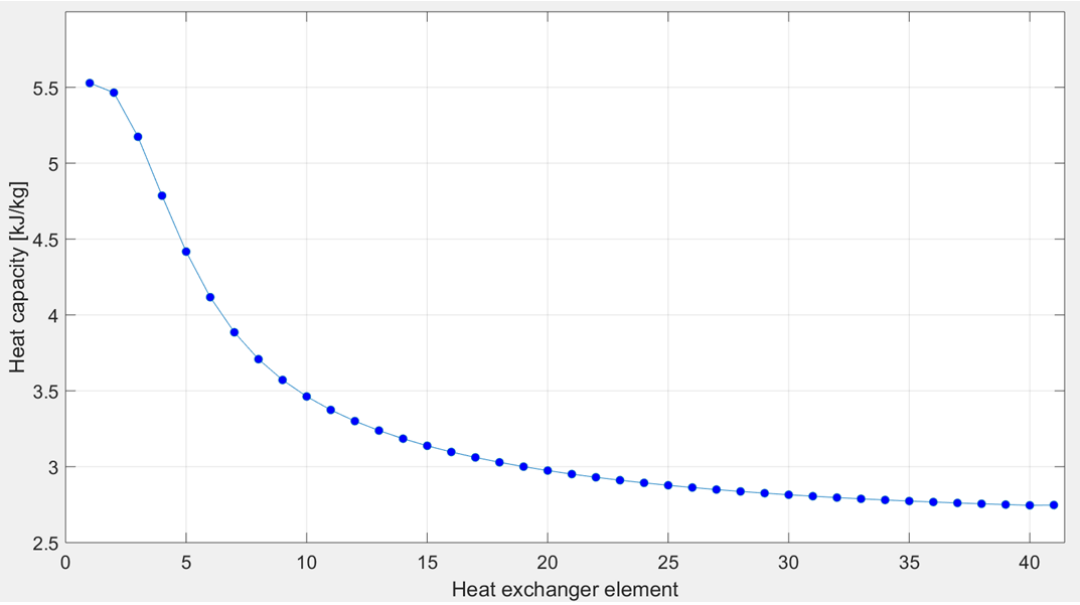

Figure 54: Heat capacity of butane. Heating oil at 80 to 160°C.

The pseudo-critical point of 6097 kPa is 182.2°C. The specific heat capacity drops sharply in the first heat exchanger elements as shown in figure 54. Meaning that there is a large heat transfer potential at the highest temperature. In this result only part of the high heat capacity at high temperature can be utilized, and it may be beneficial to either reduce the gas cooler pressure, or increase the inlet temperature, to be able to utilize the potential of the heat capacity better.

Oil temperature [°C]	100-180
Butane inlet temperature [°C]	196.25
Butane inlet pressure [kPa]	5697.9
$\dot{m}_{\text{butane}}$ [kg/s]	0.660
$\dot{m}_{\text{oil}}$ [kg/s]	1.319
Heat transfer [kW]	249.51

Table 20: Shows input and results when testing gas cooler while heating oil at 100-180°C

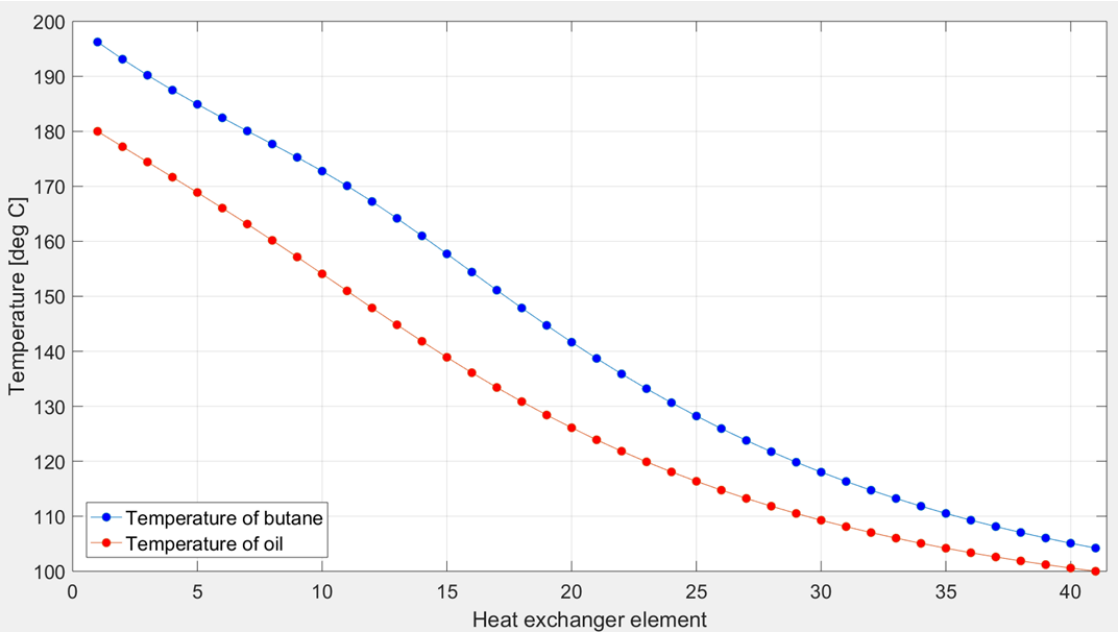

Figure 55: Temperature distribution in gas cooler. Heating oil at 100 to 180°C.

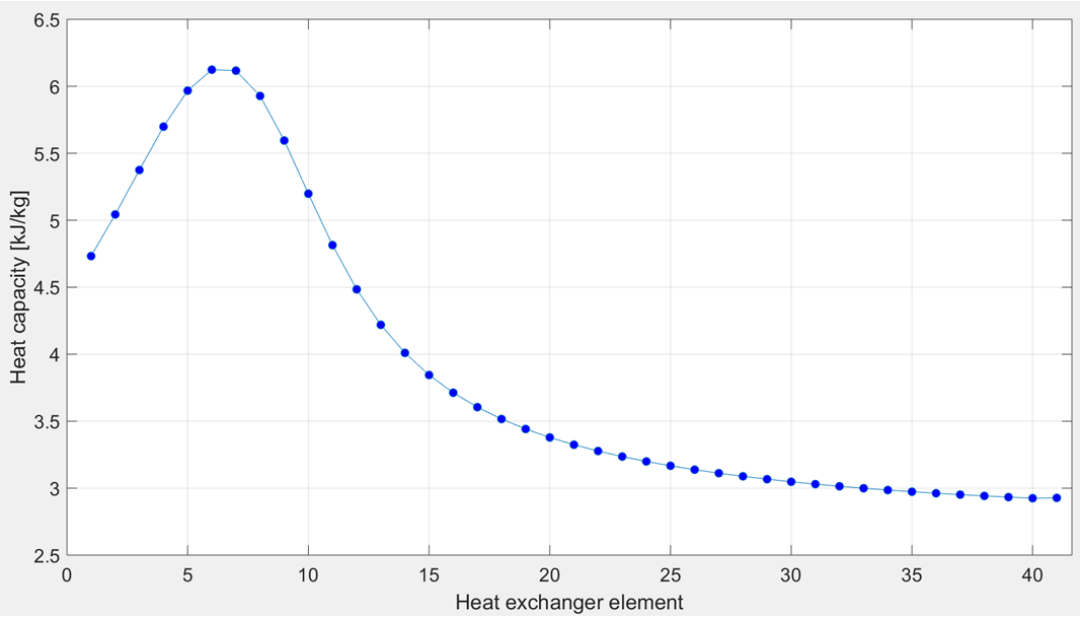

Figure 56: Heat capacity of butane in gas cooler. Heating oil at 100 to 180°C.

At 5697.9 kPa the pseudo-critical temperature is 177.7°C. Here the butane inlet temperature is increased compared to the result in figure 53. With an increased butane inlet temperature more of the high heat capacity at high temperature is utilized. Also here the heat capacity is large around high temperature, and the oil can be heated to a high temperature with almost constant temperature difference between the butane and the oil.

As can be seen in both figure 53 and 55, the pinchpoint is at one of the ends of the heat exchanger. The amount of oil mass flow is a free variable in the simulation. This leads to that the amount of oil mass flow is linearly correlated to the amount of heat delivered in the gas cooler.

8.7.4 IHX

Table 21 shows the input used to test the IHX, with some of results.

HP inlet temperature [°C]	83.66
LP inlet temperature [°C]	75.17
HP inlet pressure [kPa]	6067.2
LP inlet pressure [kPa]	905.14
$\dot{m}_{\text{butane}}$ [kg/s]	0.902
Heat transfer [kW]	15.54
Pressure loss LP side [kPa]	27.84

Table 21: Input used to test internal heat exchanger with some results

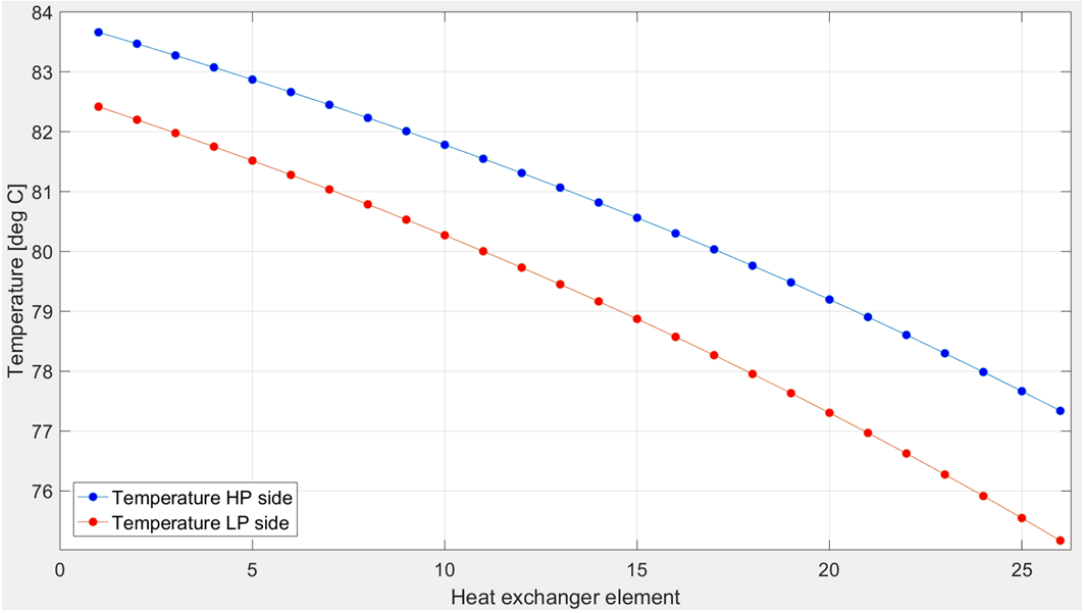

Figure 57: Temperature distribution in IHX

The temperature difference of the HP side and the LP side is almost uniform. While the temperature difference is small, the transfer of heat is effective and performed. The heat received in the IHX increases the suction temperature, ensuring that the saturation temperature can be kept high while still maintaining the suction superheat. This comes at the small cost of the pressure loss on the LP side, as shown in table 21. The pressure loss is very small compared to the otherwise required drop in pressure to ensure sufficient suction superheat. This means that the IHX may improve the compressor performance significantly.

9 Ejector

An ejector may improve the performance of a heat pump system by utilizing the expansion loss to increase the compressor suction pressure. The simulation was adapted to examine the potential of an ejector. Beside exchanging the throttling valve with an ejector, a separator is added to the system. The separator ensures that the fluid entering the compressor is in gas state, while the fluid entering the evaporator is in liquid state. The system simulated is as shown in figure 58. The goal of the simulated is to give an impression of the COP of the ejector system, and to examine whether an ejector is a viable addition to the system.

The ejector has a variable nozzle area. Meaning that the nozzle area can be changed freely within a range, this makes it possible for the user to define the nozzle outlet pressure. In the simulation the mixer area is also freely variable, in each simulation the mixer area is converged. The results may then be examined and a suggestion can be made regarding the actual fixed mixer area.

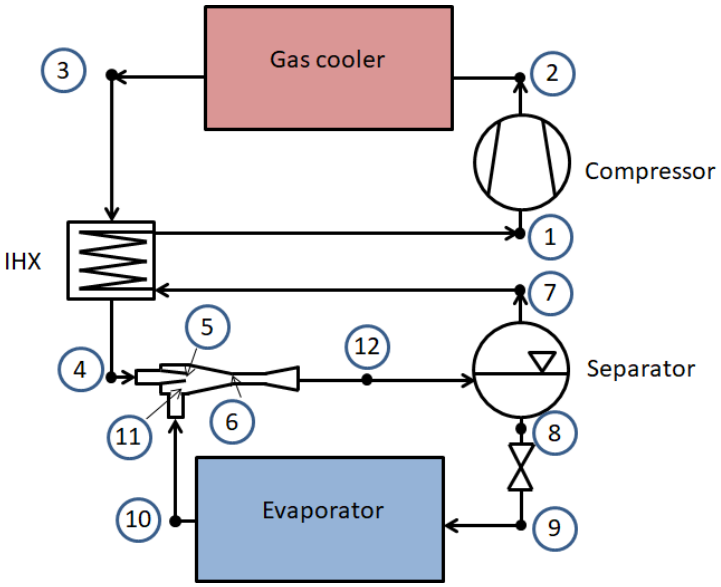

Figure 58: Principle model of the heat pump cycle with ejector

In the ejector system the compressor suction pressure is increased. As seen in previous results the compressor had a good performance at low pressure ratio when running at 90% rpm. Due to this, the rpm is at 90% in the ejector simulation. In this simulation the superheat is left as a free parameter. To have an advantage of the ejector the compressor suction pressure has to be variable. This is handled by using the separator to ensure that 100% saturated gas enters the IHX, while the IHX produces superheat before the butane enters the compressor. In the ejector cycle the pipe pressure loss is not included. There is no consideration of the performance of the separator, the system is only examined at steady state. Figure 59 shows an example of the log p-H diagram of the ejector cycle.

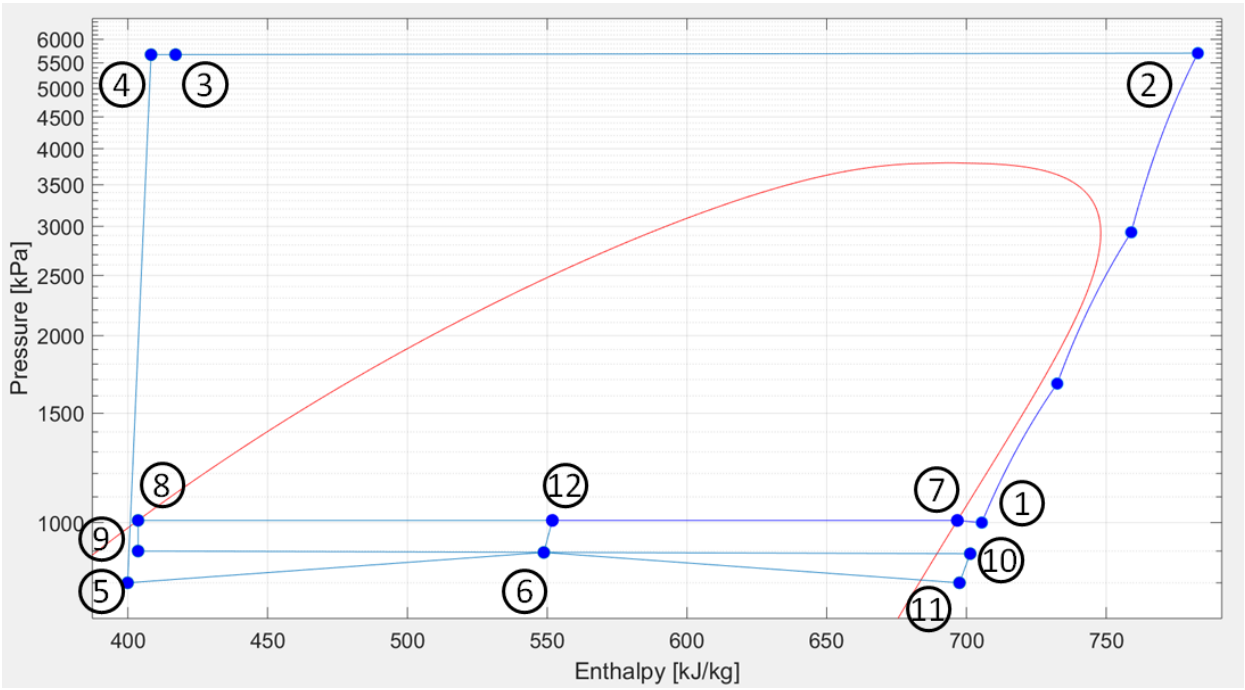

Figure 59: Log p-H diagram of ejector heat pump simulation

9.1 Simulation models

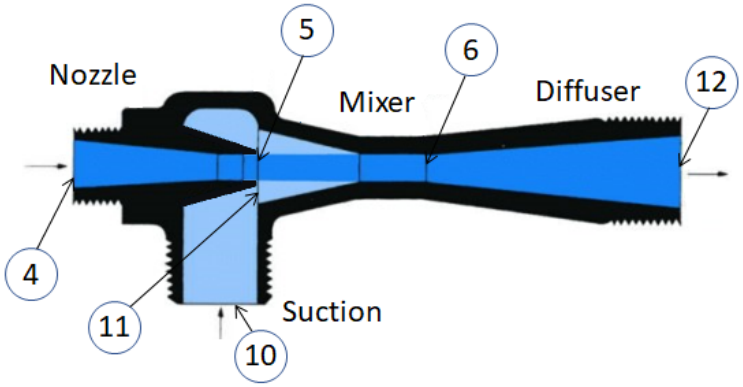

Figure 60: Illustration of ejector

Figure 60 shows the various ejector sections with point corresponding to the simulation as shown in figure 59. In the ejector there are four sections: nozzle, suction, mixer and diffuser. Each section has its own efficiency which describes how much energy of the fluid is conserved during flow through the section, shown in table 21. Table 22 shows the required input and produced output from each of the standard heat pump components.

Component	Input	Output
Compressor	π, rpm, T_1, P_1	$\dot{m}_{but}$, η_{comp}, T_2, P_2
Gas cooler	$\dot{m}_{but}$, T_2, P_2	$\dot{m}_{oil}$, Q_{GC}, T_3, P_3
IHX	$\dot{m}_{but}$, T_3, P_3, h_7, P_7	Q_{IHX}, h_1, h_4, ΔP_{HP}, ΔP_{LP}
Evaporator	$\dot{m}_{but}$, h_9, P_9	$\dot{m}_{water}$, Q_{evap}, T_{10}, h_{10}, ΔP_{evap}

Table 22: Overview of components in the ejector simulation

Component	Efficiency
Nozzle	0.85
Suction	0.85
Mixer	1
Diffuser	0.85

Table 23: Ejector efficiencies

The efficiency of the ejector sections is chosen quite freely. The study of the ejector is at this point theoretical. As discussed in the chapter 3.4.2, [Liu and Groll, 2013] presented several results regarding the efficiency of the sections in the ejector, as seen in figure 21, none of the systems used butane. Having 100% efficiency in the mixer highly simplifies the calculation as this allows for using momentum conservation across the section. The efficiencies in the equations below are defined as in [Liu and Groll, 2013]. The basis of several of the equations is shown in appendix A.4.

9.1.1 Nozzle

The adiabatic nozzle outlet enthalpy is found assuming constant entropy across the nozzle and the given outlet pressure. The outlet enthalpy is found using the efficiency of the nozzle. The nozzle outlet velocity is found using energy conservation, and the assumption that the nozzle inlet speed is 0 m/s.

$$h'_5 = h(P_5, s_5) \tag{37}$$

$$h_5 = h_4 - \eta_{noz} \cdot (h_4 - h'_5) \tag{38}$$

$$u_5 = (2 \cdot (h_4 - h_5))^{0.5} \tag{39}$$

Since the ejector is assumed to have a variable nozzle, it is possible to change the nozzle outlet pressure, the nozzle area is then found by conversion. The nozzle outlet diameter is set to converge in the range 0.0006 to 0.01 m. Conversion is done with the secant method. The conversion is done by ensuring that the mass flow in and out of the nozzle is the same. The density is decided from the enthalpy and pressure at the nozzle outlet.

$$\rho_5 = \rho(P_5, h_5) \tag{40}$$

$$\dot{m}_{noz} = \rho_5 \cdot A_5 \cdot u_5 \tag{41}$$

9.1.2 Suction

The suction area is defined as the area of the mixer minus the area of the nozzle outlet.

$$A_{11} = A_6 - A_5 \tag{42}$$

The pressure out of the suction section is the same as the outlet pressure of the nozzle, which is defined by the user.

$$P_{11} = P_5 \tag{43}$$

Assuming constant entropy across the suction section the ideal outlet enthalpy is found. The efficiency of the suction section is used to find the real outlet enthalpy.

$$h'_{11} = h(P_{11}, s_{11}) \tag{44}$$

$$h_{11} = h_{10} - \eta_{suc} \cdot (h_{10} - h'_{11}) \tag{45}$$

Finally conservation of energy is used to find the outlet velocity, with the assumption of a inlet velocity into the suction of 0 m/s.

$$u_{11} = (2 \cdot (h_{10} - h_{11}))^{0.5} \tag{46}$$

The density is calculated from the enthalpy and pressure. Then the mass flow is found.

$$\rho_{11} = \rho(P_{11}, h_{11}) \tag{47}$$

$$\dot{m}_{suc} = \rho_{11} \cdot A_{11} \cdot u_{11} \tag{48}$$

9.1.3 Mixer

The mixer area is assumed initially, and is solved for in subsequent iterations. The mixer outlet pressure is found by converging the density at the mixer outlet. The mixer outlet pressure is converged in the range 840 kPa to 1050 kPa. The outlet velocity is found using momentum conservation(eq. 49) and the enthalpy is found by energy conservation(eq. 50).

$$u_6 = \frac{P_5 \cdot A_{mix} + \dot{m}_{noz} \cdot u_5 + \dot{m}_{suc} \cdot u_{11} - P_6 \cdot A_{mix}}{\dot{m}_{noz} + \dot{m}_{suc}} \tag{49}$$

$$h_6 = \frac{\dot{m}_{noz} \cdot \left(\frac{u_5^2}{2} + h_5\right) + \dot{m}_{suc} \cdot \left(\frac{u_{11}^2}{2} + h_{11}\right)}{\dot{m}_{noz} + \dot{m}_{suc}} - \frac{u_6^2}{2} \tag{50}$$

The density is calculated from the mass conservation (eq. 51) and by using the pressure and enthalpy (eq. 52). P_6 is then varied such that both densities match. With the subscript alt meaning alternative.

$$\rho_6 = \frac{\dot{m}_{noz} + \dot{m}_{suc}}{A_{mix} \cdot u_6} \tag{51}$$

$$\rho_{6,alt} = \rho(P_6, h_6) \tag{52}$$

9.1.4 Diffuser

Diffuser outlet pressure is converged in the range 850 kPa to 1200 kPa. Over the diffuser the enthalpy is used to converge the pressure. The ideal outlet enthalpy is found assuming constant entropy, which is then used to find the real outlet enthalpy. The real outlet enthalpy is also found using energy conversion, knowing the velocity and enthalpy at the diffuser inlet. The velocity at the diffuser outlet is assumed to be almost 0.

$$h'_{12} = h(P_{12}, s_{12}) \tag{53}$$

$$h_{12} = h_6 + \frac{h'_{12} - h_6}{\eta_{diff}} \tag{54}$$

$$h_{12,alt} = h_6 + \frac{u_6^2}{2} - \frac{u_{12}^2}{2} \tag{55}$$

Finally the gas quality along with the gas and liquid mass flow out of the ejector is calculated.

$$x_{12} = x(P_{12}, h_{12}) \tag{56}$$

$$\begin{aligned} \dot{m}_g &= (\dot{m}_{noz} + \dot{m}_{suc}) \cdot x_{12} \\ \dot{m}_l &= (\dot{m}_{noz} + \dot{m}_{suc}) \cdot (1 - x_{12}) \end{aligned} \tag{57}$$

9.2 Solving procedure

The oil temperature in the gas cooler is 80 to 160°C. The supply water in the evaporator enters at 80°C and leaves at 77°C. The pressure loss in the pipes between each component is ignored. The input required from the user is ejector nozzle outlet pressure, evaporation pressure and compressor discharge pressure. In addition several assumptions are used to run the initial cycle, these are shown in table 24.

Assumption	Value
Compressor suction superheat (T_1)	5 K
Compressor suction pressure (P_1)	1000 kPa
IHX inlet pressure (P_7)	1000 kPa
Evaporator outlet superheat (T_{10})	5 K
Evaporator outlet pressure (P_{10})	900 kPa

Table 24: Initial assumptions to run the ejector simulation

After running the cycle with initial guesses the system continues using the results from the previous cycle. Each time the system runs consequently it uses the results from the previous cycle. In the simulation the heat pump cycle runs five times after the initial cycle, with each cycle improving the convergence. After completing the fifth iteration the system stops and the results may be examined by the user to ensure that there is convergence.

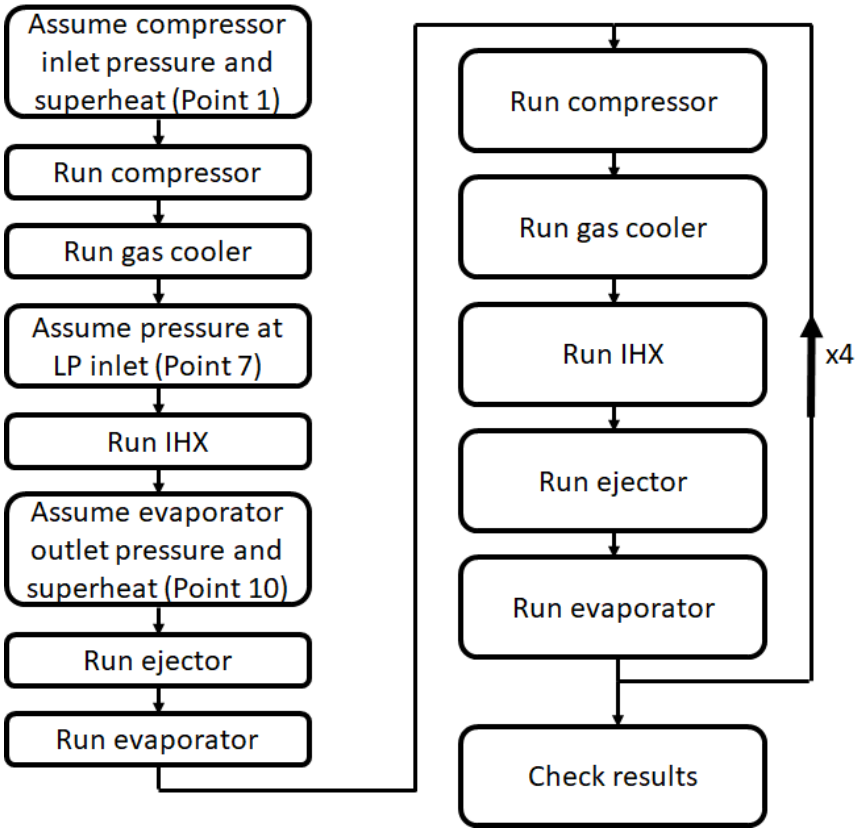

Figure 61: Flowchart of the entire ejector simulation

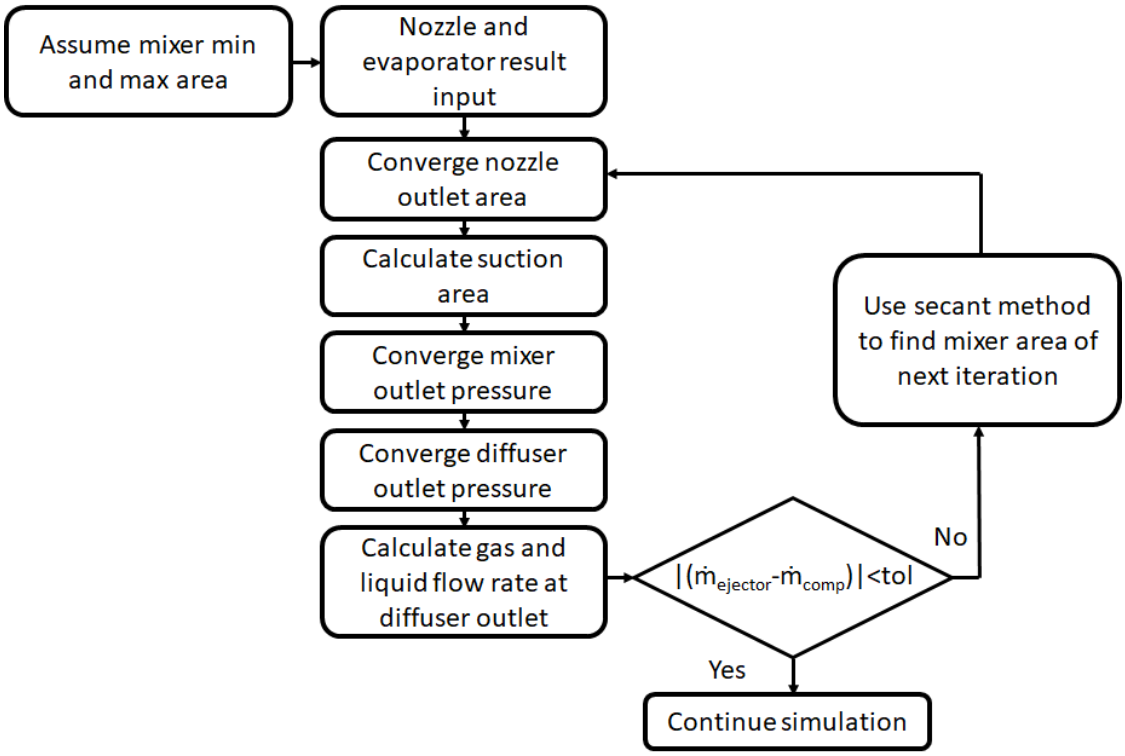

Figure 62: Flowchart of how the ejector converges mixer area

When running the ejector system it is difficult to ensure convergence. The viable discharge pressure, evaporator pressure and nozzle outlet pressure all depend on each. While at the same time the range of convergence of the nozzle outlet area and mixer and diffuser pressure has to be chosen. Table 25 shows the necessary input and produced output of each of the ejector sections.

Component	Input	Output
Nozzle (4 →5)	T_4, P_4, $\dot{m}_{noz}$ P_5 Nozzle efficiency	Nozzle outlet area h_5, u_5
Suction (10 →11)	h_{10}, P_{10} P_{11}/P_5 Suction efficiency	Suction area $\dot{m}_{suc}$ h_{11}, u_{11}
Mixer (5, 11 →6)	P_5/P_{11}, h_5, h_{11}, u_5, u_{11} Mixer efficiency	Mixer outlet area h_6, P_6, u_6
Diffuser (6 →12)	Mixer flow rate h_6, P_6, u_6 Diffuser efficiency	Diffuser outlet area $\dot{m}_g$, $\dot{m}_l$ h_{12}, P_{12}

Table 25: Description of ejector components in simulation

9.3 Results

$P_{suc,\ comp}$ [kPa]	4500	5000	5500	5700	6100
P_{evap} [kPa]	925	900	925	900	900
$P_{noz,\ out}$ [kPa]	850	800	800	800	800
$P_{suc,\ ejector}$ [kPa]	995.3	982.5	1017.9	1023.5	1010
COP [-]	4.718	4.736	4.735	4.735	4.730
Heat delivered [kW]	333.77	325.93	345.18	347.24	333.51
Work [kW]	70.74	68.82	72.90	73.34	70.51
η_{comp} [%]	68.82	72.00	72.44	74.26	75.40
π [-]	4.52	5.09	5.40	5.57	6.04
T_{dis} [°C]	170.14	176.05	181.014	182.73	185.81
$T_{sh,\ comp}$ [K]	5.95	5.17	3.75	3.68	3.54
$\dot{m}_{gas}$ [kg/s]	0.919	0.892	0.947	0.906	0.912
$\dot{m}_{liquid}$ [kg/s]	0.915	0.885	0.939	0.878	0.904
$\dot{m}_{oil}$ [kg/s]	1.821	1.778	1.883	1.807	1.819
$\dot{m}_{water}$ [kg/s]	17.056	21.260	17.593	21.419	21.473
A_{noz} [m^2]	0.0000433	0.0000446	0.0000468	0.0000461	0.0000401
A_{suc} [m^2]	0.0006085	0.0005088	0.0005033	0.0005077	0.0005274
A_{mix} [m^2]	0.0006518	0.0005535	0.0005500	0.0005538	0.0005674
A_{diff} [m^2]	0.0038543	0.0037701	0.0038709	0.0038727	0.0037503

Table 26: Ejector simulation results

In figure 63 the ejector results are compared to the results from the normal system heating oil at 80-160°C, with a discharge pressure of 6100 kPa. This point had the highest COP when examining variation in discharge pressure, with a COP of 4.0677 and a delivered amount of heat of 351.72 kW.

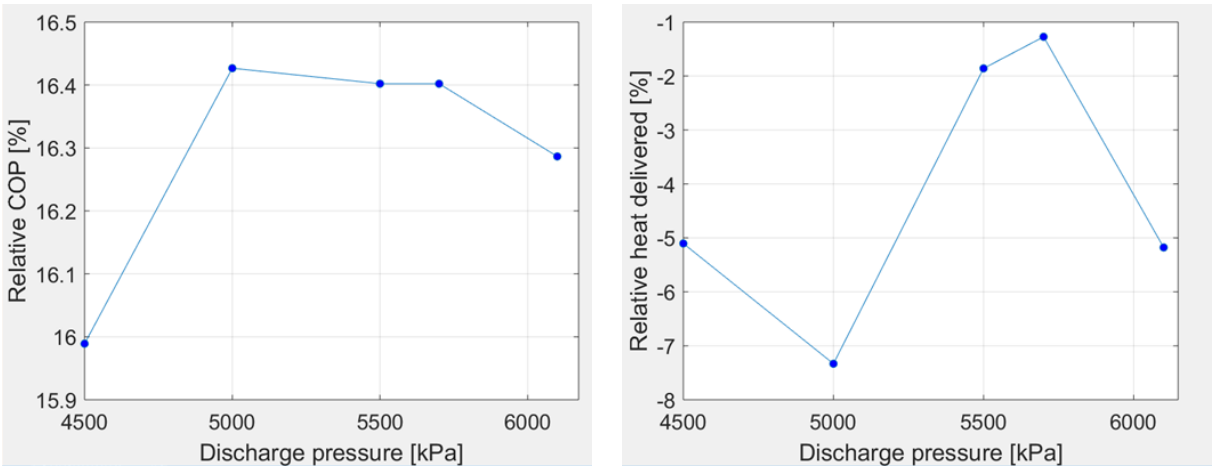

(a) Ejector system relative COP

(b) Ejector system relative heat delivered

Figure 63: Relative ejector results

From figure 63 it can be seen that the COP of the system is improved by 16% when employing an ejector. The improved COP is a result of the increased compressor efficiency, along with

a lower pressure ratio due to the increased compressor suction pressure. The compressor is working at 90% which is beneficial at lower pressure ratio, as seen in previous results. In additionally the ejector system is able to maintain a high amount of heat delivered while working at high discharge pressure compared to the standard cycle when working at 90% rpm.

Compared to the normal heat pump system at 100% rpm there is some reduction in the amount of gas through the compressor and there is a slight reduction in the discharge temperature of the compressor, as can be seen in table 26. The reduction of temperature stems mainly from the reduced pressure ratio, due to the increased compressor suction pressure which the ejector facilitates. As seen in other results, also here the discharge temperature is increased when the pressure ratio increases. The reduced butane flow rate is mainly due to the change in performance of the compressor at lower rpm, but is still acceptable.

The evaporator and nozzle outlet pressure also effect the results. To be able to achieve a water temperature of 77°C at the evaporator outlet the water flow rate is regulated. With increased evaporator pressure (which is defined by the user) the difference between the saturation temperature of the butane and the water temperature is reduced. This reduces the heat transfer, and the evaporator conforms by reducing the water flow rate. Alternatively a reduction in the evaporator pressure reduces the diffuser outlet pressure, which leads to an increased pressure ratio and a reduced amount of gas flow rate. Increased evaporation pressure seems to be beneficial as the system is able to deliver more heat, while using a lower amount of supply water. The nozzle outlet pressure has a much smaller impact on the result, it tweaks some values, but has no large impact on the performance. Variation of the nozzle outlet pressure may however be necessary to make the simulation to converge.

The compressor suction superheat is freely variable in the ejector simulation, as can be seen from the results in table 26 the superheat varies from 5.95 K to 3.54 K. The variation in superheat has an impact on the compressor performance. When varying the superheat in the normal system it has a direct impact on the compressor suction pressure, in the ejector simulation however the pressure is decided by the ejector. In the ejector system the compressor suction superheat is decreased as the discharge pressure increases. This is due to the increase in heat at high temperature, the larger amount of heat allows the gas cooler to increase the amount of oil. The increased amount of oil also requires more heating at low temperatures, and the butane temperature out of the gas cooler is thereby reduced, and the available heat at the HP side in the IHX is reduced. In the simulations done there has been sufficient compressor suction superheat to ensure that there is no condensation in any of the compressor stages. If the discharge pressure is increased further it may be the case that the compressor suction temperature becomes too low.

Depending on which parameter is prioritized the ideal compressor discharge, evaporator and nozzle outlet pressure varies. The COP is stable over all the results with only minor change, there is however some change in the amount of heat delivered in the gas cooler. In addition a high discharge temperature is beneficial as it may allow for a large range of oil temperature. The results may suggest that the mixer area should be somewhere in the range 0.00055 to 0.00057 m^2.

An ejector seems like a viable solution as it increases the COP of the system with 16% while still being able to maintain a high amount of delivered heat. It should however be further investigated how the ejector system performs at delivering higher discharge temperature. If

the oil inlet temperature is increased the temperature of the butane on the HP side of the IHX increases. This may significantly increase the heat delivered in the IHX and thereby increase the compressor suction superheat. The increase in superheat does not linearly increase the discharge temperature, but a sufficiently large increase in the suction superheat will lead to some increase in the discharge temperature. The ejector system is only tested with a oil temperature of 80 - 160°C. If the oil temperature is increased to 100-180°C then perhaps the increase of temperature in the IHX would be enough to produce sufficiently high discharge temperature.

Additional ejector results with a nozzle outlet pressure of 850 kPa are supplied in the appendix in table 32.

10 Sources of error

The limitations regarding the validity of the results and assumptions should be addressed. The simulation is created using correlations and efficiencies gathered from research literature and manufactures. The assumptions used are made in dialog with experienced engineers, who have knowledge of the system simulated. The simulation gives reasonable estimations of performance and feasibility of the system. The error margins should be within reasonable limits.

There are several simplifications and assumptions which reduce the accuracy of the results, two are noted:

- The Compal software calculation used to create the compressor correlations does not include the machine loss, such as the windage loss in the compressor motor.
- There is no consideration of the heat loss from the system. At the high temperatures used the dissipation of heat may be large.

Both of these will reduce the overall performance of the system.

11 Discussion

Simulation	100% rpm	90% rpm	Ejector	No IHX	Design
P_{dis} [kPa]	6100	4600	5000	5700	5700
$P_{suc,\ comp}$ [kPa]	843.3	875.3	982.5	809.3	842.2
COP [-]	4.068	4.731	4.736	4.033	3.833
Heat delivered [kW]	351.72	255.54	325.93	334.28	249.50
Work [kW]	86.47	54.01	68.82	82.89	65.09
η_{comp} [%]	71.93	76.66	72.00	71.60	79.73
π [-]	7.23	5.25	5.09	7.04	6.77
T_{dis} [°C]	189.88	171.96	176.05	186.12	196.26
$T_{sh,\ comp}$ [K]	10	10	5.17	10	30
$\dot{m}_{butane}$ [kg/s]	0.902	0.685	$0.892(\dot{m}_g)/0.885(\dot{m}_l)$	0.863	0.660
$\dot{m}_{oil}$ [kg/s]	1.918	1.394	1.778	1.822	1.3185
$\dot{m}_{water}$ [kg/s]	21.070	16.006	21.260	19.974	14.643
$\rho_{suc,\ butane}$ [kg/m^3]	19.74	20.50	24.38	18.94	18.00

Table 27: Shows point of highest COP for various simulations

Summary of results:

- All the simulations aimed at oil heating in the temperature range 80-160°C, are able to do so with a COP above 3.5.
- The highest COP at 4.7 and highest compressor efficiency, with 10 K suction superheat, is achieved when the compressor works at 90% rpm. However, without an ejector the amount of heat delivered is reduced significantly, additionally the pressure ratio is limited which effectively limits the discharge temperature. The increased efficiency is mainly from a large reduction in friction loss in the compressor.
- The ejector system is able to work at a COP of 4.7, while at the same time deliver a large amount of heat, and has a large range of viable discharge pressure. However there is a reduction in the compressor discharge temperature compared to the standard cycle, due to the reduced pressure ratio.
- The system allows for a large variation in the amount of water delivered. Seemingly being able to handle a water flow rate between 7 kg/s and 32 kg/s, while working at a COP above 3.5 and deliver more than 300 kW of heat.
- With increased compressor suction temperature the compressor performance is improved, but the butane mass flow is reduced, partially due to reduced butane density.
- When working with oil temperature of 100 to 180°C, the system is able to heat the oil at a COP of 3.8, but the amount of heat delivered is reduced below 300 kW. The reduction is mainly due to the reduced butane flow rate from the increased suction superheat temperature. The density of butane is reduced, as well as the volumetric capacity of the compressor.
- For a given evaporation temperature the pressure ratio and the discharge pressure is more important than the suction temperature in determining the compressor discharge temperature.

- At the design point the highest compressor efficiency is achieved, suggesting that increased suction superheat is advantageous for the compressor performance.

Overall the system is performing well compared to the goal of the project. Within each individual simulation the COP and the amount of heat produced is very stable. This is in part due to the relatively large heat exchangers which are aimed at a high temperature.

The compressor should be specifically designed for the pressure ratio which is wanted. There is a large change in performance depending upon the pressure ratio and the suction temperature. It is found that the heat pump is most efficient when the compressor is working at 90% rpm, with a suction superheat of 10 K. This is most likely due to the narrow design range of turbo compressors. If the turbo compressor had been specifically designed for the 80°C to 160°C range, it would most likely have the highest efficiency at 100% rpm. Kaida et al. [2015] found for the SGH165, that the greatest heat pump performance was when working on 60-80% of the possible steam generation rate. In that work however a screw compressor was utilized, while in this thesis a turbo compressor is used. When using the system there has to be a compromise regarding the efficiency of the cycle, amount of heat delivered, and the temperature level of the oil, which was also found by Kaida et al. [2015].

It will be of interest to examine the ejector system at higher oil temperatures. At higher gas cooler outlet temperature, the potential of the ejector increases, due to the potential increase in the throttling loss at higher temperature. It is clear that the IHX already is doing a large part in using the high quality heat after the gas cooler. The current ejector results are all very stable. If a given mixer area is chosen this is going to change, the system will have a more distinct performance curve. [Sarkar et al., 2007] found that there was an ideal gas cooler pressure for a given transcritical system. Attempts can be made to find the ideal gas cooler pressure with an ejector with a fixed mixer area.

	Previous reports			Simulation		
System	HeatBooster	SGH165	Mayekawa pentane	Standard	Design	Ejector
COP [-]	3	2.5	3	4	3.8	4.7
T_{sink} [°C]	150	165	150	160	180	160
T_{source} [°C]	90	70	80	80	80	80

Table 28: Compares results from the simulations done with previous results

Table 28 presents the temperature levels and COP achieved by the systems presented in chapter 2.3 and the simulations. It should be kept in mind that the simulation results are theoretical. The previous examined systems are subcritical, they deliver heat at constant temperature. This is advantageous when the heat sink is constant temperature process, such as water evaporation. A transcritical system is more efficient when delivering heat to a variable temperature heat sink. The theoretical efficiency of the simulation exceeds the performance of the previous systems on all fronts. However, if used for steam production at constant high temperature the efficiency could be reduced depending on the evaporation temperature of the water/steam. There is not a large amount of scientific data to compare this work to, as butane is not a commonly used working fluid in general heat pump systems.

12 Conclusion and suggestions for further work

Development of new technology is necessary to reduce the environmental impact of high temperature heat production. Efficient and economically viable options are required. In this thesis it is found that a high temperature transcritical heat pump is a viable option for heating high temperature oil. The utilization of waste heat in the process makes the solution more relevant. Butane is presented as a viable working fluid for such a transcritical system, being able to ensure a large heat capacity, as well as an environmentally friendly system.

It is found that the system is able to achieve the goal of delivering above 300 kW of heat when heating oil from 80 to 160 °C, while working at a COP of 4. The system is able to perform in a large range of conditions such as: reduced supply water flow rate, variation of suction superheat in a large range and variation of discharge pressure in the transcritical area.

The addition of an ejector is examined and seems promising, it enables the system to produce the highest COP, while at the same time maintaining a larger flexibility and delivered amount of heat. With the ejector a theoretical COP of 4.7 is achieved. The system is most efficiency with the compressor working at 90% rpm, due to a reduction in the compressor friction loss. It is important to note that the design specification is heating oil from 100°C to 180°C, and therefore when heating at 80°C to 160 °C the compressor is more efficient at reduced rpm, and the heat exchangers are relatively large. Due to the narrow efficiency range of turbo compressors it is important to design them for the appropriate conditions.

The compressor discharge pressure and pressure ratio is found to be the most important parameters in delivering sufficiently high temperature. When increasing discharge pressure, not only is the discharge temperature increased, but the heat capacity is shifted towards higher temperatures, which further increases the potential at high pressure.

The heat loss from the system and some of the compressor losses are not included in the simulation. To confirm the performance these losses need to be examined in practical tests of the system.

12.1 Suggestions for further work

Based on the work completed in this thesis, the following is suggested as further work:

- Compare the simulation results with the test results which will be produced by Mayekawa.
- Evaluate heat loss from cycle.
- Evaluate reduction in the compressor efficiency due to friction.
- Examine the performance of the system using water/steam as the heat sink in the gas cooler.
- Examine the ejector system with oil temperature of 100-180°C in the gas cooler.

References

Alfa Laval. Heat exchanger calculation software. https://www.alfalaval.com/industries/hvac/product-selection-tool/#.

Marshall Brain. How steam engines work. https://science.howstuffworks.com/transport/engines-equipment/steam2.htm, 2008. Accessed: 20.09.2017.

Yunus A. Cengel and John M. Cimbala. *Fluid Mechanics Fundamentals and Applications*, chapter 8 Internal flow, pages 355–356. McGraw-Hill Education, 2013. ISBN 9780073380322. URL https://www.amazon.com/Fluid-Mechanics-Fundamentals-Applications-Cengel/dp/0073380326?SubscriptionId=0JYN1NVW651KCA56C102&tag=techkie-20&linkCode=xm2&camp=2025&creative=165953&creativeASIN=0073380326.

Concepts NREC. *COMPAL*. Woburn, Massachusetts. URL http://www.conceptsnrec.com/solutions/software/computer-aided-engineering/preliminary-design/compal.

H. Crowther and E. Smithart. *Frictionless-compressor technology*, volume 76. January 2004. URL http://lit.daikinapplied.com/bizlit/DocumentStorage/WaterCooledChiller/Articles/2F-6000.pdf. Accessed: 19.10.2017.

Trygve M. Eikevik. *Compendium TEP4255*. NTNU, 2016.

Trygve M. Eikevik and Armin Hafner. *Compendium TEP09*. NTNU, 2016.

ETSU and United Kingdom WS Atkins Consultants Ltd. Energy efficiency best practice programme: A training package for engineers - guidance for engineers. http://www.zuj.edu.jo/?wpdmdl=12236, 2000. Accessed: 20.10.2017.

How It Works. How it works: Centrifugal compressor. http://howitsworkss.blogspot.no/2015/06/centrifugal-compressor.html, 2015. Accessed: 06.02.2018.

Rainer Jakobs. Status and outlook: Industrial heat pumps. In *3rd EHPA European Heat Pump Forum*, 2010. Accessed: 16.01.2018.

T. Kaida, I. Sakuraba, K. Hashimoto, and H. Hasegawa. Experimental performance evaluation of heat pump-based steam supply system. *Experimental performance evaluation of heat pump-based steam supply system*, 90(1):012076, 2015. ISSN 1757-8981. Accessed: 29.09.2017.

M. Karlsson, M. Åbom, M. Lalit, and R. Glav. A note on the applicability of thermo-acoustic engines for automotive waste heat recovery. *SAE International Journal of Materials and Manufacturing*, 9(2):286–293, 2016. ISSN 19463979. Accessed: 26.01.2018.

Werner Kast. *VDI Heat Atlas (VDI-Buch)*, chapter L1.2 Pressure drop in flow through pipes. Springer, 2010. ISBN 978-3-540-77876-9. URL https://www.amazon.com/VDI-Heat-Atlas-VDI-Buch-Gesellschaft/dp/3540778764?SubscriptionId=0JYN1NVW651KCA56C102&tag=techkie-20&linkCode=xm2&camp=2025&creative=165953&creativeASIN=3540778764.

Jiyoung Kim, Seong-Ryong Park, Young-Jin Baik, Ki-Chang Chang, Ho-Sang Ra, Minsung Kim, and Yongchan Kim. Experimental study of operating characteristics of compression/absorption high-temperature hybrid heat pump using waste

heat. *AFORE 2011(Asia-Pacific Forum of Renewable Energy 2011)*, 54:13–19, June 2013. ISSN 0960-1481. URL http://www.sciencedirect.com/science/article/pii/S0960148112006039. Accessed: 24.01.2018.

O. Kleefkens and S. Spoelstra. R&d on industrial heat pumps. In *11th IEA Heat Pump Conference 2014, May 12-16 2014, Montréal (Québec) Canada*, 2014. URL https://www.ecn.nl/publications/PdfFetch.aspx?nr=ECN-M--14-039. Accessed: 20.09.2017.

Christoph Lauterbach, Shahrdad Javid, Bastian Schmitt, and Klaus Vajen. *FEASIBILITY ASSESSMENT OF SOLAR PROCESS HEAT APPLICATIONS*. August 2011. Accessed: 17.01.2017.

Eungchan Lee, Hoon Kang, and Yongchan Kim. Flow boiling heat transfer and pressure drop of water in a plate heat exchanger with corrugated channels at low mass flux conditions. *International Journal of Heat and Mass Transfer*, 77(Supplement C):37–45, October 2014. ISSN 0017-9310. URL http://www.sciencedirect.com/science/article/pii/S0017931014004190. Accessed: 20.10.2017.

E. W. Lemmon, M. L. Huber, and M. O. McLinden. NIST Standard Reference Database 23: Reference Fluid Thermodynamic and Transport Properties-REFPROP, Version 9.1, National Institute of Standards and Technology, 2013. URL https://www.nist.gov/srd/refprop.

Fang Liu and Eckhard A. Groll. Study of ejector efficiencies in refrigeration cycles. *Applied Thermal Engineering*, 52(2):360, 2013. ISSN 1359-4311. Accessed: 10.11.2017.

Alan Malmcom. Steam generators vs. steam boilers. https://turbofuture.com/industrial/steamgenerators-vs-steamboilers, 2016. Accessed: 20.09.2017.

MATLAB version 9.1.0.441655 (R2016b). The Mathworks, Inc., Natick, Massachusetts, 2016.

Mayekawa. *Natural Five*, 2009. URL http://www.mayekawa.com/activities/natural5/. Accessed: 13.10.2017.

Nelson Mugabi, Akito Machida, Kazutoshi Ito, and Hideki Fuchikami. Development of a steam generation heat pump using a natural refrigerant. In *Grand Renewable Energy 2014, Tokyo Big Sight, Tokyo Japan*, 2014. Accessed: 10.09.2017.

Kosaku Nishida, Mizuo Kudo, Keizo Kobayashi, Akito Machida, Kiyoshi Saito, Yutaka Ohta, and Masafumi Katsuta. Development of an industrial high performance and high temperature heat pump heat transfer characteristics of supercritical R600 in plate heat exchangers [Japanese], 2016. Accessed: 13.10.2017.

Kousaku Nishida. Meetings and mail correspondence. Mayekawa, 2017.

Bob Parsons. *Ashrae Handbook: Heating, Ventilating, and Air-Conditioning Systems and Equipment/I-P Edition*. ASHRAE, 1992. Accessed: 20.09.2017.

J. Sarkar, Souvik Bhattacharyya, and M. Ram Gopal. Natural refrigerant-based subcritical and transcritical cycles for high temperature heating. *International Journal of Refrigeration*, 30(1):3–10, January 2007. ISSN 0140-7007. URL http://www.sciencedirect.com/science/article/pii/S0140700706000661. Accessed: 19.10.2017.

Bhodan Soroka. Industrial heat pumps, energy efficiency. *European Copper Institute & Laborelec*, 2007. Accessed: 20.09.2017.

SWEP. https://www.swep.net/.

U.S. Department of Energy. Industrial heat pumps for steam and fuel savings. 2003. Accessed: 20.09.2017.

Viking Heat Engines. New industrial heat pump produces heat in the very high temperature range, viking's industrial high-temperature heat pump available to order. http:/www.vikingheatengines.com/news/new-industrial-heat-pump-produces-heat-in-the-very-high-temperature-range, https://tinyurl.com/y7lky2t7, 2017. Accessed: 12.01.2018.

V. V. Wadekar. Compact heat exchangers. *Chemical Engineering Progress*, 96(12):39–49, 2000. ISSN 03607275. Accessed: 20.10.2017.

Choyu Watanabe, Yohji Uchiyama, Satoshi Hirano, and Takeshi Hikawa. Pioneering industrial heat pump technology in japan. http://etkhpcorderapi.extweb.sp.se/api/file/1139, 2014. Accessed: 15.10.2017.

Stefan Wolf, Jochen Lambauer, Markus Blesl, Ulrich Fahl, and Alfred Voß. *Industrial heat pumps in Germany: Potentials, technological development and market barriers*. September 2012. Accessed: 20.09.2017.

Jingwei Zhu and Stefan Elbel. *A New Control Mechanism for Two-Phase Ejector in Vapor Compression Cycles Using Adjustable Motive Nozzle Inlet Vortex*. July 2016. Accessed: 10.11.2017.

A Appendix

A.1 Pressure drop from evaporator to IHX

Information about the pipes between the evaporator and the IHX. The data is not included in simulation as the pressure loss was found to be low.

Component	Type	Characteristics	Length/Amount	Comment
Pipes	32A	Di 35.5	919.9	Half flow rate
	65A	Di 65.9	1489	-
Turns	32A	R 47.6	3	Half flow rate
	65A	R 95.3	2	-
Splitter/mixer	65A	ζ 0.75	1	Splitter
Valves	-	-	-	-

Table 29: Evaporator to IHX pipes

A.2 Compressor maximum flow rate at 90 and 100% rpm

The maximum mass flow depends on the compressor suction superheat, and the suction pressure.

	5 K	10 K	30 K	50 K
1.249 kPa	1.65	1.568	1.30	1.092
0.9062 kPa	1.128	1.077	0.906	0.77
0.6382 kPa	0.76	0.728	0.621	0.534

Table 30: Compressor maximum flow rate at 100% rpm

	3 K	5 K	10 K	30 K	50 K
1.249 kPa	1.353	1.319	1.241	0.98	0.777
0.9062 kPa	0.906	0.8856	0.837	0.674	0.545
0.6382 kPa	0.6282	0.578	0.5496	0.451	0.372

Table 31: Compressor maximum flow rate at 90% rpm

A.3 Ejector results

P_{dis} [kPa]	4500	5000	5500
P_{evap} [kPa]	925	900	925
$P_{noz,\ out}$ [kPa]	850	850	850
$P_{suc,\ ejector}$ [kPa]	995.3	975.5	1017
COP [-]	4.7181	4.7357	4.7339
Heat delivered [kW]	333.77	321.45	344.55
Work [kW]	70.74	67.88	72.78
η_{comp} [%]	68.82	72.39	72.49
pi [-]	4.52	5.13	5.41
T_{dis} [°C]	170.14	176.06	181.02
$T_{sh,\ comp}$ [K]	5.95	5.36	3.79
$\dot{m}_{gas}$ [kg/s]	0.919	0.879	0.945
$\dot{m}_{liquid}$ [kg/s]	0.915	0.877	0.937
$\dot{m}_{oil}$ [kg/s]	1.821	1.754	1.880
$\dot{m}_{water}$ [kg/s]	17.056	21.024	17.558
A_{noz} [m^2]	0.00004329	0.00003422	0.00003737
A_{suc} [m^2]	0.00060855	0.00070998	0.00063525
A_{mix} [m^2]	0.00065184	0.00074420	0.00067261
A_{diff} [m^2]	0.00385434	0.00376307	0.00386867

Table 32: Shows additional ejector results, nozzle outlet pressure of 850 kPa

A.4 Ejector equations

Equations found in [Liu and Groll, 2013].

A.4.1 Nozzle equations

$$\eta_{noz} = \frac{h_4 - h_5}{h_4 - h_5'} \tag{58}$$

$$h_4 + \frac{u_4^2}{2} = h_5 + \frac{u_5^2}{2} \tag{59}$$

A.4.2 Suction equations

$$\eta_{noz} = \frac{h_{10} - h_{11}}{h_{10} - h_{11}'} \tag{60}$$

$$h_{10} + \frac{u_{10}^2}{2} = h_{11} + \frac{u_{11}^2}{2} \tag{61}$$

A.4.3 Mixer equations

$$P_6 \cdot A_{mix} + (\dot{m}_{noz} + \dot{m}_{suc}) \cdot u_6 = P_5 \cdot A_{mix} + (\dot{m}_{noz} \cdot u_5 + \dot{m}_{suc} \cdot u_{11})\eta_{mix} \tag{62}$$

η_{mix} is the efficiency of the mixer, which is assumed to be 1.

$$(\dot{m}_{noz} + \dot{m}_{suc})(h_6 + \frac{u_6^2}{2}) = \dot{m}_{noz}(h_5 + \frac{u_5^2}{2}) + \dot{m}_{suc}(h_{11} + \frac{u_{11}^2}{2}) \tag{63}$$

A.4.4 Diffuser equations

$$\eta_{diff} = \frac{h_6 - h_{12}}{h_6 - h'_{12}} \tag{64}$$

$$h_6 + \frac{u_6^2}{2} = h_{12} + \frac{u_{12}^2}{2} \tag{65}$$

A.5 Oil properties

Oil properties received from Mayekawa.

Temp.	Vapour pressure	Heat capacity	Thermal conductivity	Density	Dynamic viscosity	Kinematic viscosity
℃	kPa	kJ／kg・K	W／m・K	kg／m^3	mPa・s	mm^2／s
0	—	1. 842	0. 140	844	233	276
20	—	1. 916	0. 139	832	69. 3	83. 3
40	—	1. 990	0. 137	820	27. 9	34. 0
60	—	2. 064	0. 136	807	13. 8	17. 1
80	—	2. 138	0. 134	796	7. 91	9. 93
100	—	2. 213	0. 133	784	5. 03	6. 42
120	—	2. 287	0. 131	772	3. 46	4. 49
140	—	2. 361	0. 130	760	2. 53	3. 32
160	—	2. 435	0. 128	748	1. 93	2. 58
180	0. 1	2. 509	0. 127	736	1. 52	2. 07
200	0. 2	2. 584	0. 125	724	1. 24	1. 71
220	0. 4	2. 658	0. 124	712	1. 03	1. 45
240	0. 9	2. 732	0. 122	700	0. 87	1. 24
260	1. 9	2. 806	0. 121	688	0. 75	1. 08
280	4. 0	2. 881	0. 119	676	0. 65	0. 96
300	7. 7	2. 955	0. 118	664	0. 57	0. 85

Figure 64: Properties of the heat medium oil used